

AN ABSTRACT OF THE DISSERTATION OF

Dongwha Sohn for the degree of Doctor of Philosophy in Oceanography presented on March 15, 2016.

Title: Distribution, Abundance, and Settlement of Slope-spawning Flatfish during Early Life Stages in the Eastern Bering Sea.

Abstract approved: _____

Lorenzo Ciannelli

Changes in environmental conditions in marine ecosystems could directly or indirectly influence distribution, abundance, settlement, and size at settlement of flatfish. Understanding species-specific and age-specific responses to environmental variability is important for managing commercially important flatfish stocks. Slope-spawning flatfish whose offspring rely on extensive drift from the slope (spawning) to the shelf (settlement) and which require specific habitat for settlement could be especially vulnerable to environmental variability. Arrowtooth flounder (ATF; *Atheresthes stomias*), Greenland halibut (GH; *Reinhardtius hippoglossoides*), and Pacific halibut (PH; *Hippoglossus stenolepis*) are commercially and ecologically important slope-spawning flatfish species in the eastern Bering Sea (EBS), which has experienced fluctuating warm and cold periods since 2000. Although the three species share many attributes, their population trajectories have fluctuated differently. This difference could result from contrasting responses to environmental variability during early life history. To understand how physical variability of the Bering Sea can differentially affect flatfish ecology from pre-settlement to post-settlement phases, I used a combination of field data, biophysical modeling, and statistical modeling to characterize early life stage attributes (chapter 2), settlement success (chapter 3), and size, abundance, and distribution at settlement (age-0) and age-1 (chapter 4).

Based on historical ichthyoplankton survey data for GH and PH, I found that there were species-specific differences in the spatial distribution (vertically and horizontally) and juvenile nursery areas between the two species during early life stages in the EBS. Specifically, I found that PH larvae abruptly move to shallower water as they grow, and cross onto the shelf earlier than GH. This ontogenetic movement has the benefit of allowing PH larvae to take advantage of

on-shelf transport to reach their settlement locations. However, an early transition from the slope to the shelf may not equally benefit GH, whose settlement locations are further from the spawning ground.

Using a bio-physical modeling approach parameterized on the field data summarized in chapter 2, I found that species-specific variability of early life attributes causes interannual and species-specific variability of GH and PH settlement success in the EBS. GH settlement increased with increasing along-shelf (northwestward) flow whereas PH settlement decreased. GH that spawned in November and December were highly successful at settling while PH settlement was most successful when they spawned in January and February. Furthermore, GH settlement is affected by temperature dependence of pelagic larval duration, but not PH, indicating a strong resilience of PH to temperature induced variations in development and dispersal duration.

Using otolith microstructure analysis, I found that variations in size at settlement for ATF are significantly correlated with latitude of sampling location. For GH, their size at settlement is associated with bottom water temperature and sea ice extent. Especially, sea ice coverage has a strong negative correlation with on-shelf winds, which drive along-shelf Ekman transport to southeast impacting dispersal pathways and duration. Size at settlement for ATF increased with increasing latitude of sampling location, which could be impacted by currents. For GH, size at settlement decreased with decreasing bottom water temperature and increasing sea ice extent. Also, my results showed that settlement habitat increases for GH in cold years whereas that of ATF increases in warm years. The bottom temperature of age-0 habitat for both ATF and GH affected on their age-1 abundance; GH age-1 abundance increased with decreasing bottom temperature of age-0 habitat, but no clear directionality was found for ATF.

The findings from this study have implications for understanding settlement success and recruitment of slope-spawning flatfish in the EBS. In most cold years when along-shelf flow is generally strong, the level of larval supply of GH to their settlement areas is higher than in warm years. Size at settlement for GH decreased in cold years. The larger amount of suitable habitat for settlement and post-settlement stages could result in lower competition and less predation in comparison to warm years. In support of this hypothesis, I found greater age-1 abundance in cold years, indicating size at settlement in GH may not be critical compared to suitability of habitat

features and larval supply to settlement grounds. On the other hand, in cold years with strong along-shelf transport to northwest, PH (or ATF), which settle in the southern part of the EBS, have lower numbers of successful settlers. Size at settlement for ATF increased in cold years, and I assumed that size at settlement for PH may have similar patterns. The amount of suitable habitat after settlement would be smaller, resulting in lower recruitment due to increased competition for limited resources.

By studying how physical factors and their variability influence these three flatfish during early life stages, this study provides valuable insight into the response of flatfish stocks to past and future climate changes in the eastern Bering Sea – a system that is especially vulnerable to warming.

©Copyright by Dongwha Sohn
March 15, 2016
All Rights Reserved

Distribution, Abundance, and Settlement of Slope-spawning Flatfish during Early Life Stages in
the Eastern Bering Sea

by
Dongwha Sohn

A DISSERTATION

submitted to

Oregon State University

in partial fulfillment of
the requirements for the
degree of

Doctor of Philosophy

Presented March 15, 2016
Commencement June 2016

Doctor of Philosophy dissertation of Dongwha Sohn presented on March 15, 2016

APPROVED:

Major Professor, representing Oceanography

Dean of College of Earth, Ocean, and Atmospheric Sciences

Dean of the Graduate School

I understand that my dissertation will become part of the permanent collection of Oregon State University libraries. My signature below authorizes release of my dissertation to any reader upon request.

Dongwha Sohn, Author

ACKNOWLEDGEMENTS

I would like to thank my advisor Lorenzo Ciannelli for his endless of support, encouragement and thoughtful guidance during my graduate life including both Masters and Ph.D. programs. Without his constant support, I could not complete my Ph.D. program successfully and become a better scientist. Also, he is one of the wonderful role models for me.

I would like to thank my dissertation committee members, Janet Duffy-Anderson, Harold P. Batchelder, Jessica A. Miller, and Michael Behrenfeld for insightful comments and guidance for my research. Especially, Janet has supported me as a committee member and has shared her knowledge and experience during both Masters and Ph.D. programs. I appreciate her endless support, encouragement, and warmth. Also, I thank Hal and Jessica for sharing their thoughtful advice and insightful comments on Chapter 3 and Chapter 4, respectively. Furthermore, I would like to thank Yvette Spitz for sharing her wisdom and valuable insights throughout my graduate life.

I would like to thank all of the members of the EcoFOCI group of the Alaska Fisheries Science Center: Kevin Bailey, Jeffrey Napp, Ann Matarese, Debbie Blood, Morgan Busby, Dan Cooper, Lisa DeForest, Annette Dougherty for providing data, sharing their scientific knowledge, and allowing me to use their facilities. I also thank William T. Stockhausen for providing the particle-tracking model (DisMELS) used in Chapter 3 and insightful comments on Chapter 3. Furthermore, I thank Delsa M. Anderl for providing otolith samples, allowing me to use her facilities, and reviewing Chapter 4. Moreover, I thank Jim Ianelli, Robert R. Lauth, Stan Kotwicki, Timothy Loher, Kerim Y. Aydin, Troy W. Buckley, and Geoffrey M. Lang for providing data and sharing their scientific knowledge about arrowtooth flounder, Greenland halibut, and Pacific halibut. In addition, I thank Richard D. Brodeur and William Pearcy for interest in my research and encouragement. I would like to thank Enrique Curchitser who developed Regional Oceanographic Modeling System for the northeast Pacific (ROMS NEP version 4).

I am grateful to all of the members of the Fisheries Oceanography Lab including past, for their friendships and help to fulfill my graduate student life. In particular, I thank Cathleen Vestfals for providing the transport indices of Bering Slope Current in the eastern Bering Sea used in Chapter 3. I also thank Mary Hunsicker and Kathryn Sobocinski for providing valuable

feedback on my manuscripts and being wonderful mentors. Additionally, I thank Angela Johnson, Sandi Neidetcher, Bobby Ireland, Jason Phillips, Caren Barceló, Morgan Bancroft, and Michelle Stowell for their friendships, valuable feedback, and the conversations about graduate student life.

I thank my friends and colleagues at the CEOAS, in particular, Gaby Mayoga and her family, Susan Schnur, Robyn Matteson, Byungho Lim, Martin Hoecker- Martinez, Atul Daghe, Lin Li, Emily Lemagie, Gonzalo Saldias, Fabian Gomez, Morgaine McKibben, Clara Llebot, Iria Giménez, and Mei Sato. Your friendships mean the world to me and I am grateful to know you all. Especially, Susan and Martin reviewed the earlier version of my manuscripts and Byungho taught me how to write MATLAB codes for downloading the wind data in Chapter 3. I also thank Robert Allan, Lori Hartline, Chuck Sears, Bruce Marler, Tom Leach, and Mary Hitch for their help and support. I would like to thank the all of the people I have met in the CEOAS who have helped me adjust to American life and graduate student life. I would like to thank all my Korean friends throughout my journey at Oregon State University.

A special thanks goes to Suam Kim and Sukyung Kang for their constant support, encouragement, and love. For my family, I would like to thank my Mom who believes in and loves me. I could not make it without her support and endless love. I also thank my wonderful parents-in-law for their support, encouragement, and love. I deeply thank you to my husband Changsung Moon for helping and taking care of me with steadfast love. To my son, Ryan Moon who was born in 2013, thank you for making me happy and smile. To my daughter who is in my tummy, thank you for being there.

My research was supported by grants from the North Pacific Research Board, National Science Foundation, the Ecology of Marine Nekton Award at the CEOAS, Bill Wick Marine Fisheries Award scholarship at the Hatfield Marine Science Center, and International Student and Advising Services at Oregon State University.

CONTRIBUTION OF AUTHORS

Dr. Lorenzo Ciannelli contributed to the analysis and writing of all chapters. Dr. Janet T. Duffy-Anderson contributed to the data of Chapter 2 and 4 and to reviewing and commenting on Chapter 2 and 3. Dr. Harold P. Batchelder contributed to the analysis and reviewing and commenting on Chapter 3. Dr. William T. Stockhausen developed the particle-tracking model (DisMELS) used in Chapter 3. Dr. Cathleen Vestfals characterized the transport indices of Bering Slope Current in the eastern Bering Sea used in Chapter 3. Dr. Jessica A. Miller contributed to reviewing and commenting on Chapter 4. Dr. Delsa M. Anderl contributed to the data and facilities for Chapter 4.

TABLE OF CONTENTS

	<u>Page</u>
Chapter 1. Introduction.....	1
Chapter 2. Distribution of early life Pacific halibut and comparison with Greenland halibut in the eastern Bering Sea.....	6
ABSTRACT.....	7
INTRODUCTION.....	7
MATERIALS AND METHODS.....	10
Study area.....	10
Data sources.....	11
Data analyses.....	13
RESULTS.....	15
Horizontal distribution of Pacific halibut and Greenland halibut larvae.....	15
Vertical distribution of Pacific halibut and Greenland halibut larvae.....	16
Distribution of Pacific halibut and Greenland halibut settled juveniles.....	17
DISCUSSION.....	17
ACKNOWLEDGMENTS.....	22
Chapter 3. Predicting settlement success of two slope-spawning flatfish in the eastern Bering Sea.....	37
ABSTRACT.....	38
INTRODUCTION.....	38
MATERIALS AND METHODS.....	41
Spatial characterization of settlement locations.....	42
Dispersal pathways simulations.....	43
DisMELS model.....	43
Individual-based model parameters for DisMELS.....	44
Estimation for successful settlement.....	46
Correlations between settlement success and age-0 catch and recruitment data.....	47
Correlations between settlement success and oceanic indices.....	47
Sensitivity analysis of the simulation model.....	48

TABLE OF CONTENTS (Continued)

	<u>Page</u>
RESULTS.....	49
Settlement locations.....	49
Interannual variability and spatial and temporal patterns of successful settlement....	49
Correlations between settlement success with ocean circulation indices, age-0 catch and recruitment data.....	50
Model sensitivity.....	51
DISCUSSION.....	51
CONCLUSIONS.....	57
ACKNOWLEDGEMENTS.....	57
Chapter 4. Interannual variability of size at settlement and distributions for two slope- spawning flatfish in the eastern Bering Sea.....	70
ABSTRACT.....	71
INTRODUCTION.....	71
MATERIALS AND METHODS.....	75
Data sources.....	75
Otolith analysis and criteria for settlement check mark on ATF and GH otoliths.....	76
Otolith measurements.....	77
Statistical analysis.....	78
Effect of water temperature on abundance and distribution of ATF and GH Juveniles.....	79
RESULTS.....	80
Interannual variability of size at settlement.....	80
Effect of water temperature on the abundance and distribution of ATF and GH Juveniles.....	81
DISCUSSION.....	82
CONCLUSION.....	85
ACKNOWLEDGMENTS.....	86
Chapter 5. Summary and implication.....	101

TABLE OF CONTENTS (Continued)

	<u>Page</u>
BIBLIOGRAPHY.....	108
APPENDICES.....	119

LIST OF FIGURES

<u>Figure</u>	<u>Page</u>
<p>Fig. 1.1. Conceptual plots that link chapter 2 (early life stage attributes), 3 (settlement success), and 4 (size, abundance, and distribution at settlement) of this dissertation. Circle (dash with blue color) represents settlement areas for age-0 Greenland halibut as an example. Rectangle (purple color) indicates potential spawning locations for Greenland halibut and Pacific halibut. Blue arrow represents one of the drift pathways from spawning to settlement locations.....</p>	5
<p>Fig. 2.1. Study area with schematic representation of the major currents - the Aleutian North Slope Current (ANSC; black line), Bering Slope Current (BSC; black line), Alaska Coastal Current (ACC; dashed line), flows (long dashed line) along the isobaths in the shelf in the eastern Bering Sea.....</p>	31
<p>Fig. 2.2. Pacific halibut horizontal distribution of (a) preflexion larvae (6.0 mm – 13.5 mm standard length (SL)) from February to August, (b) flexion larvae (13.6 mm – 17.8 mm SL) from February to August, and (c) postflexion larvae (17.9 mm – 28.0 mm SL) from February to August in the eastern Bering Sea. Bubble sizes are proportional to the log transformed catch per unit effort (CPUE)+1. MOCNESS and MBT stand for Multiple Opening/Closing Net Sampling System and modified beam trawl, respectively. Gray lines indicate 50 m, 100 m, 200 m, 500 m, 1000 m, and 2000 isobaths.....</p>	32
<p>Fig. 2.3. Partial effects of (a) sampling location and (b) day of year on Pacific halibut larval body-length estimated from the Generalized Additive Model (GAM). Image colour and red contour lines indicates predicted larval body-length from the GAM in which sampling location (latitude and longitude) and day of the year where included as covariate. The body-length increases going from blue to green and yellow being largest. Open circles in (a) and (b) indicate the observation data. Shaded areas on (b) are intervals of the modeled independent variables.....</p>	33
<p>Fig. 2.4. Horizontal distributions of (a) Pacific halibut and (b) Greenland halibut larvae between February to September collected from 60 bongo (BON), modified beam trawl (MBT), and methot trawl (METH) samplings between 1972 and 2012. Plus signs represent non-catch stations across the sampling years. Gray lines indicate 50 m, 100 m, 200 m, 500 m, 1000 m, and 2000 isobaths.....</p>	34
<p>Fig. 2.5. Vertical distribution of Pacific halibut larval abundance (one standard deviation (line); top left) and standard length (standard deviation (line); top right) over 10 years (1992-1995 and 2005-2010) and vertical distribution of Greenland halibut larval abundance (standard deviation (line); bottom left) and standard length (one standard deviation (line); bottom right) in 1992-1994, 2007-2008, and 2010 in the eastern Bering Sea. N refers to number of tows (number of positive tows) for the left panel and number of fish for the right panel.....</p>	35

LIST OF FIGURES (Continued)

<u>Figure</u>	<u>Page</u>
Fig. 2.6. Distributions of (a) abundance (ln (catch per unit effort (CPUE) + 1)) per 10,000 m ² and of (b) body-length for Pacific halibut settled juveniles (33.7 mm – 90.0 mm total length (TL)) and distributions of (c) abundance (ln (CPUE + 1)) per 10,000 m ² and of (d) body-length for Greenland halibut settled juveniles (60.0 mm – 90.0 mm TL) from the eastern Bering Sea summer bottom trawl (1982 – 2011) and beam trawl (2010 and 2012) surveys. Bubbles in (a) and (c) indicate natural log transformed CPUE+1 and open circles in (b) and (d) indicate locations where individuals in each body-length category were found. Gray lines indicate 50 m, 100 m, 200 m, 500 m, 1000 m, and 2000 m isobaths. Black line polygon in (a) indicates geographic area sampled by bottom trawl while black dash line polygon indicates geographic area sampled by beam trawl.....	36
Fig. 3.1. Study area with major currents in the eastern Bering Sea. Aleutian North Slope Current (ANSC) and Bering Slope Current (BSC). Also shown is the Alaska Coastal Current (ACC) along the Alaska Peninsula. Circles indicate known settlement areas for age-0 Greenland halibut (dashed with blue color) and age-0/age-1 Pacific halibut (dotted with green color).....	63
Fig. 3.2. Greenland halibut and Pacific halibut egg release locations for the DisMELS dispersal pathway simulations in the eastern Bering Sea. 1 and 2 were two locations from preliminary analysis. Three potential spawning locations (location 42-44; purple circles) were closely spaced (< 4 km) in order to check small-scale spatial variability.....	64
Fig. 3.3. The probability map of age-0 Greenland halibut (≤ 100 mm total length, TL; left) and age-0/age-1 Pacific halibut (≤ 150 mm TL; right) occurrence predicted by a binomial generalized additive model (GAM) using data from the eastern Bering Sea summer Groundfish Survey between 1982 to 2011. The color image shows the effect of station position on the presence/absence of each species estimated from the GAM. Red contours indicate the occurrence probability value for Greenland halibut (left; 0.2) and Pacific halibut (right; 0.2) that identify potential settlement locations for each species. Beige color indicates a relatively higher occurrence and green color indicates a relatively lower occurrence.....	65
Fig. 3.4. Percentage of successful settlers for Greenland halibut (blue) and Pacific halibut (red) from the DisMELS dispersal pathway simulations between 1982/1983 and 2003/2004.....	66
Fig. 3.5. The horizontal distributions of predicted Greenland halibut (left) and Pacific halibut (right) successful settlers over all simulation years. Red circles indicate an individual successful settler for each species that have probability of occurrence above 0.2 for Greenland halibut and Pacific halibut from 1982/1983 to 2003/2004.....	67

LIST OF FIGURES (Continued)

<u>Figure</u>	<u>Page</u>
<p>Fig. 3.6. Mean number of successful settlers by spawning date for Greenland halibut in good years (above multi-year mean; please see Fig. 3.3) and in bad years (below multi-year mean; please see Fig. 3). Error bars represent standard error. Spawning date 1 indicates November 2 and spawning date 30 indicates February 26 (four-day intervals).....</p>	68
<p>Fig. 3.7. Mean number of successful settlers by spawning date for Pacific halibut in good years (above multi-year mean; please see Fig. 3.3) and in bad years (below multi-year mean; please see Fig. 3). Error bars represent standard error. Spawning date 1 indicates November 2 and spawning date 30 indicates February 26 (four-day intervals).....</p>	69
<p>Fig. 4.1. Sampling locations of otoliths for arrowtooth flounder (≤ 170 mm total length; 2004-2006, 2008-2011; upper panel) and Greenland halibut (≤ 170 mm total length; 2000-2003, 2007-2011; bottom panel), collected during summer bottom trawl groundfish surveys in the eastern Bering Sea.....</p>	91
<p>Fig. 4.2. Right otolith pictures for (A) arrowtooth flounder and (B) Greenland halibut juveniles from summer bottom trawl groundfish surveys in the eastern Bering Sea. In (A), dashed lines and intervals indicate otolith and kernel widths, while solid lines and intervals indicate otolith and kernel lengths. Similar structural metrics were used in Greenland halibut otoliths.....</p>	92
<p>Fig. 4.3. Relationships between otolith length (mm) and body length (mm) and between kernel length (mm) and body length (mm) for Greenland halibut larvae and juveniles in 2009-2011....</p>	93
<p>Fig. 4.4. Relationships between body length (mm total length) and otolith length (mm) of arrowtooth flounder (≤ 170 mm total length) in 2004-2006 and 2008-2011 from summer bottom trawl groundfish surveys in the eastern Bering Sea. Red dots indicate kernel length on otoliths of arrowtooth flounder.....</p>	94
<p>Fig. 4.5. The relationships between body length (mm total length) and otolith width (mm) of Greenland halibut (≤ 170 mm total length) in 2000-2003 and 2007-2011 from summer bottom trawl groundfish surveys in the eastern Bering Sea. Blue dots indicate kernel width on otoliths of Greenland halibut.....</p>	95
<p>Fig. 4.6. Box plots for the estimated body length at settlement (mm total length) based on relationships between body length and otolith length for arrowtooth flounder (upper panel; 2004-2006 and 2008-2011) and between body length and otolith width for Greenland halibut (bottom panel; 2000-2003, 2007-2011) in the eastern Bering Sea.....</p>	96

LIST OF FIGURES (Continued)

<u>Figure</u>	<u>Page</u>
Fig. 4.7. Rate of change of local age-0 arrowtooth flounder (≤ 100 mm total length) abundance in relation to unit changes of bottom temperature from the best-fitted variable coefficient generalized additive model.....	97
Fig. 4.8. Rate of change of local age-1 arrowtooth flounder (110 mm – 160 mm total length) abundance in relation to unit changes of bottom temperature. The shaded regions indicate the average distribution of age-1 arrowtooth flounder abundance estimated from the best-fitted variable coefficient generalized additive model. Light and dark shading show areas of high and low abundance, respectively. Bubbles indicate the rate of ATF change for a unit change of water temperature (blue = negative, red = positive).....	98
Fig. 4.9. Rate of change of local age-0 Greenland halibut (≤ 120 mm total length) abundance in relation to unit changes of bottom temperature. The shaded regions indicate the average distribution of age-0 Greenland halibut abundance estimated from the best-fitted variable coefficient generalized additive model. Light and dark shading show areas of high and low abundance, respectively. Bubbles indicate the rate of GH change for a unit change of water temperature (blue = negative).....	99
Fig. 4.10. Rate of change of local age-1 Greenland halibut (130 mm – 180 mm total length) abundance in relation to unit changes of bottom temperature. The shaded regions indicate the average distribution of age-1 Greenland halibut abundance estimated from the best-fitted variable coefficient generalized additive model. Light and dark shading show areas of high and low abundance, respectively. Bubbles indicate the rate of GH change for a unit change of water temperature (blue = negative, red = positive).....	100
Fig. 5.1. Schematic representations of Greenland halibut settlement, size at settlement, and habitat availability in cold years (a) and warm years (b) in the eastern Bering Sea. Blue arrows represent the strength of along-shelf transport. The size of settling individuals is representative of their observed size at settlement (i.e., smaller in (a) and larger in (b)). Circles indicate known settlement areas for age-0 Greenland halibut (dashed with blue color).....	106
Fig. 5.2. Schematic representations of Pacific halibut settlement, size at settlement, and habitat availability in cold years (a) and warm years (b) in the eastern Bering Sea. Blue arrows represent the strength of along-shelf transport. The size of settling individuals is representative of their observed size at settlement (i.e., larger in (a) and smaller in (b)). Circles indicate known settlement areas for age-0/age-1 Pacific halibut (dotted with green color).....	107

LIST OF TABLES

<u>Table</u>	<u>Page</u>
Table 2.1. Cruise information for Pacific halibut (PH) and Greenland halibut (GH) larvae from the Alaska Fisheries Science Center’s EcoFOCI Program Ichthyoplankton database. *Bongo (BON), Multiple Opening/Closing Net and Environmental Sensing System (MOCNESS), Tucker trawl (TUCK), modified beam trawl (MBT), and Methot trawl (METH).....	23
Table 2.1. Continued.....	24
Table 2.1. Continued.....	25
Table 2.2. Data collected for Pacific halibut (PH) and Greenland halibut (GH) juveniles (≤ 90 mm total length) from the Alaska Fisheries Science Center’s Groundfish survey (1) and juveniles flatfish survey (2) database.....	26
Table 2.3. Range, mean, and standard deviation (SD) of Pacific halibut standard length (mm) and catch per unit effort (CPUE; number of individuals per 10 m ²) over geographic area from preflexion to postflexion larvae. *Bongo (BON), Multiple Opening/Closing Net and Environmental Sensing System (MOCNESS), Tucker trawl (TUCK), modified beam trawl (MBT), and Methot trawl (METH).....	27
Table 2.3. Continued.....	28
Table 2.4. Model selection results of Generalized Additive Models for Pacific halibut larval standard length (mm) from 1979 to 2012 in the eastern Bering Sea. Estimated degrees of freedom are shown for independent variables with nonparametric terms. Asterisks denote significance at the following alpha levels: *0.1, **0.005, and ***0.001. GCV stands for generalized cross validation score and AIC stands for akaike information criterion. Bottom depth is log-transformed.....	29
Table 2.5. Range, mean, and standard deviation (SD) of Greenland halibut standard length (mm) and catch per unit effort (CPUE; number of individuals per 10 m ²) over geographic area from preflexion to postflexion larvae. *Bongo (BON), Multiple Opening/Closing Net and Environmental Sensing System (MOCNESS), modified beam trawl (MBT), and Methot trawl (METH).....	30
Table 3.1. Dispersal pathway simulation parameters for Greenland halibut and Pacific halibut eggs to newly-settled juveniles used in the Dispersal Model for Early Life Stages (DisMELS). Transformation larvae are competent to settle after 15 days.....	59

LIST OF TABLES (Continued)

<u>Table</u>	<u>Page</u>
Table 3.2. Results of the effect of sampling location on Greenland halibut (≤ 100 mm total length, TL) and Pacific halibut (≤ 150 mm TL) presence/absence from the binomial generalized additive model (GAM).....	60
Table 3.3. Correlations between successful settlement for Greenland halibut and Pacific halibut and annual along-shelf and cross-shelf transport indices (Vestfals et al. 2014) in the eastern Bering Sea (*= p-value ≤ 0.1 , **= p-value ≤ 0.05 , ***= p-value ≤ 0.01 , ****= p-value ≤ 0.001). F-M: February-March and A-M: April-May.....	61
Table 3.4. Results from sensitivity analyses testing changes in Greenland halibut and Pacific halibut settlement success in relation to changes in pelagic larval duration length (25% increase or 25% decrease) for dispersal pathway simulations from 1996/1997 to 1999/2000.....	62
Table 4.1. Number of useful otolith samples for Greenland halibut pelagic larvae (< 80 mm standard length) and settled juvenile arrowtooth flounder and Greenland halibut (≤ 170 mm total length) in the eastern Bering Sea.....	87
Table 4.2. Correlations between size at settlement for arrowtooth flounder and Greenland halibut and environmental variables in the eastern Bering Sea (*= p-value ≤ 0.1 , **= p-value ≤ 0.05 , ***= p-value ≤ 0.01 , ****= p-value ≤ 0.001).....	88
Table 4.3. Model selection results of variable coefficient generalized additive models for age-0 arrowtooth flounder (≤ 100 mm total length) abundance/CPUE between 1992 and 2012 and age-0 Greenland halibut (≤ 120 mm total length) abundance between 1982 and 2012 from summer groundfish surveys in the eastern Bering Sea. GCV stands for generalized cross validation score and AIC stands for akaike information criterion. (*= p-value ≤ 0.1 , **= p-value ≤ 0.05 , ***= p-value ≤ 0.01 , ****= p-value ≤ 0.001).....	89
Table 4.4. Results of variable coefficient generalized additive models for age-1 arrowtooth flounder (110 mm – 160 mm total length) abundance between 1992 and 2012 and age-1 Greenland halibut (130 mm -180 mm total length) abundance between 1982 and 2012 from summer groundfish surveys in the eastern Bering Sea. GCV stands for generalized cross validation score and AIC stands for akaike information criterion. BT stands for bottom temperature in present survey year and BT1 stands for bottom temperature of age-0 habitat in previous survey year. (*= p-value ≤ 0.1 , **= p-value ≤ 0.05 , ***= p-value ≤ 0.01 , ****= p-value ≤ 0.001).....	90

LIST OF APPENDICES

<u>Appendix</u>	<u>Page</u>
Appendix 3.1. The relationship between observed percentage of presence stations (red line), percentage of absence stations (blue line), and percentage of presence stations minus percentage of absence stations and predicted probability of occurrence for Greenland halibut (left panel) and Pacific halibut (right panel).....	120
Appendix 3.2. Mean number of successful settlers by spawning date in 75 th percentile years and in 25 th percentile years for Greenland halibut (upper panels) and Pacific halibut (bottom panels). Error bars represent standard error. Spawning date 1 indicates November 2 and spawning date 30 indicates February 26 (four-day intervals).....	121
Appendix 3.3. Mean number of successful settlers by spawning location over the simulated years for Greenland halibut (left panel) and Pacific halibut (right panel). Error bars represent standard error.....	122
Appendix 3.4. Time series of standardized average annual transport in the Bering Slope Current between Feb. 1 st and March 31 st (upper panel) and between April 1 st – May 31 st (bottom panel) and standardized annual Greenland halibut settlement. Transport has been standardized to transect length (Sv/km) to facilitate comparison between transects. Positive values represent northwestward transport; negative values represent southeastward transport.....	123
Appendix 3.5. Time series of standardized average annual transport in the Bering Slope Current between Feb. 1 st and March 31 st (upper panel) and between April 1 st – May 31 st (bottom panel) and standardized annual Pacific halibut settlement. Transport has been standardized to transect length (Sv/km) to facilitate comparison between transects. Positive values represent northwestward transport; negative values represent southeastward transport.....	124
Appendix 4.1. Mean value for environmental variables including along-shelf/on-shelf winds, ICI, and bottom temperature in the eastern Bering Sea.....	125
Appendix 4.2. Correlations between environmental variables in the eastern Bering Sea using the Pearson’s product-moment correlation (*’= p-value ≤ 0.1, **’= p-value ≤ 0.05, ***’= p-value ≤ 0.01, ****’= p-value ≤ 0.001).....	126
Appendix 4.3. Results of variable coefficient generalized additive models for age-1 arrowtooth flounder (110 mm – 160 mm total length) between 1992 and 2012 from summer groundfish surveys in the eastern Bering Sea. Mean bottom temperature experienced during age-1 ATF habitat was used as the only factor in the model (*’= p-value ≤ 0.1, **’= p-value ≤ 0.05, ***’= p-value ≤ 0.01, ****’= p-value ≤ 0.001).....	127

LIST OF APPENDICES (Continued)

<u>Appendix</u>	<u>Page</u>
Appendix 4.4. Results of variable coefficient generalized additive models for age-1 Greenland halibut (130 mm -180 mm total length) between 1982 and 2012 from summer groundfish surveys in the eastern Bering Sea. GCV stands for generalized cross validation score and AIC stands for akaike information criterion. Mean bottom temperature experienced during age-1 GH habitat was used as the only factor in the model (*'= p-value \leq 0.1, '**'= p-value \leq 0.05, '***'= p-value \leq 0.01, '****'= p-value \leq 0.001).....	128

Distribution, Abundance, and Settlement of Slope-spawning Flatfish during Early Life Stages in the Eastern Bering Sea

Chapter 1. Introduction

Most marine fish utilize different geographical areas for nursery, feeding, and spawning throughout ontogeny. Thus, achievement of spatial life-cycle closure of marine fish is critical for their survival, as highlighted in the Harden Jones's triangle of migration (Harden Jones 1968). Based on the triangle of migration, offspring have to depend on currents to reach appropriate nursery areas during early life stages (eggs and larvae). Then offspring have to return to the natal spawning area for reproduction. Especially during dispersal from spawning to nursery locations, larvae are subject to high mortality due to aberrant currents (Hjort 1914, Iles and Sinclair 1982, Houde 2008). Hjort (1914) emphasized that year-class strength of marine fish is determined during larval stage due to both starvations after yolk absorption ("critical period hypothesis") and loss by aberrant currents ("aberrant drift hypothesis"). Iles and Sinclair (1982) extended Hjort's second idea and developed the "Members/Vagrant hypothesis" that highlighted the importance of circulation features for larval retention in appropriate nursery.

Direct influences of physical circulation features on early life survival are particularly important in flatfish, which are typically subject to long developmental phases and dispersal to bridge the distance from spawning to nursery locations. (Bailey *et al.* 2005, Nash and Geffen 2012, Duffy-Anderson *et al.* 2014). Several studies have shown that changes in the prevailing ocean currents can influence dispersal pathways during the early life history stages of marine fish – a process which is known to play an important role in determining variations in flatfish recruitment (Rijnsdorp *et al.* 1992, Van der Veer *et al.* 1998, Wilderbuer *et al.* 2002, Bailey *et al.* 2005, Bailey *et al.* 2008, Bolle *et al.* 2009, Hufnagel *et al.* 2013, Petitgas *et al.* 2013). Deepwater and slope-spawning flatfish species may be particularly vulnerable to changes in ocean circulation because of their relatively long pelagic larval durations (PLD), which provide a protracted opportunity for unfavorable or interrupted transport. During the settlement and post settlement phase, mortality can also be high due to abiotic (e.g., bottom temperature) and biotic (e.g., predation, food availability) factors (Bailey 1994; Rijnsdorp *et al.* 1992; Leggett and Frank 1997; Van der Veer *et al.* 2000; Gibson *et al.* 2002). For example, during the settlement phase, slower growing and smaller individuals in relatively cold water can suffer high mortality due to

size-selective predation and size-selective feeding success (Houde 1989; Ellis and Gibson 1995; Van der Veer *et al.* 1997; Gibson *et al.* 2002).

In the eastern Bering Sea (EBS), arrowtooth flounder (ATF; *Atheresthes stomias*), Greenland halibut (GH; *Reinhardtius hippoglossoides*), and Pacific halibut (PH; *Hippoglossus stenolepis*) are ecologically and commercially (the last two species) important slope-spawning flatfish species. ATF, GH, and PH share several life history attributes, but they exhibit different population biomass trajectories; ATF and PH have increased over the past 3 decades, while GH has declined. The three species spawn eggs in batches in deep water (> 400 m) along the continental slope during winter months. They have relatively long pelagic durations from eggs to newly settled juveniles and must cross from the slope (spawning locations) to shelf areas (settlement locations) for settlement. There are also species-specific differences in spawning depth and ontogenetic changes in vertical distribution as well as pelagic durations and the timing of on-shelf movement and settlement. These species-specific differences could result in different population dynamics under similar conditions of environmental forcing. However, little is known about the distribution, dispersal, and settlement of ATF, GH, and PH in early life stages and the influence of physical factors on them; most studies have focused on the ecology of adult population dynamics for the purpose of stock assessment and management in the EBS.

Interannual variations in wind, sea-ice coverage, temperature, and currents in the EBS alter the distribution, dispersal pathways, trophic interaction, and recruitment of marine fish populations (Overland *et al.* 1999, Overland *et al.* 2002, Wilderbuer *et al.* 2002, Schumacher *et al.* 2003, Bond and Overland 2005, Mueter and Litzow 2008, Spencer 2008, Hunt *et al.* 2011, Stabeno *et al.* 2012, Ladd 2014). Wilderbuer *et al.* (2002), using a modeling approach, found that broad-scale shifts in climatological forcing (e.g., Aleutian Low) and associated changes in oceanographic processes affect the dispersal and recruitment of flatfish, including flathead sole, northern rock sole, and ATF in the EBS. Stabeno *et al.* (2012) showed that interannual variability in the spatial extent of sea ice during spring and also prolonged warm periods with low ice extent (2001-2005) were recorded prior to cold periods with extensive sea ice (2007-2010) (Stabeno *et al.* 2012). The extent, timing, and persistence of sea ice also influence the extent and retreat of the near-bottom cold pool (< 2 degree Celsius) in the middle shelf of the EBS. Spencer (2008) revealed that ATF avoid the cold pool, while GH prefer to stay in the cold pool. Ladd (2014),

using altimetry data, found that strong interannual variability in the speed of the Bering Slope Current is correlated with the North Pacific Index (NPI) and Multivariate ENSO Index (MEI). The speed of the Bering Slope current increases with negative NPI (strong Aleutian Low), and is also high in El Niño years.

In the presence of large physical variability in the Bering Sea and critical knowledge gaps about distribution, abundance, settlement, and size at settlement during flatfish early life stages in relation to variations in environmental variables, I focused my dissertation on the study of slope-spawning flatfish early life stages from eggs to juveniles (age-1) (Fig. 1.1). My study provides valuable insights into physical factors affecting ATF, GH, and PH distribution, abundance, settlement, size at settlement, and nursery habitat availability in the EBS (Fig. 1.1). In chapter 2, I characterize the horizontal and vertical distributions of abundance and body-size of PH larvae in the EBS and described nursery habitats for PH juveniles. Furthermore, I compare the larval distributions of GH and PH larvae. In chapter 3, I hypothesize that interannual variability in currents encountered by early life history stages may differentially affect GH and PH settlement success. To test the hypothesis, I develop a bio-physical model using early life parameters discovered in chapter 2, to simulate dispersal from eggs to newly settled juveniles for GH and PH. I also identify settlement locations for GH and PH in the EBS using historical observation data. In chapter 4, using otolith analysis, I estimate size at settlement for ATF and GH over the examined years and linked them to environmental variables, particularly physical factors affecting dispersal trajectories and duration. I also examine how bottom temperature affected settlement habitats of ATF and GH. Individual chapters do not address all three flatfish species, as data on one or more species are lacking on some aspects investigated. For example, eggs of GH and PH are not visually distinguishable due to overlapping sizes and similar morphology, thus egg data were not included in chapter 2. ATF and Kamchatka flounder (*Atheresthes evermanni*) are not easily distinguishable during their larval stages due to similar morphology, therefore, ATF were not examined as GH and PH in chapter 2. Likewise, in chapter 4, I could not examine size at settlement of PH because otolith samples for settled PH juveniles are not available.

The findings of these investigations will provide important ATF, GH, and PH life history information for fisheries scientists and managers, relevant to understanding recruitment

processes. This research improves our understanding of the influence of hydrographic variability associated with climate changes on the distribution, abundance, settlement, size at settlement, and nursery habitat availability of these Bering Sea slope-spawning flatfish species. Although other mechanisms including prey availability and predation could influence variability on their settlement, there is not enough knowledge, data, and research about their major prey items and predators during their early life stages in the Bering Sea to conduct a formal analysis now; they would be interesting topics for future study. While this study focuses on slope-spawning flatfish species in the Bering Sea, the concepts and techniques developed here may be applicable to other marine species with larval dispersal and settlement phases in their life histories.

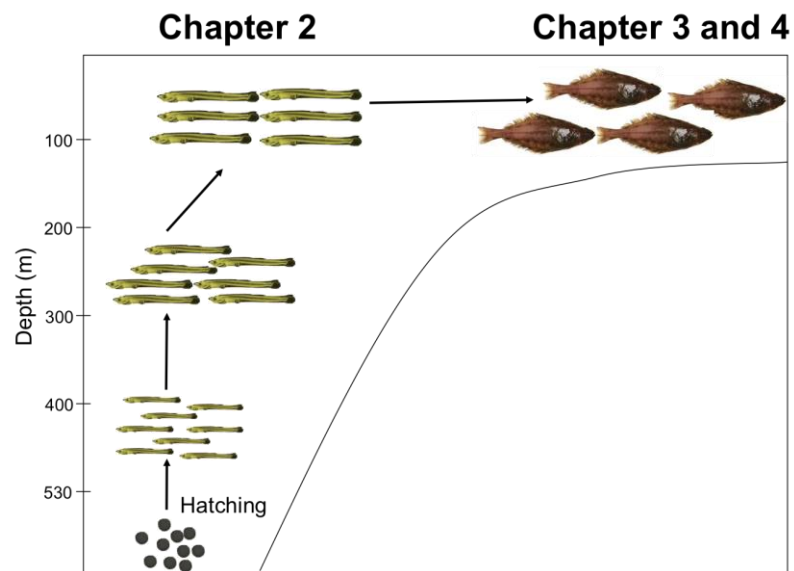
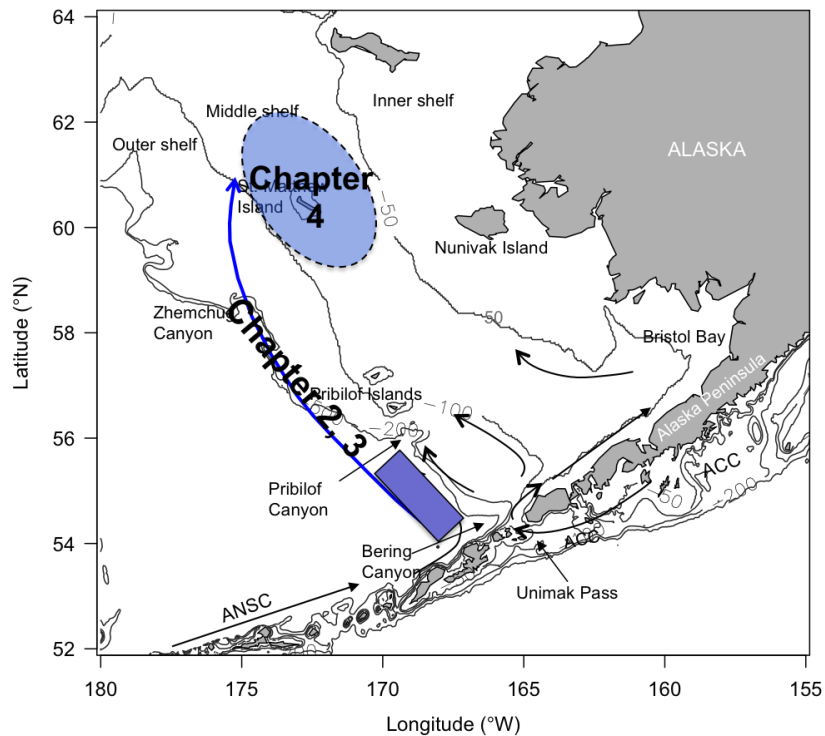


Fig. 1.1. Conceptual plots that link chapter 2 (early life stage attributes), 3 (settlement success), and 4 (size, abundance, and distribution at settlement) of this dissertation. Circle (dash with blue color) represents settlement areas for age-0 Greenland halibut as an example. Rectangle (purple color) indicates potential spawning locations for Greenland halibut and Pacific halibut. Blue arrow represents one of the drift pathways from spawning to settlement locations.

**Chapter 2. Distribution of early life Pacific halibut and comparison with Greenland halibut
in the eastern Bering Sea**

Dongwha Sohn, Lorenzo Ciannelli, Janet T. Duffy-Anderson

Journal of Sea Research
Elsevier Science Bv, Po Box211
Amsterdam, Netherlands
107: 31-42

ABSTRACT

Information about spatial distribution patterns during early life stages of fish is key to understanding dispersal trajectories and connectivity from spawning to nursery areas, as well as adult population dynamics. More than 30 years of historical field data were analyzed in order to describe the horizontal and vertical distributions of Pacific halibut early life stages (larvae to juveniles) in the eastern Bering Sea and to compare the distributions between Pacific halibut and Greenland halibut. Our results indicate that spawning for both species likely occurred in Bering and Pribilof canyons, along the slope between the two canyons, and on the eastern side of the Aleutian Islands during winter, but Pacific halibut spawning was protracted until early spring. Larvae of both species rose to shallower depths in the water column as they developed, but Pacific halibut larvae had an abrupt movement toward shallower depths. Geographically, larvae for both species either advected northwestward along the Bering Sea Slope or crossed onto the shelves from the slope regions, but the timing in Pacific halibut larval progression onto the shelf and along the slope was earlier than for Greenland halibut larvae. Pacific halibut juveniles (≤ 90 mm total length (TL)) were mostly found in the inner shelf between Bristol Bay and Nunivak Island, along the Alaskan Peninsula, and in the vicinity of the Pribilof Islands. The range of Greenland halibut juvenile (≤ 90 mm TL) distribution was expanded to south of the Pribilof Islands in the middle shelf and to the inner shelf. Although the two species share some attributes (i.e., spawning location) during early life stages, there were species-specific differences associated with spatial distribution (vertically and horizontally), timing differences in larval progression onto the shelves, pelagic larval duration, and juvenile nursery areas.

INTRODUCTION

Knowledge of the distribution and dispersal trajectories of marine fish during early life is critical for understanding recruitment and adult population dynamics. The early life stages of marine fishes are influenced by interactions between abiotic (i.e., currents, geographical feature, temperature, and dissolved oxygen) and biotic (i.e., food availability, predation, growth, body-length, and behaviors) factors. Changes in prevailing currents induced by variable atmospheric forcing play an important role in variations of dispersal trajectories and recruitment of marine

fish (Van der Veer et al., 1998; Wilderbuer et al., 2002; Bailey et al., 2005; Cowen and Sponaugle, 2009). Currents may transport fish larvae to unsuitable areas resulting in high mortality rates and low recruitment (Houde, 2008). Flatfish may be particularly vulnerable to advective loss due to their long pelagic phases as larvae (Bailey et al., 2005) and their strict benthic habitat requirements as juveniles (Petitgas et al., 2013). It has been shown in several studies that slope-spawning flatfish may be vulnerable to changes in currents during their dispersal phases, when they rely on extensive drift to connect from spawning to settlement areas (Wilderbuer et al., 2002; Bailey et al., 2008; Duffy-Anderson et al., 2013; Vestfals et al., 2014; Duffy-Anderson et al., 2015). Further, variations in connectivity between spawning and nursery habitats influence recruitment in flatfish populations (Hufnagl et al., 2013; Petitgas et al., 2013).

Pacific halibut (*Hippoglossus stenolepis*) and Greenland halibut (*Reinhardtius hippoglossoides*) are two ecologically and commercially important slope-spawning flatfish in the eastern Bering Sea (EBS). Both species are piscivorous and substantial predators - adults feed on abundant juvenile gadid species (e.g., walleye pollock (*Gadus chalcogrammus*), cod (*Gadus macrocephalus*)) and other flatfish species in the EBS (Aydin and Mueter, 2007). The abundances of Pacific halibut and Greenland halibut in the EBS have differentially fluctuated during the last three decades although they share many life history attributes. Pacific halibut had been stable prior to 2000, but over the last decade, biomass has continuously decreased because of poor recruitment and decreasing adult body-size at age (Stewart et al., 2013). Greenland halibut has decreased since late 1970s due to low recruitment and spawning biomass, however, there are signs of improved recruitment after 2006 (Barbeaux et al., 2013).

Distribution, dispersal trajectory, and population dynamics of Greenland halibut and Pacific halibut may be affected differently by changes in environmental conditions (e.g., changes in water temperature and currents) due to species-specific differences (i.e., vertical distribution, pelagic duration, and settlement location) during the early life stages. Greenland halibut is a circumpolar species while Pacific halibut is a subarctic species and comparing the two species may provide insight on how environmental variability affects the two species with contrasting ecological niches. The EBS has exhibited a prolonged cold period (2007–2012) after a prolonged warm period (2001–2005) with respect to variations in the timing of sea ice retreat and water temperature (Stabeno et al., 2012). The habitat occupied by Greenland halibut juveniles and

adults has expanded to the south in the middle shelf with a series of cold periods in the EBS (Ianelli et al., 2011). Previous studies showed that differences in advective connectivity in flatfish are influenced by depth-discrete currents (Lanksbury et al., 2007; Duffy-Anderson et al., 2013). Therefore, it is important to understand the spatial distribution (vertically and horizontally), dispersal trajectories, and connectivity between spawning and nursery areas for the two species of halibut in order to understand their diverging population dynamics.

Little is known about Pacific halibut early life history in the EBS. From studies in the Gulf of Alaska (GOA) it is known that Pacific halibut spawn in relatively deep water (<400 m) along the continental slope during the winter, from December to March. Pacific halibut eggs have been found at depths between 100 and 400 m water, and newly hatched larvae below 425 m, along the continental slope (Thompson and Van Cleve, 1936; Skud, 1977). Pacific halibut hatching time was 20 days at 5 °C (Forrester and Alderdice, 1973). Larvae were reported to move to shallower depths as they developed, and 3 to 5 months after hatching were found at 100 m or shallower. The larvae are advected by currents from offshore to inshore and settle in shallow nursery habitat in May and June, 6 to 7 months after spawning (Skud, 1977; Norcross et al., 1997). In the EBS, Best (1981) mentioned that Pacific halibut spawn at depths between 250 and 550 m along the continental edge from Unimak Island and the Pribilof Islands and along the Aleutian Islands between December and January based on an International Pacific Halibut Commission (IPHC) cruise data. St-Pierre (1989), using 1985 and 1986 field survey data, reported that Pacific halibut postflexion larvae (16 – 25 mm) were found in Unimak Pass, along the eastern side of the Aleutian Islands, and along Unimak Island. Best (1974, 1977) and Best and Hardman (1982) showed that settled juveniles (<100 mm) and larger individuals were found in shallower water along the Alaskan Peninsula and in the inner shelf (<50 m isobaths) near Bristol Bay. Recently, Seitz et al. (2011) based on tagging data, found that localized spawning population may exist in the EBS. However, the horizontal and vertical distributions and dispersal trajectories of Pacific halibut larvae in the EBS are yet unknown. These knowledge gaps impede an understanding of whether and how dispersal and circulation differently affect Pacific halibut and Greenland halibut recruitment variability.

In contrast to Pacific halibut, there have been more studies about Greenland halibut ecology and biology during early life stages in the EBS, particularly in recent years. Alton et al.

(1988) reported on the history of harvest and management for Greenland halibut and distribution of adult stages. Swartzman et al. (1992) showed that Greenland halibut adults moved to deeper water as they grew. McConnaughey and Smith (2000) found that the spatial distribution of Greenland halibut (>141 mm fork length (FL)) was related to sediment characteristics – a mixture of mud and fine sand. Distribution and dispersal trajectories of Greenland halibut during the early life stages have been studied based on observational data or/and passive modeling approaches (Sohn et al., 2010; Duffy-Anderson et al., 2013). Greenland halibut spawn along the slope near Bering Canyon and along the eastern Aleutian Islands during winter. Eggs have been found at depths between 200 and 600 m and larvae have been found between surface and 600 m (Sohn, 2009; Duffy-Anderson et al., 2013). After hatching, Greenland halibut larvae slowly move upward in the water column as they develop. Settlement areas are located over the middle shelf in the vicinity of St. Matthew Island (Sohn et al., 2010). Greenland halibut have a long pelagic larval duration of over six months from spawning to settling areas (Sohn et al., 2010).

The goals of this study are to (1) characterize the distribution and dispersal trajectories for Pacific halibut larvae by ontogenetic stage, (2) describe age-0 nursery habitats for Pacific halibut, and (3) compare the larval progression (horizontally and vertically) of Pacific halibut larvae to that of Greenland halibut. Using more than 30 years of historical data (1979 to 2012), I examined the spatial (horizontal and vertical) distributions of larval Pacific halibut (preflexion, flexion, and postflexion) abundance and body length, and then compared these results to a similar set of results for Greenland halibut. I also examined Pacific halibut age-0 distribution using historical field survey data. This study provides important fundamental early life history information about the ecology and biology of two commercial flatfish species in the EBS, especially for Pacific halibut. The comparison between the two species will be useful for studying habitat usages and predator–prey interactions, as well as conducting biophysical modeling, and climate impact projects for the two species and also other flatfish in the EBS.

MATERIALS AND METHODS

Study area

The EBS includes both the basin and the continental shelf that support one of the highly productive marine ecosystems from phytoplankton to mammals (Fig. 2.1). The shelf can be

divided into three domains based on bathymetry: the inner shelf (<50 m isobaths), the middle shelf (50 m–100 m isobaths), and the outer shelf (100 m–200 m isobaths) (Fig. 2.1; Coachman, 1986). There are two dominant currents; the Aleutian North Slope Current (ANSC), flowing eastward along the Aleutian Islands, and the Bering Slope Current (BSC), flowing northwestward along the Bering Slope of the EBS (Fig. 2.1; Stabeno et al., 1999). In addition, part of the Alaska Coastal Current (ACC) flows from the GOA into the EBS through Unimak Pass and flows eastward parallel to the 50 m isobath along the Alaska Peninsula (Fig. 2.1; Stabeno et al., 2002). A portion of the ACC continues westward and enters into the Bering Sea through other passes including Samalga, and some of the Aleutian Stream flows through Amukta and Amchitka Passes along the Aleutian Islands (Stabeno et al., 1999; Ladd et al., 2005; Stabeno and Hristova, 2014). Submarine canyons, including Bering, Pribilof, and Zhemchug Canyons, are located on the continental margin edge along the Bering Slope and serve as spawning grounds for skates (Rajidae), Pacific halibut, Greenland halibut (Fig. 2.1; St-Pierre, 1984; Seitz et al., 2007; Hoff, 2010; Sohn et al., 2010; Duffy-Anderson et al., 2013) and nursery grounds for Pacific Ocean perch (*Sebastes alutus*) and skates (Brodeur, 2001; Hoff, 2008), as well as conduits for slope-shelf exchanges of nutrients and larvae (Stabeno et al., 1999; Mizobata et al., 2006).

Data sources

To characterize the horizontal and vertical distributions of Pacific halibut larvae and to compare the horizontal and vertical distributions between Pacific halibut and Greenland halibut larvae in the EBS, I obtained historical Pacific halibut larval abundance and body-length data including sampling date, sampling location (latitude and longitude), and bottom depth at each sampling location between 1979 and 2012 from the ichthyoplankton survey database (EcoDAAT) at the National Oceanic and Atmospheric Administration (NOAA)'s Alaska Fisheries Science Center (AFSC; Table 2.1). During the surveys, Pacific halibut larvae were collected by various gear types including 60 cm bongo (BON), 1 m² Tucker trawl (TUCK), modified beam trawl (MBT; used in midwater towing), 5 m² frame Methot trawl (METH; Methot 1986), and 1 m² Multiple Opening/Closing Net and Environmental Sensing System (MOCNESS; Wiebe et al., 1976). The gears including BON, MOCNESS, and TUCK were

equipped with 333 or 505 μm mesh size nettings. Both MBT and METH were equipped with 3 mm mesh size nettings. Tows were conducted from the surface to various depths in the shelf and slope/basin mostly tows were to 10 m off bottom in the shelf and to about 200 or 500 m in the slope and basin. All tows were oblique. All sampling gears were fitted with flow meters to estimate the volume of water filtered. Ichthyoplankton samples were preserved in buffered 5% formalin and were sorted at the Plankton Sorting and Identification Center in Szczecin, Poland. All larvae were measured to the nearest 1.0 mm standard length (SL). Larval identifications were verified at the AFSC in Seattle, Washington, USA. More detailed sampling protocols can be found in Matarese et al. (2003).

To describe nursery habitats for Greenland halibut and Pacific halibut juveniles in the EBS, I utilized abundance and body-length data for juvenile stages (≤ 90 mm total length (TL)) and associated environmental data at each sampling station. Most of the historical catch data were acquired from the AFSC's EBS summer bottom trawl groundfish surveys which were conducted by the Groundfish Assessment Program (hereafter: Groundfish Survey) between 1982 and 2011 (Table 2.2). The Groundfish Survey has been conducted annually beginning as early as May and extending as late as October, although most recently, surveys have been conducted during June and July. These surveys provide extensive geographic coverage over the EBS shelf (http://www.afsc.noaa.gov/RACE/groundfish/gfprof_coverage.htm). The Groundfish Survey covered about 376 standard stations within 20×20 nautical mile grids. The gear is 25.3×34.1 m eastern otter trawl with 25.3 m headrope and 34.1 m footrope. The net is attached to paired chains and dandyines, and a net mensuration system is used to measure net height and width while towing. Tows are typically 30 min. in duration. Estimates of net width are used in calculations of area swept. All individual fish that were captured were measured to the nearest mm TL for flatfish or FL for other fish. More specific information about the Groundfish Surveys can be found in Lauth (2011). Other Pacific halibut and Greenland halibut juveniles catch data were also obtained from the AFSC juvenile flatfish surveys that were conducted in September in 2010 and 2012 using a 3.05 m plumb staff beam trawl rigged with 7 mm mesh, a 4 mm cod end liner, and tickler chains (Gunderson and Ellis, 1986). The 2010 survey was primarily conducted at shallow depths (< 50 m depth) between Nunivak Island and Cape Newenham, whereas the 2012 survey was conducted over the inner, middle, and outer shelves between 55° N and 60° N.

Each fish length was recorded to the nearest mm TL. A total of 123 stations were sampled between the two surveys. More specific information about these surveys can be found in Cooper et al. (2014).

Data analyses

The use of data from different gears is necessary in order to capture the larval distribution of Pacific halibut and Greenland halibut throughout their different early life history stages. PH and GH larval catch data from BON, MOCNESS, and TUCK with 333 and 505 μm mesh and MBT and METH with 3 mm mesh were utilized for analysis. The difference between MBT and METH is that the former has a weighted frame instead of having a depressor (Methot, 1986; Duffy-Anderson et al., 2006), therefore larval abundance data from these two gears were combined.

I analyzed the horizontal and vertical distributions of Pacific halibut and Greenland halibut larvae separately by gear to avoid complications due to differences in capture efficiency. Larval abundance was expressed as individuals per 10 m^2 for analysis of horizontal distributions. The larval abundance data of Pacific halibut and Greenland halibut from nets at different MOCNESS sampling depths were integrated to provide a whole-water column estimate when examining horizontal larval distribution. I pooled data over years because larvae for the two species were rarely collected in each ichthyoplankton survey. However, to characterize the dispersal progression throughout the ontogeny, the distribution is shown for different months. Pacific halibut larvae were grouped in development stages based on their body-length: preflexion larvae (6.0 – 13.5 mm SL), flexion larvae (13.6 – 17.8 mm SL), and postflexion larvae (17.9 – 27.9 mm SL) (Thompson and VanCleve, 1936; Matarese et al., 1989). Greenland halibut larvae were also grouped in development stages: preflexion larvae (9.0 – 19.2 mm SL), flexion larvae (19.3 – 21.9 mm SL), and postflexion larvae (22.0 – 44.9 mm SL) (Sohn et al. 2010; Duffy-Anderson et al. 2013). Each stage was analyzed separately.

To characterize Pacific halibut dispersal trajectories and movement across bathymetry throughout early ontogeny, I examined the spatial and temporal progression of body length during the larval stage using a generalized additive model (GAM). The full model was constructed using a Gaussian family with an identity link function using individual larval body-

length at each station as the response variable. Independent variables in the model (prior to variable elimination) were day of year, sampling location (latitude and longitude), and bottom depth. A stepwise backwards selection process was used to determine the best-fit model by minimizing the generalized cross validation (GCV) and Akaike information criterion (AIC). The GCV is a measure of the predicted mean squared error of the fitted model. The AIC is a measure of the relative goodness of fit of a statistical model (likelihood), penalized by the number of parameters. The GAMs were implemented using the *mgcv* library in R (Wood, 2004 and 2006; R Statistical Computing Software, <http://www.r-project.org/>). To consider the possibility of bias due to selectivity in larval body-length in relation to gear type, Welch's t-tests were applied (R Statistical Computing Software, <http://www.r-project.org/>): no significant differences were found in larval size between gear type (BON and MOCNESS) ($t = 1.43$, $df = 38$, and $p\text{-value} = 0.16$) or between mesh sizes (333 and 505 μm) ($t = -0.05$, $df = 29$, and $p\text{-value} = 0.96$). Sample sizes of larval length from other gear types including TUCK, MBT, and METH were insufficient to conduct statistical analysis.

For the analysis of vertical distributions, I utilized Pacific halibut larval data from MOCNESS samplings in 1992 – 1995 and 2005 – 2010 while Greenland halibut larval data were grouped in 1992 – 1994, 2007-2008, and 2010. I analyzed both larval body-length (mm SL) and density (expressed as individuals per 1000 m^3) distributions grouped over the following binned depth strata: 0 – 100 m, 101 – 200 m, 201 – 300 m, 301– 400 m, and 401 – 530 m. The depth bins were grouped to a relatively low resolution because the sampled depth varied over survey years or stations.

To describe settlement locations for both Pacific halibut and Greenland halibut in the EBS, I used juvenile catch data with body-length ≤ 90 mm TL from the Groundfish Survey and the juvenile flatfish survey, which represent age-0. Pacific halibut and Greenland halibut juveniles (≤ 90 mm TL) were not collected in every year from the Groundfish Survey (Table 2.2). In the juvenile flatfish survey, Greenland halibut juveniles (≤ 90 mm TL) were only found in 2010. Due to low catches of the juvenile Pacific halibut and Greenland halibut in each survey year, it was necessary to pool datasets over the survey years. Abundance of Greenland halibut and Pacific halibut juveniles was calculated as the number of individuals caught per 10,000 m^2 swept.

RESULTS

Horizontal distribution of Pacific halibut and Greenland halibut larvae

Pacific halibut preflexion larvae ($n = 210$) were collected during spring (February – May) from BON ($n = 155$), MOCNESS ($n = 48$), and TUCK ($n = 7$) samplings (Table 2.3). Smaller preflexion larvae (< 8.3 mm SL) were found in February, March, and May (Table 2.3). Spatially, preflexion larvae were mostly found in the continental slope regions along the Bering Sea slope between Bering and the Pribilof Canyons and along the eastern end of the Aleutian Islands (Fig. 2.2. (a)). A few preflexion larvae were found in the middle shelf between 50 m and 100 isobaths along Unimak Island and near St. Paul Island (Fig. 2.2. (a)). Pacific halibut flexion larvae ($n = 349$) were caught between February and July from BON ($n = 309$), MOCNESS ($n = 36$), TUCK ($n = 3$), and METH ($n = 1$) samplings (Table 2.3). Pacific halibut flexion larvae were mainly observed in three areas; the same area where the majority of preflexion larvae were found, the outer shelf (100 m - 200 m isobaths), and at shallower depths (< 50 m isobath) along the Alaskan Peninsula (Fig. 2.2. (b)). Flexion larvae were also found north of the Pribilof Islands near Zhemchug Canyon (Fig. 2.2. (b)). Pacific halibut postflexion larvae ($n = 94$) were captured between February and August from BON ($n = 60$), MBT/METH ($n = 16$), MOCNESS ($n = 15$), and TUCK ($n = 3$) samplings (Table 2.3). Postflexion larvae were mostly observed in the outer and middle shelves along the Unimak Island and around the Pribilof Islands (Fig. 2.2. (c)). Some postflexion larvae still remained in the slope edge along the eastern side of the Aleutian Islands and along the Bering Sea Slope between Pribilof and Zhemchug Canyons (Fig. 2.2. (c)). The best-fitted GAM (Model 3 in Table 2.4) explained 74.8% of the deviance in observed larval body-length (Table 2.4). Sampling location and day of year had significant effects on larval body-length (Table 2.4). Results of the GAM analysis showed that Pacific halibut larvae progress from the slope to the shelves through Bering Canyon and along the slope to northwest as they grow (Fig. 2.3 (a)). Some preflexion larvae were predicted along the central side of the Aleutian Islands (Fig. 2.3 (a)). Other preflexion larvae were predicted to occur along the slope between 55° N and 59° N (Fig. 2.3 (a)). Also, a preflexion larva was predicted to occur in the middle shelf around the Pribilof Islands between 57° N and 58° N (Fig. 2.3 (a)). Pacific halibut larval body-length increased over time (Fig. 2.3 (b)), at about 0.08 mm d^{-1} .

Greenland halibut preflexion larvae (n = 537) were also caught during spring (February – May) from BON (n = 441) and MOCNESS (n = 96) samplings (Table 2.5). Smaller preflexion larvae (< 10.1 mm SL) were found between February and April (Table 2.5). Greenland halibut flexion larvae (n = 182) were collected between April and May from BON (n = 167) and MOCNESS (n = 15) samplings (Table 2.5). Greenland halibut postflexion larvae (n = 268) were captured between April and August from BON (n = 57), MBT/METH (n = 205), and MOCNESS (n = 6) samplings (Table 2.5).

Larvae of both Greenland halibut and Pacific halibut were mainly found along the Bering Sea slope between 53 ° and the 60 ° N and along the eastern side of the Aleutian Islands between February and April (Fig. 2.4). Larvae of the two species were also observed in the outer shelf between May and July (Fig. 2.4). However, Pacific halibut larvae were found in the middle shelf near Unimak Island in April and in the middle shelf and shallower areas (< 50 m isobaths) along the Alaskan Peninsula in May and June (Fig. 2.4 (b)), but Greenland halibut were not. Pacific halibut larvae were also found through Unimak Pass (Fig. 2.4 (b)). A small number of Greenland halibut larvae were found in the north of St. Matthew Island, while Pacific halibut were observed south of St. Matthew Island (Fig. 2.4 (a) and (b)). The smallest body-length class for both species (< 10 mm SL) was found along the Bering Sea slope near Bering Canyon. As they develop, larval distribution of Greenland halibut and Pacific halibut spreads northward along the slope and eastward over the shelf. A few Pacific halibut larvae (20.1 – 27.0 mm SL) were found on the shelf while many Greenland halibut larvae were found along the shelf-break and in the middle shelf near the Pribilof Islands. No Pacific halibut larvae (27.1 – 63.0 mm SL) were found in the water column in the outer and the middle shelves, while Greenland halibut larvae (27.1 – 63.0 mm SL) were still observed in this area.

Vertical distribution of Pacific halibut and Greenland halibut larvae

Vertically, both species rose to shallower depths in the water column as they developed - larger larvae were found at shallower depths while smaller larvae were found deeper (Fig. 2.5). However, the vertical distribution of Pacific halibut larvae was bi-modal with peaks 0 – 100 m and 301 – 530 m depth while Greenland halibut larvae were found throughout the water column from the surface to 530 m depth (Fig. 2.5). Pacific halibut preflexion larvae, which were < 13.6

mm SL, were found between 301 m and 530 m while both flexion and postflexion larvae that were between 14 and 20 mm SL were observed above 100 m depth.

Distribution of Pacific halibut and Greenland halibut settled juveniles

Pacific halibut juveniles (≤ 90 mm TL) were found over the shelf, especially in the inner shelf between Bristol Bay and Nunivak Island, along the west side of the Alaskan Peninsula, and in the vicinity of the Pribilof Islands (Fig. 2.6 (a) and (b)). The smallest Pacific halibut settled juvenile found in the juvenile flatfish survey was 33.7 mm TL and was found in shallow water (<50 m depth) along the eastern side of the Alaska Peninsula ((Fig. 2.6 (b)). The smallest settled juvenile collected from the Groundfish Survey was 40 mm TL and it was also found in the inner shelf (<50 m depth) near Bristol Bay ((Fig. 2.6 (b)). Greenland halibut (≤ 90 mm TL) were mostly found in the middle shelf around St. Matthew Island and between 57° and 59° N in the inner shelf (Fig. 2.6 (c) and (d)). A few Greenland halibut juveniles were observed above 60° N and south close to Unimak Island of the outer shelf (Fig. 2.6 (c) and (d)). The smallest Greenland halibut settled juvenile was 60 mm TL from the Groundfish Survey and 69 mm TL from the juvenile flatfish survey.

DISCUSSION

Given the distribution of Pacific halibut larvae from the analysis of the preflexion size data, it is likely that spawning occurs in both Bering and Pribilof Canyons, along the continental slope between Bering and Pribilof Canyons, and along the eastern side of the Aleutian Islands during winter and early spring in the EBS. This result is consistent with previous studies about spawning location in the EBS (Best, 1981; St-Pierre, 1984). Forrester and Alderdice (1973) reported that Pacific halibut hatching time was about 20 days at 5°C and 14 days at 7°C and that larval body-length at hatching ranged from 6.15 mm to 7.79 mm TL at 5°C and from 5.33 mm and 7.62 mm TL at 7°C . Furthermore, Liu et al. (1994) reported that time to hatching for Pacific halibut was about 14 days at 6.5°C and newly-hatched larval body-length ranged from 6.0 mm to 6.6 mm TL. Our GAM results showed that Pacific halibut body-length between preflexion and postflexion larvae increased at about 0.08 mm d^{-1} . This is likely an

underestimation of actual growth due to the continuous influx of newly hatched individuals. Liu et al. (1993) reported that the average daily body-length increment during 20 days after hatching was 0.17 mm at 8 °C. Considering Pacific halibut hatching time, larval body-length at hatching (Forrester and Alderdice, 1973; Liu et al., 1994) and larval body-length daily increment from our results, small larvae that were found in February, March, and May could have been spawned in January, February, and April, respectively. These results are in agreement with earlier studies which show spawning occurs from November through March in the EBS (Best, 1981; St-Pierre, 1984). Also, our results indicate that Pacific halibut have a protracted spawning window during winter and early spring (April) in the EBS.

From depth-discrete MOCNESS sampling, the smallest Pacific halibut larva (7 mm SL) was found between 401 and 530 m. Assuming that eggs slowly rise during embryogenesis, this suggests that Pacific halibut eggs are hatched below 500 m depth. However, the actual spawning depth of Pacific halibut in the EBS is still unknown because Pacific halibut and Greenland halibut eggs cannot presently be differentiated by morphological traits alone. In the GOA, Pacific halibut eggs have been found between 100 and 400 m water depth (consistent with our results), and newly hatched larvae below 425 m, along the continental slope (Thompson and Van Cleve, 1936; Skud, 1977). Based on female spawning behaviors from unpublished Pop-up Archival Transmitting (PAT) tagging study in the EBS, Pacific halibut may release their eggs between 200 and 400 m depth (Andrew Seitz, University of Alaska, personal communication). Egg densities of Pacific halibut that were fertilized and incubated at 33%, increased from 1.025 and then stabilized at 1.026 between about 8 and 13 days after fertilization (Forrester and Alderdice, 1973). It is therefore likely that Pacific halibut eggs are released at relatively shallow depths (around 250 m), then sink due to change in their density. Additionally, vertical distribution of Pacific halibut larvae in the EBS is different than in the GOA. Pacific halibut larvae (< 13 mm SL) in our study were observed between 301 and 530 m in the EBS, but they have been found between 150 and 380 m in the GOA (Bailey and Picquelle, 2002). This discrepancy in vertical depth might result from differences in environmental conditions (i.e., water temperature, salinity, and topographic features) influencing larval growth and distribution.

Interestingly, developmental stages of Pacific halibut co-occurred along the central (west of Samalga Pass and east of Amchitka Pass as defined by Mordy et al., 2005) Aleutian Islands,

indicating the existence of separate spawning groups and the retention of larvae in this region. Previous studies suggested that there could be a separate spawning group in the Aleutian Islands. Nielsen et al. (2010) reported genetic differences between Pacific halibut in the Aleutian Islands and Pacific halibut in the EBS and the GOA. Moreover, Seitz et al. (2011) suggested localized spawning groups in the EBS and the Aleutian Islands regions based on tagging results. Alternatively or in addition to multiple spawning groups in the EBS, it is possible that Pacific halibut larvae enter the Aleutian Islands of the Bering Sea from the GOA through the central passes (i.e., Amukta, Seguam, Tanaga, and Amchitka Passes). Some of the Alaskan Stream flows through the central passes along the Aleutian Islands into the Bering Sea (Stabeno et al., 1999; Ladd et al., 2005; Mordy et al., 2005; Ladd and Stabeno, 2009).

Pacific halibut preflexion larvae were mostly observed over the slope while postflexion larvae were found in the shelf regions, indicating larval advection from the slope to the shelf as they grow. Vertically, Pacific halibut larvae have a bi-modal depth distribution between preflexion and flexion larval stages, indicating an abrupt movement toward shallower depths as they develop. This vertical ontogenetic migration might enhance cross-shelf transport from spawning locations over the slope to nursery areas on the shelves in the EBS. Based on modeling results, BSC transport from April to early September varies with water depth: below 30 m, flow is primarily northward along the slope edge, while above 30 m onshore transport occurs (Regional Oceanographic Modeling System for the northeast Pacific (ROMS NEP version 4); Duffy-Anderson et al., 2013). Slope-shelf exchanges of Pacific halibut larvae in the EBS could be influenced by variability in the BSC. Satellite- tracked drifters, oceanographic models, and field observation data show seasonal and interannual variability in onshore and offshore transports in the EBS (Danielson et al., 2011; Stabeno et al., 2012; Ladd, 2014; Vestfals et al., 2014). Intra-annual variability in the BSC exists; the BSC is close to the slope edge during winter and far from the edge during the rest of year (Ladd, 2014). Interannual shifts in the BSC position are likely due to mesoscale variability, such as eddies or meanders (Ladd, 2014). Vestfals et al. (2014) found that Pacific halibut recruitment increased with increased cross-shelf transport through Bering and Pribilof Canyons, and decreased with increased transport along the Bering Sea slope (Vestfals et al., 2014). Thus, changes in the BSC could influence variations of distribution, dispersal trajectories, and habitat connectivity during Pacific halibut early ontogeny.

Flexion and postflexion Pacific halibut larvae were found in the Unimak Pass indicating some larvae observed in the EBS may have advected from the GOA through the eastern passes (passes east of Samalga Pass as defined by Ladd et al., 2005) including Unimak. This finding is in agreement with previous studies in which Pacific halibut larvae were found near the Unimak Pass and appeared to flow from the GOA to the EBS through the Unimak Pass associated with circulation pattern (Skud, 1977; Best, 1981; St-Pierre, 1989). Satellite-tracked drifter data support Pacific halibut larval connectivity between the EBS and GOA through Unimak Pass (Ladd et al., 2005). Unimak Pass is also known to be important for exchange of nutrients and other organisms (e.g., northern rock sole (*Lepidopsetta polyxystra*)) between the EBS and the GOA (Stabeno et al., 2005; Ladd et al., 2005; Lanksbury et al., 2007; Siddon et al., 2011). Furthermore, Nielsen et al. (2010) found that the genetic structure of Pacific halibut is not different between the GOA and southeast Bering Sea, but is different in the Aleutian Islands. Larvae could also enter the Bering Sea through other eastern passes. The portion of the Aleutian Stream flows through Aleutian passes, especially Amukta Pass and forms the eastward flowing the ANSC (Stabeno et al., 1999). The ACC flows in the EBS through Unimak Pass while a portion of the ACC continuously flows along the Aleutian Islands until Samalga Pass (Ladd et al., 2005; Stabeno and Hristova, 2014).

Based on our analysis of the juvenile data, Pacific halibut utilize specific settlement and nursery habitat for age-0 fish: water < 50 m depth, between Bristol Bay and Nunivak Island, along the Alaska Peninsula, and around the Pribilof Islands in the inner and middle shelves of the EBS. These results are consistent with previous studies (Best, 1974, 1977; Best and Hardman, 1982). Best (1974 and 1977) and Best and Hardman (1982) found juveniles (< 100 mm TL) in shallow depths (< 50 m) along the Alaskan Peninsula, in the inner shelf between Bristol Bay and Nunivak Island, and in the middle shelf of southeastern Bering Sea. The smallest settled juvenile (33.7 mm TL) in our dataset was in the inner shelf along the Alaska Peninsula, suggesting that this body-length is a potential body-size at settlement for Pacific halibut. Best (1977) reported that many age-0 Pacific halibut in the EBS were found in bottom water temperature between 3.5 and 5.5 °C while few halibut were found at 2 °C or less than 2 °C. Thus, climate variability in the EBS can alter the distribution of Pacific halibut juveniles. Recently, the EBS has exhibited a prolonged cold period (2007–2012) after a prolonged warm period (2001–2005; Stabeno et al.,

2012). Settled juvenile Greenland halibut (< 100 mm TL) range has expanded to south of the Pribilof Islands, which is likely due to an increase in the extent of the cold pool (summer bottom temperatures < 2 °C) and associated expansion of their habitat due to expanded winter sea ice coverage during the cold period (Ianelli et al., 2011). The distributions of age-0 and age-1 northern rock sole in the EBS also appears to be influenced by changes in water temperature and flows due to climate change (Cooper et al., 2014). Thus, it is possible that changes in size of suitable nursery habitat for Pacific halibut could be impacted between the warm and cold periods in the EBS, influencing Pacific halibut distribution and recruitment.

Although Greenland halibut and Pacific halibut share several attributes during early life stages, there are species-specific differences in vertical distribution, timing of cross-shelf transport (larval progression in time and space), and settlement locations. Both species spawn along the slope near Bering Canyon during winter, larvae ascend into surface waters after hatching, and are advected from the slope to the shelf for settlement. However, Pacific halibut spawning may be protracted until April. Also, Pacific halibut cross to the shelf earlier than Greenland halibut. Vertically, Pacific halibut have an abrupt vertical ascent through the water column. Furthermore, Pacific halibut settle earlier than Greenland halibut indicating that Pacific halibut pelagic larval duration is comparatively shorter than that of Greenland halibut. Both species occupy specific habitats for settlement. Greenland halibut settle in the middle shelf around St. Matthew Island at water temperatures ~1 °C (Sohn et al., 2010) though their settlement area can be expanded to south when water temperatures decrease (Ianelli et al., 2011). In contrast, Pacific halibut settle farther south in shallower depth (< 50 m) along the Alaskan Peninsula, between Bristol Bay and Nunivak Island, and around the Pribilof Islands. These species-specific differences during early ontogeny in the same environment can cause different distribution and transport characteristics with climate variability in the EBS, which in turn may differently influence their settlement success, recruitment, and population dynamics.

Based on the results of our study, I propose that species-specific differences in early life stages for Pacific halibut and Greenland halibut could result in differences of recruitment success and population dynamics within the same oceanographic system. As a future study, particle-tracking models for Pacific halibut and Greenland halibut during early life stages, combined with outputs from regional ocean modeling systems may help to further elucidate the proposed

hypothesis. In that regard, our results provide baseline data for future modeling work of drift trajectories for the Pacific halibut during early life history stages. Furthermore, our study provides fundamental or updated early life history information about ecology and biology for the two commercial flatfish species in the EBS that would be useful for studying habitat usages, predator–prey interactions, and climate impact projects for other flatfish species in the EBS.

ACKNOWLEDGMENTS

I thank A. Dougherty, M. Busby, J. Napp, M. Hunsicker, K. Sobocinski, M. Hoecker-Martinez, and three anonymous reviewers for reviewing the manuscript and giving insightful comments. I would like to thank to the members of NOAA's Ecosystems and Fisheries Oceanography Coordinated Investigations (EcoFOCI) for collecting and processing of the ichthyoplankton and juvenile samples. I also thank the officers and crew of the NOAA Ships Miller Freeman and Oscar Dyson for ichthyoplankton sampling in the field and crew and scientists who work for the summer bottom trawl groundfish surveys and flatfish juvenile survey in the Bering Sea. This research was supported by the North Pacific Research Board (NPRB), project #619 and #905. This paper is NPRB contribution number 561. This research is contribution EcoFOCI-N833 to NOAA's Ecosystems and Fisheries Oceanography Coordinated Investigations.

Table 2.1. Cruise information for Pacific halibut (PH) and Greenland halibut (GH) larvae from the Alaska Fisheries Science Center's EcoFOCI Program Ichthyoplankton database. *Bongo (BON), Multiple Opening/Closing Net and Environmental Sensing System (MOCNESS), Tucker trawl (TUCK), modified beam trawl (MBT), and Methot trawl (METH)

Year	Cruise	Gear*	Total no. of tows	Positive tows of PH	Positive tows of GH	Sampling duration
1992	2MF92	MOCNESS	8	4	6	4/16 – 4/22
1993	3MF93	MOCNESS	17	7	15	4/17 – 4/28
1994	4MF94	MOCNESS	9	1	7	4/16 – 4/27
1995	7MF95	MOCNESS	6	0	0	5/5 – 5/17
2005	5MF05	MOCNESS	21	3	0	5/10 – 5/17
2006	3MF06	MOCNESS	12	5	0	5/9 – 5/15
2007	4MF07	MOCNESS	3	2	2	5/9 – 5/15
2008	1MF08	MOCNESS	8	4	4	2/19 – 2/26
2009	1KN09	MOCNESS	55	4	1	6/14 – 7/10
2010	1TT10	MOCNESS	90	3	2	7/1 – 7/12
1979	3MF79	BON	126	1	8	6/1 – 7/23
1986	MF862	BON	48	1	1	2/16 – 2/28
1988	1DN88	BON	46	5	0	4/11 – 5/8
	1OC88	BON	61	7	8	3/17 – 4/4
1991	0MF91	BON	20	6	10	3/11 – 3/15
	1MP91	BON	61	1	5	4/14 – 5/8
1992	2MF92	BON	36	11	9	4/16 – 4/18
1993	3MF93	BON	119	33	79	4/15 – 4/30
1994	4MF94	BON	128	34	37	4/15 – 4/30
1995	2MF95	BON	1	1	0	3/8
	6MF95	BON	137	30	15	4/17 – 4/30
	7MF95	BON	134	14	10	5/4 – 5/18
1996	6MF96	BON	5	2	3	5/15

Table 2.1. (Continued)

1997	4WE97	BON	66	1	2	7/1 – 7/13
	5MF97	BON	34	5	3	4/16 – 4/25
	6MF97	BON	32	5	7	5/4 – 5/13
1999	1MF99	BON	37	1	0	4/14 – 4/18
	4MF99	BON	16	3	3	5/15 – 5/20
2002	3MF02	BON	81	14	11	5/13 – 5/21
2003	4MF03	BON	60	5	0	5/18 – 5/24
2004	1KR04	BON	3	2	0	8/10 – 8/22
2005	5MF05	BON	91	17	1	5/10 – 5/20
	6MF05	BON	2	2	0	5/22
	3TT05	BON	42	0	1	5/16 – 5/27
2006	1TT06	BON	92	0	1	4/15 – 5/9
	3MF06	BON	90	10	2	5/9 – 5/18
	4MF06	BON	3	2	0	5/22
2007	1HE07	BON	64	2	2	4/11 – 5/11
	4MF07	BON	101	18	25	5/8 – 5/18
2008	1AR08	BON	14	1	0	6/3 – 6/16
	1MF08	BON	44	23	18	2/18 – 2/26
	3DY08	BON	65	4	1	5/13 – 5/21
2009	1DY09	BON	27	11	5	2/26 – 3/4
	2DY09	BON	12	3	1	4/27 – 5/3
	3DY09	BON	87	7	6	5/9 – 5/18
2010	1AK10	BON	21	1	0	6/6 – 6/26
	2DY10	BON	102	1	8	5/6 – 5/17

Table 2.1. (Continued)

2011	1DY11	BON	37	1	0	5/21 – 5/28
	2AK11	BON	10	1	0	6/25 – 7/11
2012	1DY12	BON	58	10	7	4/29 – 5/9
	2DY12	BON	195	6	6	5/17 – 6/1
1979	3MF79	TUCK	128	2	0	6/2 – 7/23
1986	MF862	TUCK	12	1	0	2/16 – 2/26
1993	3MF93	TUCK	8	6	0	4/16
1995	6MF95	TUCK	13	1	0	4/17 – 5/1
1997	4WE97	TUCK	25	1	0	7/6 – 7/13
1996	1OM96	MBT	34	0	4	7/21 – 7/29
1997	1OM97	MBT	28	0	12	7/21 – 7/29
1998	1OM98	MBT	25	0	1	7/25 – 7/30
1999	1OM99	MBT	20	0	6	7/26 – 8/1
2000	1OM00	MBT	21	0	1	7/28 – 8/1
2001	1OM01	MBT	23	0	6	7/21 – 7/24
2002	1OM02	MBT	26	0	1	8/1 – 8/9
2004	1OM04	MBT	25	0	2	7/28 – 8/4
2005	1OM05	MBT	24	1	1	7/15 – 7/21
1992	1MM92	METH	4	1	0	7/9 – 7/14
1994	7MF94	METH	15	0	4	7/15 – 9/6
1996	9MF96	METH	32	0	2	7/21 – 8/7
1997	4WE97	METH	32	9	22	7/5 – 7/13
	9MF97	METH	13	0	1	9/11 – 9/17
1999	7MF99	METH	38	0	2	9/4 – 9/14

Table 2.2. Data collected for Pacific halibut (PH) and Greenland halibut (GH) juveniles (≤ 90 mm total length) from the Alaska Fisheries Science Center's Groundfish survey (1) and juveniles flatfish survey (2) database.

Survey	Year	Gear	Total no. of tows	Positive tows of PH	Positive tows of GH	Sampling duration
1	1983	Bottom trawl	353	0	1	6/7 – 8/1
	1985	Bottom trawl	358	0	3	6/8 – 10/5
	1986	Bottom trawl	354	0	6	6/3 – 8/1
	1988	Bottom trawl	373	1	0	6/4 – 7/30
	1989	Bottom trawl	374	0	1	6/6 – 8/11
	1990	Bottom trawl	371	0	10	6/4 – 8/1
	1991	Bottom trawl	373	0	3	6/7 – 8/13
	1993	Bottom trawl	375	0	1	6/4 – 7/26
	1997	Bottom trawl	376	1	0	6/7 – 7/26
	1999	Bottom trawl	373	2	0	5/23 – 7/11
	2000	Bottom trawl	372	3	1	5/23 – 7/20
	2001	Bottom trawl	400	0	1	5/29 – 7/19
	2002	Bottom trawl	375	0	2	6/2 – 7/24
	2003	Bottom trawl	376	1	0	6/2 – 7/22
	2004	Bottom trawl	375	4	1	6/5 – 7/25
	2005	Bottom trawl	402	1	0	6/3 – 7/22
	2006	Bottom trawl	405	5	1	6/2 – 7/25
	2007	Bottom trawl	376	1	4	6/11 – 7/28
	2008	Bottom trawl	375	0	7	6/4 – 7/24
	2009	Bottom trawl	376	1	10	6/2 – 7/19
2010	Bottom trawl	376	2	6	6/7 – 8/4	
2011	Bottom trawl	376	3	1	6/5 – 7/25	
2	2010	Beam trawl	58	11	6	9/11 – 9/18
	2012	Beam trawl	64	1	0	8/20 – 10/7

Table 2.3. Range, mean, and standard deviation (SD) of Pacific halibut standard length (mm) and catch per unit effort (CPUE; number of individuals per 10 m²) over geographic area from preflexion to postflexion larvae. *Bongo (BON), Multiple Opening/Closing Net and Environmental Sensing System (MOCNESS), Tucker trawl (TUCK), modified beam trawl (MBT), and Methot trawl (METH)

Stage	Month	Gear type*	Body-length range	Mean body-length (SD)	CPUE range	Mean CPUE (SD)	No. fish
Preflexion larvae	2	BON	6.1 – 12.8	9.4 (1.4)	3.4 – 12.1	7.8 (1.7)	78
	2	MOCNESS	7.0 – 13.5	9.6 (1.4)	0.7 – 1.4	1.1 (0.3)	29
	2	TUCK	11.1		2.7		1
	3	BON	6.0 – 11.8	9.7 (1.0)	5.2 – 17.2	8.1 (3.2)	43
	4	BON	10.0 – 13.5	12.6 (0.9)	5.4 – 14.2	8.7 (2.4)	19
	4	MOCNESS	10.0 – 13.0	12.0 (0.9)	1.8 – 4.4	2.9 (1.0)	17
	4	TUCK	11.0 – 13.0	12.2 (0.7)	2.8 – 3.8	3.3 (0.7)	6
	5	BON	8.2 – 13.5	12.2 (1.9)	3.8 – 9.8	6.8 (1.9)	15
	5	MOCNESS	11.0 – 13.5	12.3 (1.8)	1.2 – 2.1	1.6 (0.7)	2
Flexion larvae	2	BON	13.8		9.4		1
	2	MOCNESS	13.9		1.3		1
	3	BON	13.6 – 15.0	14.3 (1.0)	7.2 – 7.8	7.5 (0.4)	2
	4	BON	13.6 – 17.8	15.6 (1.1)	4.7 – 10.4	7.5 (1.1)	144
	4	MOCNESS	14.0 – 16.2	15.0 (0.8)	2.3 – 3.1	2.6 (0.3)	12
	4	TUCK	14.0 – 15.5	14.7 (0.8)	3.1		3
	5	BON	13.7 – 17.8	15.9 (0.9)	3.5 – 11.4	6.9 (1.5)	160
	5	MOCNESS	15.0 – 17.8	16.5 (0.8)	0.9 – 2.0	1.5 (0.3)	18
	6	BON	17.0 – 17.5	17.3 (0.4)	6.8 – 7.1	7.0 (0.2)	2
	6	MOCNESS	15.0 – 17.6	16.5 (1.0)	0.8 – 1.5	1.2 (0.3)	5
7	METH	17.5		0.08		1	

Table 2.3. (Continued)

Postflexion	2	BON	18.2		8.3		1
larvae	4	BON	18.0 – 26.0	19.6 (2.6)	5.7 – 9.3	7.4 (1.1)	9
	5	BON	17.9 – 26.5	19.3 (1.7)	4.1 – 10.0	6.3 (1.3)	46
	5	MOCNESS	18.0 – 19.1	18.8 (0.4)	1.2 – 1.6	1.4 (0.2)	7
	6	BON	22.6		3.3		1
	6	MOCNESS	18.0 – 22.0	19.7 (1.5)	1.1 – 6.1	2.7 (2.0)	8
	6	TUCK	20.7		2.9		1
	7	BON	21.0 – 22.0	21.5 (0.7)	4.9 – 5.0	5.0 (0.1)	2
	7	MBT	21.0		1.0		1
	7	METH	18.0 – 23.2	20.6 (1.5)	0.0 – 0.3	0.1 (0.1)	15
	7	TUCK	18.5 – 22.8	20.7 (3.0)	0.01 – 1.3	0.7 (0.9)	2
	8	BON	22.0		3.7		1

Table 2.4. Model selection results of Generalized Additive Models for Pacific halibut larval standard length (mm) from 1979 to 2012 in the eastern Bering Sea. Estimated degrees of freedom are shown for independent variables with nonparametric terms. Asterisks denote significance at the following alpha levels: *0.1, **0.005, and ***0.001. GCV stands for generalized cross validation score and AIC stands for akaike information criterion. Bottom depth is log-transformed.

Model	No. fish	GCV	AIC	R-square	Deviance explained	Sampling location	Bottom depth	Day of year
1	651	3.414	2647.39	0.74	74.9 %	0.1	0.004**	< 2e-16***
2	651	3.454	2656.29	0.73	72.7 %	Excluded	1.45e-08 ***	< 2e-16***
3	651	3.441	2652.22	0.74	74.8 %	4e-05 ***	Excluded	< 2e-16***

Table 2.5. Range, mean, and standard deviation (SD) of Greenland halibut standard length (mm) and catch per unit effort (CPUE; number of individuals per 10 m²) over geographic area from preflexion to postflexion larvae. *Bongo (BON), Multiple Opening/Closing Net and Environmental Sensing System (MOCNESS), modified beam trawl (MBT), and Methot trawl (METH)

Stage	Month	Gear type*	Body-length range	Mean body-length (SD)	CPUE range	Mean CPUE (SD)	No. fish
Preflexion larvae	2	BON	9.5 – 16.0	10.9 (1.6)	6.1 – 14.2	7.8 (1.9)	20
	2	MOCNESS	9.9 – 10.0	10.0 (0.1)	0.9 – 1.5	1.2 (0.4)	2
	3	BON	9.0 – 15.0	11.9 (1.2)	3.6 – 41.3	9.8 (9.3)	92
	4	BON	9.5 – 19.2	17.1 (1.6)	5.8 – 14.2	8.6 (1.4)	278
	4	MOCNESS	12.0 – 19.2	16.2 (1.4)	2.3 – 6.0	3.7 (1.1)	93
	5	BON	12.0 – 19.1	17.8 (1.4)	4.4 – 10.1	7.1 (1.6)	51
Flexion larvae	5	MOCNESS	17.1		2.0		1
	4	BON	19.4 – 21.2	20.1 (0.5)	5.8 – 15.2	7.9 (1.5)	104
	4	MOCNESS	19.5 – 21.8	20.1 (0.7)	2.0 – 5.1	3.4 (1.2)	13
	5	BON	19.3 – 21.9	20.7 (0.8)	4.0 – 10.1	7.4 (1.6)	63
Postflexion larvae	5	MOCNESS	20.6 – 21.1	20.9 (0.4)	2.0		2
	4	BON	22.0 – 22.8	22.2 (0.4)	7.3 – 9.0	8.2 (0.8)	5
	4	MOCNESS	22.0 – 22.4	22.2 (0.3)	2.8		2
	5	BON	22.0 – 25.5	22.8 (0.9)	4.9 – 9.3	7.3 (1.2)	39
	5	MOCNESS	22.0 – 25.0	23.5 (2.1)	1.3 – 2.0	1.7 (0.5)	2
	6	BON	22.0 – 34.6	27.1 (4.0)	3.9 – 7.2	6.3 (1.2)	9
	6	MOCNESS	30.0		6.7		1
	7	BON	35.1 – 39.0	36.9 (1.9)	5.4 – 6.9	6.0 (0.7)	4
	7	MOCNESS	32.9		1.7		1
	7	MBT	25.0 – 44.8	35.6 (4.5)	0.0 – 0.9	0.3 (0.3)	53
	7	METH	24.0 – 44.5	33.7 (4.4)	0.0 – 0.3	0.1 (0.1)	148
8	MBT	38		0.6		1	
8	METH	29.8 – 39.5	33.4 (5.3)	0.0 – 0.2	0.1 (0.1)	3	

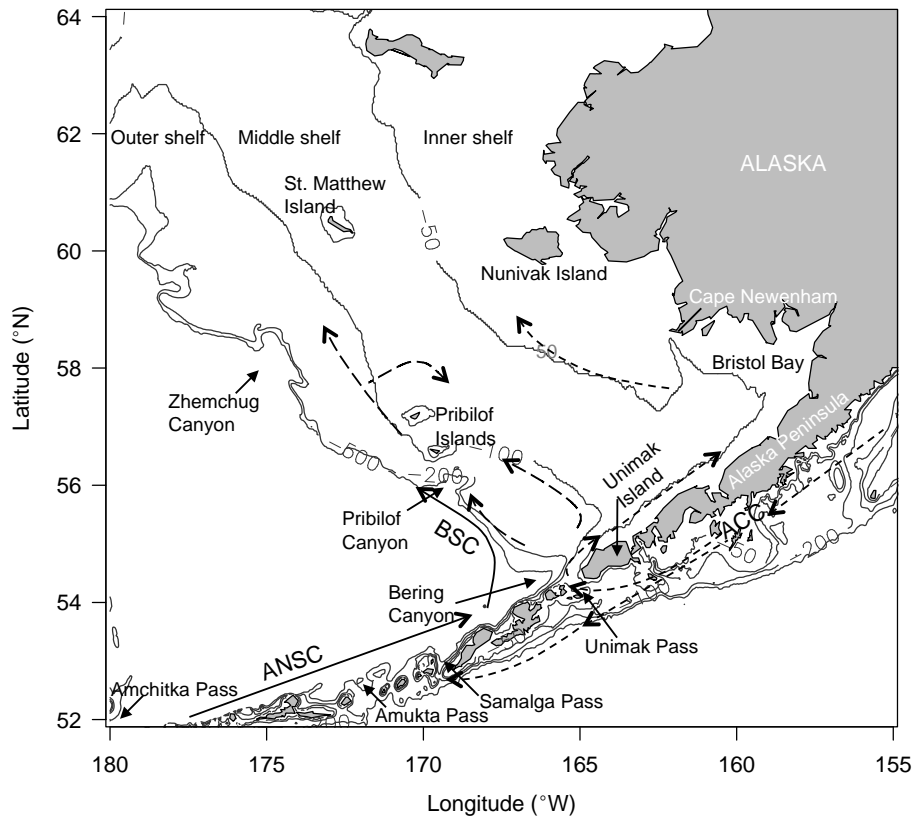


Fig. 2.1. Study area with schematic representation of the major currents - the Aleutian North Slope Current (ANSC; black line), Bering Slope Current (BSC; black line), Alaska Coastal Current (ACC; dashed line), flows (long dashed line) along the isobaths in the shelf in the eastern Bering Sea.

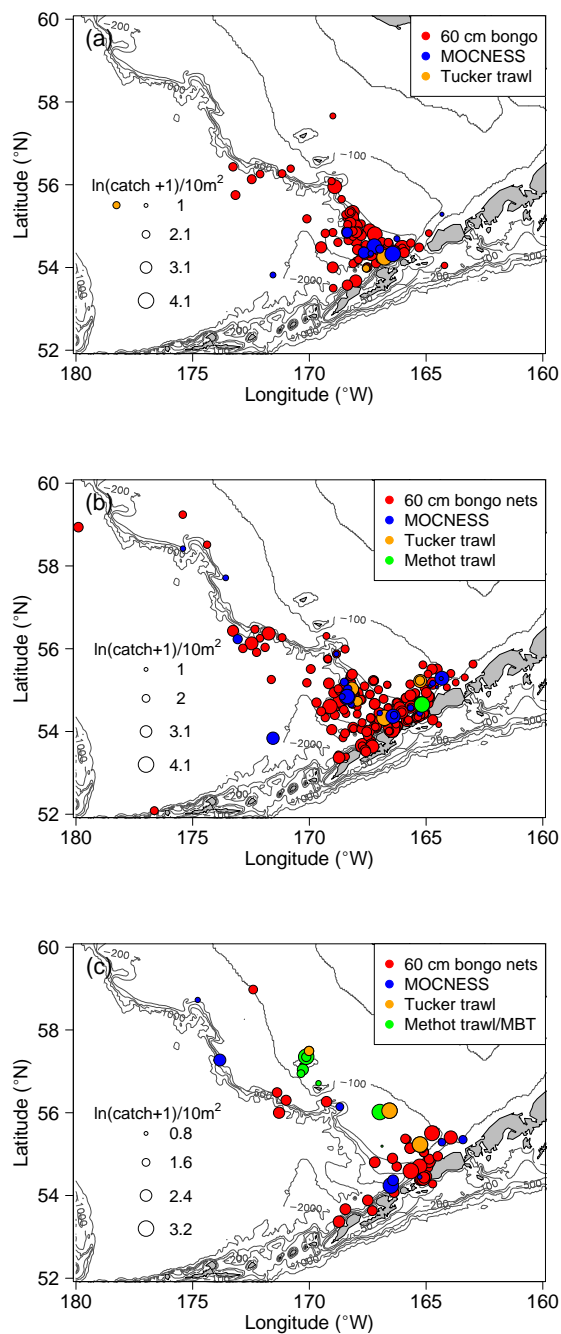


Fig. 2.2. Pacific halibut horizontal distribution of (a) preflexion larvae (6.0 mm – 13.5 mm standard length (SL)) from February to August, (b) flexion larvae (13.6 mm – 17.8 mm SL) from February to August, and (c) postflexion larvae (17.9 mm – 28.0 mm SL) from February to August in the eastern Bering Sea. Bubble sizes are proportional to the log transformed catch per unit effort (CPUE)+1. MOCNESS and MBT stand for Multiple Opening/Closing Net Sampling System and modified beam trawl, respectively. Gray lines indicate 50 m, 100 m, 200 m, 500 m, 1000 m, and 2000 m isobaths.

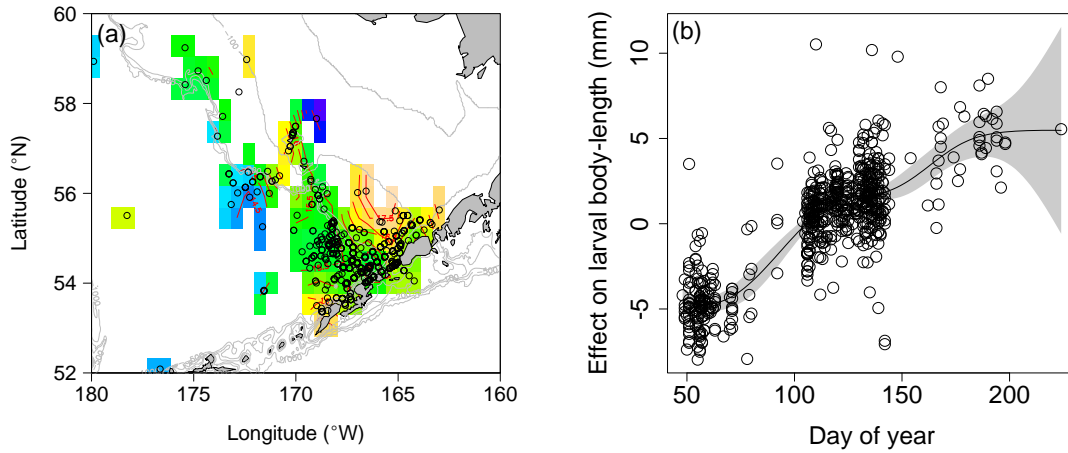


Fig. 2.3. Partial effects of (a) sampling location and (b) day of year on Pacific halibut larval body-length estimated from the Generalized Additive Model (GAM). Image colour and red contour lines indicates predicted larval body-length from the GAM in which sampling location (latitude and longitude) and day of the year where included as covariate. The body-length increases going from blue to green and yellow being largest. Open circles in (a) and (b) indicate the observation data. Shaded areas on (b) are intervals of the modeled independent variables.

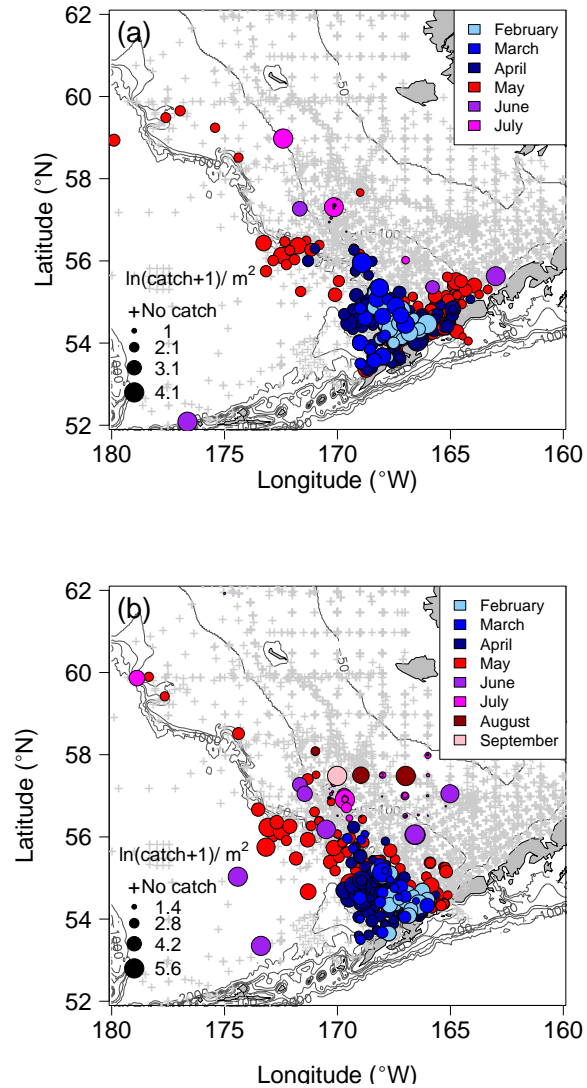


Fig. 2.4. Horizontal distributions of (a) Pacific halibut and (b) Greenland halibut larvae between February to September collected from 60 bongo (BON), modified beam trawl (MBT), and methot trawl (METH) samplings between 1972 and 2012. Plus signs represent non-catch stations across the sampling years. Gray lines indicate 50 m, 100 m, 200 m, 500 m, 1000 m, and 2000 m isobaths.

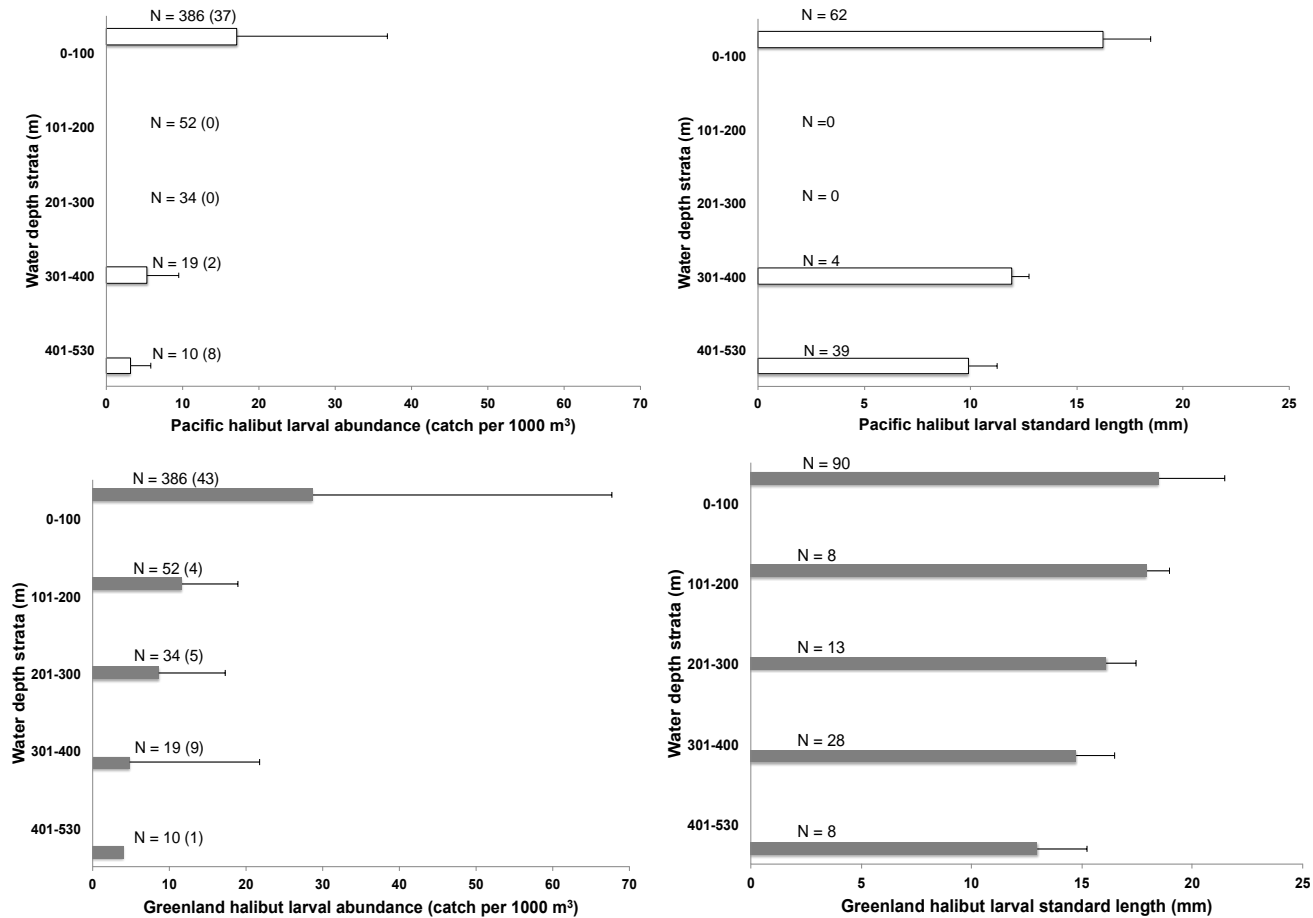


Fig. 2.5. Vertical distribution of Pacific halibut larval abundance (one standard deviation (line); top left) and standard length (standard deviation (line); top right) over 10 years (1992-1995 and 2005-2010) and vertical distribution of Greenland halibut larval abundance (standard deviation (line); bottom left) and standard length (one standard deviation (line); bottom right) in 1992-1994, 2007-2008, and 2010 in the eastern Bering Sea. N refers to number of tows (number of positive tows) for the left panel and number of fish for the right panel.

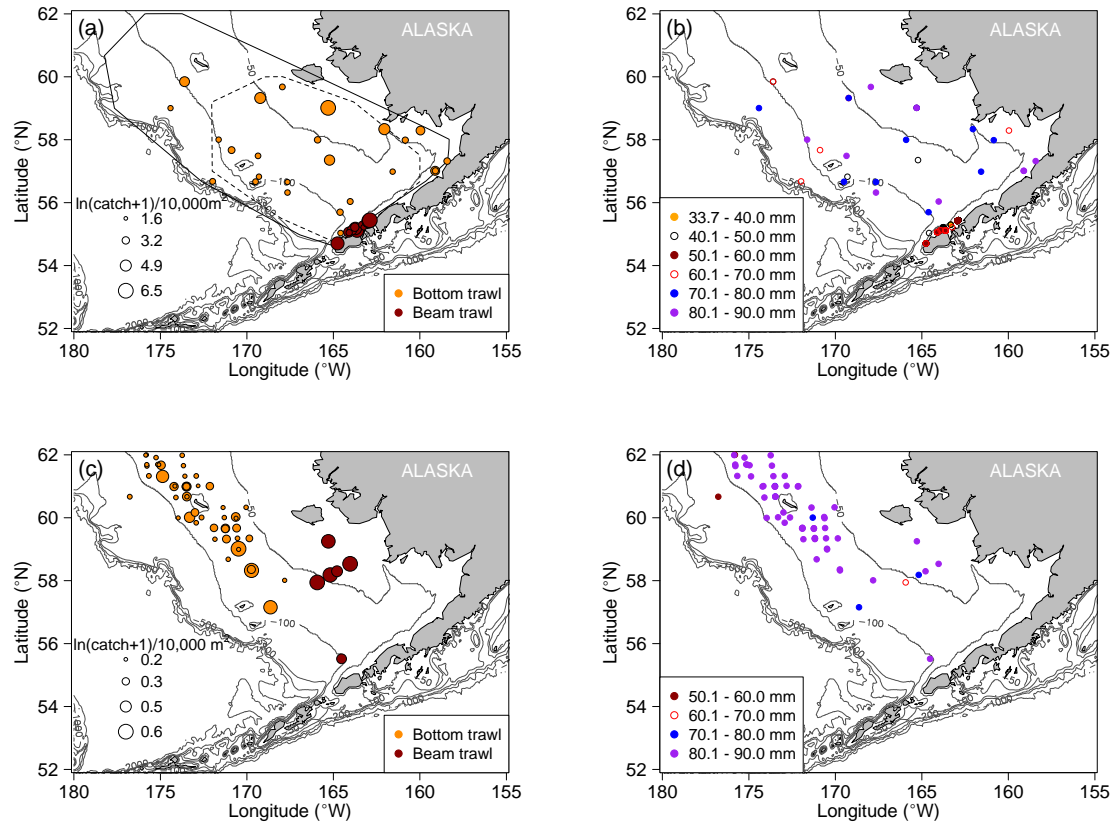


Fig. 2.6. Distributions of (a) abundance ($\ln(\text{catch per unit effort (CPUE)} + 1)$) per 10,000 m² and of (b) body-length for Pacific halibut settled juveniles (33.7 mm – 90.0 mm total length (TL)) and distributions of (c) abundance ($\ln(\text{CPUE} + 1)$) per 10,000 m² and of (d) body-length for Greenland halibut settled juveniles (60.0 mm – 90.0 mm TL) from the eastern Bering Sea summer bottom trawl (1982 – 2011) and beam trawl (2010 and 2012) surveys. Bubbles in (a) and (c) indicate natural log transformed CPUE+1 and open circles in (b) and (d) indicate locations where individuals in each body-length category were found. Gray lines indicate 50 m, 100 m, 200 m, 500 m, 1000 m, and 2000 m isobaths. Black line polygon in (a) indicates geographic area sampled by bottom trawl while black dash line polygon indicates geographic area sampled by beam trawl.

**Chapter 3. Predicting settlement success of two slope-spawning flatfish
in the eastern Bering Sea**

Dongwha Sohn, Lorenzo Ciannelli, Janet T. Duffy-Anderson, Harold P. Batchelder,
William T. Stockhausen, and Cathleen D. Vestfals

In preparation:

Marine Ecology Progress Series

Inter-Research

Nordbunte 23

Oldendorf Luhe, Germany

ABSTRACT

Settlement and recruitment of marine fish are affected by variability in prevailing currents that influence dispersal pathways from spawning to nursery locations. Two ecologically and commercially important slope-spawning flatfishes Greenland halibut (GH, *Reinhardtius hippoglossoides*) and Pacific halibut (PH, *Hippoglossus stenolepis*) in the eastern Bering Sea (EBS) may be particularly vulnerable to changes in ocean circulation because of their relatively long pelagic larval durations (PLD), which provide a protracted opportunity for unfavorable or interrupted transport. I hypothesized that interannual variability in currents may differentially affect GH and PH settlement success, due to differences in pelagic duration, vertical depths, and specific settlement habitat requirements of early life history stages. To test this hypothesis, I combined biophysical modeling, synthesis of field data, and statistical analyses to 1) identify settlement areas for GH and PH juveniles in the EBS, 2) simulate dispersal pathways from spawning to settling locations for years 1982/83 to 2003/2004, and 3) examine the environmental factors influencing the interannual variability of predicted GH and PH settlement. Our results indicate substantial variability in GH and PH settlement success among years. Significant correlations between settlement and transport along and across the eastern Bering Sea slope support the hypothesis that the variability of settlement success is driven by the flow regime, which differentially affects the dispersal of the two species during their early life stages. Species-specific differences in pre-settlement traits (i.e., spawning depth, vertical depth in each developmental stage, and pelagic larval duration) between GH and PH more strongly impact interannual variability of GH and PH settlement than pre-defined habitat for settlement of each species. GH that spawned in November and December were highly successful at settling whereas PH were more successful if they spawned in January and February. Also, GH settlement is more sensitive to temperature dependence of PLD than PH settlement. In addition to characterizing interannual variability of settlement success, our study generates new lines of inquiry addressing the link between ocean currents and recruitment of two commercially important flatfish.

INTRODUCTION

Changes in the prevailing ocean currents can influence dispersal pathways during the

early life history stages of marine fish – a process which is known to play an important role in determining variations in flatfish settlement and recruitment (Rijnsdorp et al. 1992, Van der Veer et al. 1998, Bailey & Picquelle 2002, Wilderbuer et al. 2002, Bailey et al. 2005, Bailey et al. 2008, Bolle et al. 2009). Deepwater and slope-spawning flatfish species may be particularly vulnerable to changes in ocean circulation because of their relatively long pelagic larval durations (PLD), which provides a protracted opportunity for unfavorable or interrupted transport. During their dispersal from spawning to nursery locations, eggs and larvae are subject to numerous sources of mortality, among which is the loss of individuals due to aberrant dispersal (Houde 2008). Thus, it is important to understand physical processes controlling dispersal pathways and settlement success.

The slope-spawning flatfishes, Greenland halibut (*Reinhardtius hippoglossoides*, GH) and Pacific halibut (*Hippoglossus stenolepis*, PH), are two ecologically and commercially important species in the eastern Bering Sea (EBS) whose offspring rely on extensive drift to connect from spawning locations along the continental slope to specific settlement or nursery locations over the continental shelf (Bailey & Picquelle 2002, Bailey et al. 2008, Sohn et al. 2010, Duffy-Anderson et al. 2013). Interestingly, the 2 species have geographically similar patterns of egg and larval distribution; however, they exhibit different habitat preferences for settlement (Best 1974, Best 1977, Best & Hardman 1982, Matarese et al. 2003, Sohn et al. 2010, Duffy-Anderson et al. 2013, Sohn et al. 2016). In the EBS, eggs and larvae of both species have been found primarily along the slope between Bering Canyon and Pribilof Canyon (Fig. 3.1). Settlement locations of age-0 GH (≤ 100 mm in total length, TL) are located over the middle shelf region (50 – 100 m isobaths) around St. Matthew Island (Sohn et al. 2010). Since 2009, their range has expanded to south of the Pribilof Islands, which is likely due to an increase in the extent of the cold pool (summer bottom temperatures $< 2^{\circ}\text{C}$) in the middle shelf of the EBS and associated expansion of their habitat (Ianelli et al. 2011). This may suggest that summer bottom temperature could be one of the primary factors controlling GH settlement habitat. In contrast, PH appear to have four primary nursery grounds (age-0 and age-1) over the inner shelf region (< 50 m isobath): 1) along the northern Alaska Peninsula, 2) near the Pribilof Islands, 3) in Bristol Bay, and 4) near Nunivak Island (Best 1974, Best 1977, Best & Hardman 1982). Although GH and PH share several life history attributes, species-specific differences in their pelagic durations,

water depths during early life ontogeny, and specific habitat availability under the same environmental forcing can result in differences in their dispersal pathways, which in turn may influence their settlement success, recruitment, and population dynamics.

Slope currents, submarine canyons, on-shelf flows, and eddies are important features that influence the dispersal pathways of GH and PH during their early life stages (Bailey et al. 2008, Duffy-Anderson et al. 2013, Vestfals et al. 2014). In the Bering Sea, there are two dominant slope currents; the Aleutian North Slope Current flowing eastward along the Aleutian Islands and the Bering Slope Current (BSC) flowing northwestward along the slope of the eastern shelf (Stabeno et al. 1999, Fig. 3.1). Variations in the strength and position of the BSC could potentially affect GH and PH dispersal pathways, which in turn, can influence recruitment success (Sohn et al. 2010, Duffy-Anderson et al. 2013, Vestfals et al. 2014). Submarine canyons, including Bering, Pribilof, and Zhemchug canyons, serve as spawning grounds for both GH and PH and are believed to be important conduits for slope-shelf exchange of their larvae, connecting spawning locations to nursery areas (St-Pierre 1984, Seitz et al. 2007, Sohn et al. 2010, Duffy-Anderson et al. 2013). Increased on-shelf flows over the EBS continental shelf could enhance the transport of GH and PH larvae toward appropriate settling locations (Duffy-Anderson et al. 2013, Vestfals et al. 2014). Mesoscale eddies also play an episodic role in slope-shelf exchange (Stabeno et al. 1999, Stabeno & Meurs, 1999), and may also increase GH and PH connectivity between spawning and settlement locations.

In order to understand the physical mechanisms affecting the distribution, connectivity, and recruitment of flatfish species in the EBS, two- and three-dimensional hydrographic models are increasingly being used to simulate their dispersal by tracking the passive movement of particles. For example, Wilderbuer et al. (2002) used a two-dimensional ocean surface current simulation model (OSCURS) to show that recruitment variability in flathead sole (*Hippoglossoides elassodon*), northern rock sole (*Lepidopsetta polyxystra*), and arrowtooth flounder (*Atheresthes stomias*) was correlated with decadal-scale climate variability and wind-driven advection of larvae to presumed settlement areas. Lanksbury et al. (2007) used the Northeast Pacific version 4 of the Regional Ocean Modeling System (NEP4-ROMS, Curchitser et al. 2005, Hermann et al. 2009) ocean circulation model to show that differences in the vertical distribution of northern rock sole larvae in the water column affected their passive advection.

Furthermore, Cooper et al. (2012) used a coupled biophysical model to characterize the connectivity between northern rock sole spawning and nursery areas. In a recent study, Duffy-Anderson et al. (2013) used the NEP4-ROMS model to study the passive dispersal of GH larvae from 1 April to 5 September and found strong variations of cross-shelf transport, especially between particles released above and below 30 m depth. While the modeling approaches used to date have provided valuable information to improve our understanding of flatfish dispersal in the EBS, they have mostly focused on passive transport of particles to presumed settlement or nursery areas, and have excluded behavioral characteristics of flatfish through their ontogeny. Passive particle transport does not address species-specific differences in larval dispersal behavior and settlement locations, and as such, is not suitable for comparative studies of the dispersal of species with slightly different early life history traits, such as GH and PH. Moreover, modeling approaches that simulate larval drift have seldom been merged with field data, particularly during the settlement phase, to estimate the number of successful settlers in a quantitative manner. For the Bering Sea system, I therefore have a unique opportunity to build on previous modeling attempts to simulate the dispersal pathways of slope-spawning flatfish and to evaluate their settlement success in relation to ocean circulation.

In this study, I combined a coupled biophysical model and a statistical analysis of field observations to quantify the interannual variability of GH and PH settlement success in the EBS. I hypothesized that interannual variability in currents encountered by early life history stages may differentially affect GH and PH settlement success. To test this hypothesis, I first identified juvenile settlement areas for GH and PH in the EBS using field observations. I then quantified GH and PH settlement success and linked it to transport along and across the Bering Sea slope. Finally, I conducted a sensitivity analysis to quantify the robustness of model results to changes in PLD, pre-settlement traits (spawning depth, vertical depth during each development stage), and settlement locations.

MATERIALS AND METHODS

To assess the interannual variability of GH and PH settlement success, I developed an occurrence probability map of settlement locations for each species using a binomial generalized

additive model (GAM). Dispersal pathways from the egg (spawning) to newly-settled juvenile (settlement) stage were simulated from 1982 to 2004 using an individual-based model (IBM), Dispersal Model for Early Life Stages (DisMELS), which was coupled to velocity fields from the NEP4-ROMS circulation model.

Spatial characterization of settlement locations

Occurrence probability maps of settlement locations for juvenile GH and PH were estimated from the National Oceanic and Atmospheric Administration's Alaska Fisheries Science Center's (NOAA AFSC) EBS summer bottom-trawl groundfish survey (hereafter: Groundfish Survey) data from 1982 to 2011 using a binomial GAM with the logit link function. The Groundfish Survey has been conducted annually beginning as early as May and extending as late as October, although most recently, surveys have been conducted during June and July. These surveys provide extensive geographic coverage over the EBS shelf (http://www.afsc.noaa.gov/RACE/groundfish/gfprof_coverage.htm). Samples were collected by bottom trawling at 376 fixed stations that centered in each 20×20 nautical mile grid square (or corner station, in the case of high-density strata) in the continental shelf region of the EBS (Lauth and Nichol 2013). The gear used is an 25.5×34.1 m eastern otter trawl with a 25.5 m headrope and a 34.1 m footrope. The net consists of 10.2 cm stretched mesh in the body and wing, 8.9 cm stretched mesh in the intermediate and codend, and 3.2 cm mesh in the codend liner (Stauffer 2004). The net is attached to paired chains and dandyines, and a net mensuration system is used to measure net height and width while towing. Tows are typically 30 min. in duration at a speed of 3 knots. Estimates of net width are used in calculations of area swept. During the surveys, taxa were identified and total counts and weights were recorded for each individual of both species at each tow. Also, body length for a subset of individuals was measured to the nearest mm TL for flatfish. Species abundance data for each sampling station were standardized as catch per unit effort (CPUE; catch weight (kg) divided by area swept (ha) estimated as mean net width multiplied by distance towed). Environmental data, including sea surface temperature, bottom temperature, and bottom depth, were recorded at each station using a Sea-Bird SBE-39 datalogger attached to the headrope of the trawl (Lauth 2011). More specific information about the Groundfish Surveys can be found in Lauth (2011) and Stauffer (2004).

Sampling location, captured through the interaction between latitude and longitude, was the only model covariate used in the GAM. The analysis was restricted to individuals $\text{GH} \leq 100$ mm TL, which mostly include the newly-settled age-0 stage (D. Sohn, personal observation). Due to low catches of ≤ 100 mm TL juvenile PH in the survey, I examined PH juveniles ≤ 150 mm TL, which may also include some age-1 individuals. Although the Groundfish Survey is not quantitative for small sizes of fish (age-0), it can be used as a relative index of abundance and distribution. I implicitly assume that once settled, age-0 fish do not move significantly from their settlement locations in their first year. For the binomial GAM, it was necessary to pool catch data sets from 1982 to 2011 because age-0 GH and PH are comparatively rare in collections over the years. To define GH and PH settlement regions, I selected the threshold value for probability of GH and PH occurrence that produced the greatest difference between the percentage of presence stations minus the percentage of absence stations included within the threshold (see Appendix 3.1). Thus the selected probability threshold for delineating settlement locations contained the highest number of presence stations and the lowest number of absence stations for the target species. The GAM analysis was conducted using the *mgcv*-package (version 1.7-24; Wood 2006) in R version 3.0.1 (2013).

Dispersal pathways simulations

DisMELS model

DisMELS is a coupled biophysical model that combines an individual-based model with output (i.e., temperature, salinity, and velocity fields) derived from an oceanographic model. DisMELS uses a 4th order Lagrangian predictor/corrector scheme to integrate the 3D trajectories of individual fish through time. Although the latest version of ROMS for the North Pacific (e.g., NEP6-ROMS) is available, the ocean circulation model used in this analysis is the NEP4-ROMS (Curchitser et al. 2005, Hermann et al. 2009), which has been used in several studies to explore dispersal pathways or connectivity of flatfish (e.g., GH and northern rock sole) and crab in the Bering Sea (Parada et al. 2010, Cooper et al. 2012, Duffy-Anderson et al. 2013). Our research is extended from a previous study by Duffy-Anderson et al. (2013) who used the NEP4 ROMS to track GH larvae passively in different depth strata at three canyon regions including Bering, Pribilof, and Zhemchung Canyons in the EBS. Also, Vestfals et al. (2014) characterized on-shelf and along-shelf flows in the EBS using the NEP4-ROMS. Thus, I used the NEP4-ROMs to run

simulations with life history information, in order to be able to compare our results with previous studies.

The NEP4-ROMS is a free-surface, hydrostatic, primitive equation ocean circulation model that is driven by atmospheric forcing in the North Pacific. The model has 10 km horizontal grid resolution with 42 layers in the vertical, and is nested in a larger, lower resolution North Pacific model (Curchitser et al. 2005, Herrmann et al. 2009). A coarse-grain basin-scale ROMS model for the North Pacific, with a nominal resolution of 0.4° and 30 vertical layers, was used to generate initial and boundary conditions for the NEP4-ROMS (Curchitser et al. 2005). Sea-ice generation and melting were included in the model, but tidal forcing was not. While the spatial resolution of the model is too coarse to capture the smallest eddies at this grid size and simulated currents are weaker and more topographically steered than observations, simulated current directions are in good agreement with observations, and the model reproduces the main circulation features and large-scale climate variability in the North Pacific (Curchitser et al. 2005, Duffy-Anderson et al. 2013). Daily averaged model outputs were available from 1982 to 2004 for use with DisMELS.

Individual-based model parameters for DisMELS

For constructing model simulations of GH and PH dispersal pathways, model parameters were set according to the best available knowledge based on historical field survey data and literature reviews. Combined information from existing data and available literature indicated differences in GH and PH spawning depths, hatching times, associated depths via their development, and PLD. Spawning depths for GH (600-700 m) are deeper than those for PH (400-500 m) (St. Pierre 1984, Stene et al. 1999, Loher & Seitz 2008, Sohn et al. 2010, Duffy-Anderson et al. 2013), and egg hatching time is longer for GH (53 days at 4°C , Stene et al. 1999) than for PH (20 days at 5°C , Forrester & Alderdice 1973). In addition, GH have a longer PLD (> 6 months; Sohn et al. 2010) than PH (~ 6 months; Skud 1977, Norcross et al. 1997). In DisMELS, simulated individuals can actively “swim” up or down in the water column to occupy user-defined “preferred” depth ranges, and may also undergo random vertical displacement based on the total vertical velocity (V_t). That equation for the total vertical velocity (V_t) is written (Kim et al. 2015):

$$V_t = w(x, y, z, t) + V_s + V_d$$

where w is the local hydrodynamic vertical momentum (velocity), V_s is the stage-specific deterministic vertical swimming speed – this speed is 0 when individuals occupy user-defined depth ranges, and V_d is the diffusive random walk velocity:

$$V_d = r \cdot \sqrt{\frac{D}{\delta t}}$$

where r is a normally distributed random number with mean = 0 and standard deviation = 1, D is the stage-specific diffusion constant, and δt is the integration time step (1200 s). Table 3.1 shows the stage-specific duration, depth range, vertical swimming speed, and diffusion constant as simulation parameters. The individuals, at each developmental stage after the egg stage, swim up into the next preferred depth range using user-assigned vertical swimming speed and vertical diffusion (Table 3.1). Although ranges of swimming speeds of fish larvae can be about one to three body lengths per second (Fuiman 2002), in this study, the vertical swimming speeds at each stage were set up with smaller values because fish larvae may not keep their maximum swimming speed through the developmental stages (Table 3.1). For both species, I established typical water depth ranges and pelagic durations for 6 developmental stages from eggs to newly-settled juveniles based on the analysis of the AFSC historical field survey data (Table 3.1; Sohn et al. 2016).

For the initial simulation, a total of 264000 (30 spawning dates * 44 spawning locations * 200 individuals) eggs each for GH and PH were released at depths of 700 m and 500 m, respectively, at 44 selected spawning locations between Bering and Pribilof Canyons (Fig. 3.2). Three potential spawning locations (location 42-44; Fig. 3.2) were closely spaced (< 4 km) in order to check small-scale spatial variability. Preliminary research showed a significant correlation between results from the simulation with 200 eggs released per spawning location and results from a simulation with 1000 eggs released per spawning location (not shown here). Thus, I released 200 eggs per location for the GH and PH dispersal simulations in this study. Eggs of both species were released at 4-day intervals from 2 November to 26 February, which encompasses the peak spawning period for both species (St-Pierre 1984, Alton et al. 1988, Sohn et al. 2010) with thirty spawning events assumed for each simulation year (1982/1983 to 2003/2004). This was done because GH and PH are known batch spawners (Loher & Seitz 2008, Domínguez-Petit et al. 2013). Each simulated fish was tracked through its early life stages until

settlement (defined as the maximum simulation day), which was 271 days for GH and 201 days for PH (Table 3.1). I assumed that both GH and PH were “competent-to-settle” in their nursery habitats after spending 15 days in their transformation stage. Thus, the competent settlement interval was 56 days for GH and 31 days for PH (Table 3.1).

Estimation of successful settlement

Successful settlers for GH and PH over all simulation years were determined by intersecting the simulated dispersal trajectory during the competent settlement interval with the pre-defined settlement locations. Individuals that were more than 50 km away from the Groundfish Survey grid during their competent settlement interval were classified as non-survivors, since they drifted off-shelf toward unfavorable settlement habitats. However, individuals that were within 50 km of the Groundfish Survey grid were deemed potential settlers. For each day of the competent settlement phase, I computed the probability of settlement success (settlement score) for each potential settler from the binomial GAM. I then retained only the predicted maximum settlement score throughout the entire competent settlement interval, assuming that competent larvae are able to search for the highest quality settlement locations. Successful settlers for GH and PH were identified as those whose settlement score equaled or exceeded the threshold value of occurrence probability determined from the analysis of settlement regions (see Appendix 3.1). Therefore, settlement success for each species was based on the position of the simulated individuals and on the historical occurrences of other settlers in the Groundfish Survey. After calculating GH and PH settlement success, I grouped settlement of each species by good years and bad years to check whether settlement patterns differed by spawning date. Good years were defined as those where the percentage of successful settlers was greater than the yearly mean settlement percentage for the study period. Those lower than the yearly mean were designated as bad years. In order to make differences more distinct, I also categorized GH and PH settlement into two groups: years with settlement below the yearly 25th percentile of settlement rate and the other with settlement above the yearly 75th percentile settlement rate (see Appendix 3.2). All data analyses were conducted in R version 3.0.1 (2013), and for the GAM analysis I used the mgcv-package version 1.7-24 (Wood 2006).

Correlations between settlement success and age-0 catch and recruitment data

After calculating settlement success for GH and PH, I compared the predicted number of GH and PH successful settlers to the total catch per unit effort (number of individuals caught per hectare (10000 square meters) swept; CPUE) of age-0 GH (≤ 100 mm TL) and age-0/age-1 PH (≤ 150 mm TL) from the Groundfish Survey over given simulation years using Pearson's product moment correlation. I also examined correlations between the number of GH settlers and age-0 recruitment obtained from the most recent GH stock assessment (Ianelli 2011). Comparable age-0 recruitment for PH in the EBS was not available for correlation analysis because the International Pacific Halibut Commission (IPHC) models the entire North Pacific PH population as a single stock in their assessments (Stewart et al. 2013).

Correlations between settlement success and oceanic indices

To test the hypothesis that interannual variability of currents encountered by the early life history stages of GH and PH may differentially affect their settlement success, I computed correlations between the predicted number of successful settlers and oceanic transport indices that quantify along-shelf and cross-shelf transport in the EBS. The oceanic transport indices were also derived from the NEP4-ROMS model output from 1982-2004 (Vestfals et al. 2014). Specifically, along-shelf transport was quantified across three transects, positioned in the region of Bering, Pribilof, and Zhemchug Canyons, which were placed perpendicular to the 1995 – 2004 mean path of the BSC at 30 m depth. Each transect was further subdivided into Main, Basin, and Shelf sections with Main sections bracketing mean flow greater than 0.02 m s^{-1} , Basin sections extending over the Aleutian Basin, and Shelf sections extending shelf-wards to approximately the 100 m isobath. Volume transport was calculated to 500 m depth across each section. Cross-shelf transport was also quantified around Bering, Pribilof, and Zhemchug canyons to 200 m depth, and across the 100 and 200 m isobaths. Transport indices were developed from annual anomalies, and were calculated as deviations from the 1982-2004 mean transport normalized by the standard deviation. Both the oceanic transport indices and the predicted settlement success are derived from the same ocean circulation model (NEP4-ROMS); however, the latter include species-specific differences of early life history stage behaviors (spawning depth, PLD, and settlement areas). Thus, it is appropriate to examine correlations

between the circulation indices and settlement success to identify whether interannual variability of currents encountered by GH and PH early life history stages differentially affects their settlement success.

Sensitivity analysis of the simulation model

To assess whether potential differences in GH and PH settlement success were driven by differences in pre-settlement (i.e., spawning depth, vertical depth during each developmental stage, and PLD) and/or in settlement (i.e., habitat preference during settlement) traits, I exchanged GH and PH settlement areas and early life history traits when calculating the number of settlers for the two species. Specifically, I computed GH settlement in PH settlement areas (exchange of the settlement trait) and PH settlement in GH settlement area (exchanges of pre-settlement traits) and compared each of them with the GH settlement base run using Pearson's product moment correlation. This same operation was also conducted for PH settlement success in GH settlement areas and GH settlement in PH settlement area with the PH settlement base run. The underlying rationale for this analysis was that a change of settlement success in relation to exchange of pre-settlement traits or settlement habitat between the two species would be indicative that pre-settlement or post-settlement traits are involved in driving the observed differences in settlement success between the two species.

The sensitivity of the calculated settlement success was also examined in relation to variations in the PLD of surface-oriented larval stages. PLD can change in relation to growth during the larval stage, which, in turn, is related to water temperature and feeding conditions. To assess sensitivity to changes in the PLD for each species, I conducted four dispersal trajectory simulations that spanned five consecutive years (1996 to 1997, 1997 to 1998, 1998 to 1999, and 1999 to 2000). These years were selected because of the contrasting settlement success of the two species and variable circulation features. For example, 1997 had strong along-shelf transport, high GH and low PH settlement success, while 1998 had lower along-shelf transport, low GH and high PH settlement success. For the surface-oriented larval stages (i.e., after yolk sac) I decreased and increased the PLD of each development stage by 25 % and simulated GH and PH dispersal pathways using the same protocol as the initial simulation.

RESULTS

Settlement locations

The binomial GAM explained 63.3% and 44.4% of the deviance in the presence/absence of GH (≤ 100 mm TL) and PH (≤ 150 mm TL), respectively (Table 3.2). The GAM results indicated the presence/absence of GH and PH were significantly influenced by the sampling location (latitude and longitude). Age-0 GH were preferentially found in the middle shelf, especially in the northwestern region near St. Matthew Island. Age-0 and age-1 PH occurred near Bristol Bay, Nunivak Island, the Pribilof Islands, and the Alaska Peninsula. The settlement regions for GH were well-defined by a probability of occurrence above 0.2 (Fig. 3.3). The 0.2 probability of occurrence included 90% of all stations where at least one GH was found and 11% of all stations where GH were never caught. For PH, their settlement regions were determined by a probability of occurrence of 0.2 (Fig. 3.3), which included 74% of the stations with at least one PH occurrence and 12% of all stations where PH were never caught. At the 0.2 threshold, the difference between percentage of presence and absence stations was the highest for PH and GH. The respective threshold values for GH and PH represent the minimum probability of occurrence that a simulated individual must reach during the competent settlement interval, in order to be considered settled.

Interannual variability and spatial and temporal patterns of successful settlement

The results from the dispersal pathway simulations for GH and PH revealed substantial interannual variability in settlement success over the simulation years (Fig. 3.4). The yearly mean percentage of GH settlers was 2.8 % (± 1.9 SD; 7427 out of 264000). The highest percentage of GH successful settlers (7.3 %; 19281 out of 264000) occurred in 1991/1992, while the lowest (0.3%; 678 out of 264000) occurred in 1999/ 2000 (Fig. 3.4). For PH, the yearly mean percentage was 3.3 % (± 3.5 SD; 8674 out of 264000). The highest percentage successful settlers occurred in 1984/1985 (12.7%; 33582 out of 264000), the lowest occurred in 1994/1995 (0.1%; 278 out of 264000; Fig. 3.4). The correlation between GH and PH settlement over the time period examined was not significant ($r = -0.16$, $df = 20$, and $p\text{-value} = 0.47$), indicating that the settlement of these two species is differentially affected by pre-settlement and post-settlement

dynamics. The patterns of spatial distribution of GH and PH settlers were markedly different (Fig. 3.5) – an expected result given the way in which the settlement habitat for the two species was defined. To note, PH settlers were not found in all observed settlement locations, although some individuals settled in the inner shelf near Nunivak Island in 1983/1984 and 1993/1994 and shallower than 50 m isobath along the Alaskan Peninsula in 1997/1998 (cf. Figs. 3.3 & 3.5). These results indicate that the model was consistently underestimating expected PH settlement success in inner shelf habitats, based on field observed settlement sites. Within each dispersal trajectory, for both species, the number of successful settlers changed considerably, mostly in relation to spawning time (Figs. 3.6 & 3.7). Specifically, GH settlement success was higher for individual particles released earlier during the spawning window, in November and December (Fig. 3.6). For PH, settlement success was higher for individual particles released later during January and February; Fig. 3.7). These patterns were consistently maintained in good years and bad years for both species (Figs. 3.6 & 3.7). The seasonal pattern of settlement success did not change even when the criteria for defining good and bad years was defined according to the 75th and 25th percentile (see Appendix 3.2). Settlement success for both GH and PH were not much different among selected spawning locations, although some spawning locations spaced near the slope had higher settlement than others located near the basin (see Appendix 3.3). Also, I did not find differences of GH and PH settlement success among closely positioned (< 4km) release locations (i.e., location 42-44; Fig. 3.2).

Correlations between settlement success with ocean circulation indices, age-0 catch and recruitment data

For GH, settlement success increased with increased northwestward transport along the shelf sections of the three transects including Bering, Pribilof, and Zhemchung Canyons and with increased cross-shelf transport through Pribilof Canyon (Table 3.3 and Appendix 3.4), while PH settlement success decreased with increased northwestward transport along the shelf at the three transects and with on-shelf transport through 200 m isobaths (Table 3.3 and Appendix 3.5). The number of successful GH settlers between 1982/1983-2003/2004 was not significantly correlated with total CPUE of GH (≤ 100 mm TL) from the Groundfish Survey over the same time period ($r = 0.14$, $df = 15$, and $p\text{-value} = 0.58$). Nor did not find a significant correlation between GH

settlement and age-0 recruitment ($r = -0.32$, $df = 20$, and $p\text{-value} = 0.15$). No significant correlation was found between PH settlement success and total PH CPUE ($r = 0.12$, $df = 15$, and $p\text{-value} = 0.66$).

Model sensitivity

There was no correlation between the base run of GH settlement success and that derived using PH settlement locations ($r = -0.12$, $df = 20$, and $p\text{-value} = 0.61$) or between the base run for PH settlement success and that derived using GH settlement locations ($r = -0.19$, $df = 20$, and $p\text{-value} = 0.40$). These results indicate that species-specific habitat requirements for settlement do not drive differences in settlement success between the two species. In contrast, when exchanging only the pre-settlement parameters between the two species, correlation was found between the GH base run and the modified GH run with PH pre-settlement attributes ($r = 0.60$, $df = 20$, and $p\text{-value} = 0.003$) and between the PH base run and the modified PH run with GH pre-settlement attributes ($r = 0.85$, $df = 20$, and $p\text{-value} < 0.01$). These results confirm that species-specific differences in pre-settlement attributes (i.e., spawning depth and PLD) between PH and GH are more critical in controlling interannual variability of settlement success than the location of the settlement habitat.

The sensitivity analysis on the PLD showed that GH settlement success generally increased with longer PLD in the examined four consecutive years while PH settlement success did not always increase with longer PLD in comparison to the base run. Also, when the PLD of GH decreased, their settlement was decreased considerably in each year while PH settlement did not always decrease with shorter PLD in comparison to the base run. Results for PH showed that neither a 25% increase nor a 25% decrease in PLD significantly impacted the rank of PH settlement among the four consecutive years, although there were some changes in the number of predicted settlers (Table 3.4). For GH, a 25% decrease in PLD did not influence the rank of their settlement whereas a 25% increase in PLD did.

DISCUSSION

The results from our simulation of egg and larval dispersal from spawning locations to

settlement regions are consistent with the hypothesis that interannual variability of currents encountered by the early life history stages of GH and PH differentially affect juvenile settlement in the EBS. Species-specific variability in settlement success was related to ecological differences between the 2 species including spawning depth, vertical depth during each developmental stage, and PLD.

Particle tracking models have been used previously to explore transport and settlement success in relation to recruitment of marine organisms, including flatfish (Wilderbuer et al. 2002, Fox et al. 2006, Bolle et al. 2009, Parada et al. 2010, Duffy-Anderson et al. 2013). Most of these modeling studies have emphasized the importance of hydrographic model resolution or life history characteristics in determining settlement (Levin 2006, Huret et al. 2007, Cowen & Sponaugle 2009). However, data-defined habitat requirements for settlement areas have rarely been included. For example, for slope-spawning species successful settlers are often defined by the proportion of particles or fish larvae that arrive on the continental shelf at the end of the dispersal simulation (Wilduerbuer et al. 2002), assuming that all shelf regions are of equal habitat quality. In reality, shelf areas in the EBS have heterogeneous characteristics (e.g., differences in depth, substratum, and temperature, etc.), which may be uniquely suited to selected species. Also, in the majority of studies in the EBS that have modeled larval dispersal, settlement occurs at the first acceptable site encountered during the competent-to-settle period. However, flatfish larvae that are sufficiently developed to settle may present some level of plasticity for suitable settling sites and postpone settlement until suitable habitat is found (Neuman & Able 1998). So while settlement is an abrupt event for flatfish, the window of opportunity for settlement may be deliberately prolonged. With our modeling approach I assumed that competent larvae are able to search for the highest quality settlement locations during their larval drift. To account for this, I selected successful settlers over the entire competency period. Our study is unique in that it coupled a statistical modeling approach that considered species-specific differences of habitat requirements with more traditional biophysical modeling. Statistical-biophysical models are powerful tools, especially when used to study the dispersal of species with different life history traits, because they allow for efficient parameterization, quantification of uncertainty, and improved predictive capability (e.g., Chen et al. 2014).

For GH, I found no significant correlation between the annual settlement success and the annual abundance of age-0 settled juveniles (≤ 100 mm TL) derived from the Groundfish Survey over the simulation years. This suggests that other factors (e.g., predation and food availability) in addition to advective losses during dispersal from spawning to settlement locations influence the abundance of newly-settled GH juveniles. Settlement success for GH increased with greater northwestward transport along the shelf section of the three transects located at Bering, Pribilof, and Zhemchug Canyons and with increased on-shelf transport through Pribilof Canyon, indicating that Pribilof Canyon could be an important conduit for GH larval transport to settlement areas to the north. Although Bering Canyon has previously been suggested as a pathway for GH larval transport based on field surveys (Sohn et al. 2010), I did not find significant relationships between GH settlement and on-shelf flow through this more southerly canyon. These results are not entirely unexpected since prolonged entrainment in the BSC and associated delays in shelf ingress could benefit GH larvae, as they increase the probability of delivery to their northerly nursery habitats located in the vicinity of St. Matthew Island (Fig. 3.1). However, it is important to note that it is possible that the NEP4-ROMS resolution or indices derived from averaged annual transport may obscure the relationships between GH settlement and on-shelf transport through Bering and Pribilof Canyons.

A previous study (Duffy-Anderson et al. 2013) showed that passive particles (GH larvae) released at 500 m were not advected to EBS shelf areas where age-0 settlers have been found. However, I found that ontogenetic changes in vertical distribution of GH eggs and larvae facilitated greater connections between presumed spawning sites and depths and shelf settlement regions. Slope-shelf exchanges in the EBS are influenced by the structure of the BSC (Stabeno et al. 1999). The position and strength of the BSC exhibits strong seasonal and interannual variability, with stronger flow occurring close to the shelf-break during the winter and weaker flow offshore during the summer (Overland et al. 1994, Ladd 2014, Vestfals et al. 2014). Interannual shifts in the BSC position are likely due to mesoscale variability, such as eddies or meanders in the current (Ladd 2014). Based on the results of our correlation between settlement success and flow indices, I expect that GH benefit from years with increased along-shelf flow north of Bering Canyon while PH benefit from years with weak along-shelf transport along the southern shelf. Although there is no record of significant relationships between along-shelf and

on-shelf transport and water temperature, the highest GH settlement occurred in 1991/1992 (a cold year), while the lowest GH settlement occurred in 1999/2000 (an average year). Also, GH settlement in 1997/1998 and 2000/2001-2002/2003, classified as warm years by Stabeno et al. (2012), was lower than the average settlement calculated over all simulation years. However, the patterns of settlement during warm and cold years does not always hold. For example, 1994/1995 was a cold year with low settlement success for GH, suggesting that additional processes may be involved.

Cold years could also favor GH settlement success due to increases in the extent of the cold pool, which potentially extends suitable GH settlement habitat southwards. Settled juvenile GH have been found around St. Matthew Island (Sohn et al. 2010; Fig. 3.1), which is usually surrounded by the cold pool with an average summer bottom temperature $< 2^{\circ}\text{C}$. Since 2009, the range of GH juvenile distributions has expanded to south of the Pribilof Islands, likely due to the cold pool expansion (Ianelli et al. 2011). Variability in nursery ground size caused by environmental change could generate variations in settlement success and could potentially affect GH recruitment (reference to chapter 4). Rijnsdorp et al. (1992) found a positive relationship between the size of nursery ground and recruitment success in sole (*Solea solea*) stocks in the Irish Sea and North Sea. Also, Van der Veer et al. (2000) reported that greater surface area of the nursery grounds yielded stronger year-class strength for European plaice (*Pleuronectes platessa*) in the North Sea. However, our attempt to relate interannual settlement success to interannual recruitment of age-0 GH derived from the Groundfish Survey met with limited success. The lack of correlation between the numbers of settlers and age-0 recruitment could be due to density-independent (i.e., water temperature etc.) and/or density-dependent (i.e., spawning stock biomass, predation, starvation etc.) factors not included in our models. Also, the period covered by our simulations (1982-2004) include years of low GH recruitment compared to the late 1970s and early 1980s (Ianelli et al. 2011). Therefore, our results may be missing dynamics operating in the earlier more favorable period.

For PH, I did not find a significant correlation between the annual settlement success and the annual abundance of settled juveniles (≤ 150 mm TL) from the Groundfish Survey over the simulations years. Lack of correlation may reflect the strong effects of other processes (i.e., predation and starvation etc.) on PH losses from spawning to settlement in comparison to

advective losses of PH. Alternately, the Groundfish Survey may not be quantitative for small sizes of PH (age-0/age-1) or the survey may not have covered all possible PH settlement sites as described earlier. The physical simulation model could also be incapable of transporting larvae into the predominantly shallow inner shelf nursery areas. Predicted PH settlement decreased in relation to strong northwestward flow along the shelf between Bering, Pribilof, and Zhemchung Canyons. These results suggest that PH larvae may be subject to settlement failure when they are transported northward, away from Bering Canyon. Also, PH settlement decreased with strong on-shelf flow over the 200 m isobath, contrary to my expectation that such flow could be favorable for settlement. Vestfals et al. (2014) found that there is a negative relationship between ice cover and on-shelf flow through Bering Canyon and across the 200 m isobath. Given the described influence of currents and the relationship between ice cover and on-shelf flow, I expect fewer PH settlers in cold years (i.e., 1995, 1997, and 1999) than in warm years. Our results partially agree with our expectations, as there were no successful PH settlers in 1987/1988, 1994/1995, 1996/1997, and 1998/1999 (4 cold years) and more settlers in 1997/1998, 2000/2001, 2003/2004 (3 warm years). The patterns of PH settlement during warm and cold years do not always hold though, as 1982/1983-1983/1984, 1985/1986-1986/1987, 1992/1993-1993/1994, and 2001/2002-2002/2003 were warm years with low settlement success for PH, suggesting that additional processes may be involved.

Results from the sensitivity analyses show that species-specific differences in pre-settlement (i.e., spawning depth, vertical depth, and PLD) traits are important factors that differentially influence interannual variability of GH and PH settlement in the EBS. These results support our hypothesis that interactions between EBS circulation patterns and species-specific differences in early life traits differentially affect GH and PH settlement. The interaction of spawning date with the early life histories is what determines settlement patterns, and these differ substantially for the two species. GH individuals who spawned early, from November to December, are more successful at settling than later spawned individuals in both good and bad settlement years. Indeed, the fact that only a few pre-spawning or actively spawning females were found during field sampling from mid-to-late February along the Bering Slope between Bering and Pribilof canyons support this conclusion (Duffy-Anderson et al. 2013). For PH, settlement is higher when individuals spawned later than November and December. Ladd (2014)

showed interannual and seasonal variability of the BSC in the eastern Bering Sea. In particular, the BSC is closely positioned near the shelf-break and flows strongly northwestward during winter (October-December and January-March). After winter, the BSC is reduced in speed and located farther west (Ladd 2014). GH settlement areas are located on the northern side of the EBS, thus, early spawned GH individuals have more chances to be entrained and be delivered to their settlement location due to the strong northwestward flow of the BSC during winter. For PH, later spawned individuals meet with favorable flows that help in reaching their settlement areas located in the southern part of the EBS. I found that GH settlement success is highly sensitive to changes in PLD of surface oriented early life history stages. In contrast, PH settlement success is not as sensitive to changes in PLD. Water temperature is one of the dominant factors that directly influences growth and development rates of flatfish (Nash and Geffen 2014), impacting their PLD. For marine fish, PLD decreases exponentially with increasing temperature (Benoit 2000). Given the relatively long PLD of GH and the narrow availability of suitable settlement habitats compared to PH, it is not surprising to observe a strong dependence of GH settlement success to PLD. These results however also point to the fact that PH may have a stronger resilience to climate variability in comparison to GH in the EBS region.

It is important to note that the Groundfish Survey data used to define habitat requirements during settlement only extends as far northward as 62.5°N, and may miss important additional GH and PH nursery habitats. Since GH has a circumpolar distribution, it may settle in northern areas outside of the survey grid. Likewise, the Groundfish Survey does not cover the region inshore along the northern Alaskan Peninsula, which are believed to be important settlement areas for PH (Dan Cooper at AFSC, personal communication). These limitations could contribute to underestimated GH and PH potential settlement areas and their subsequent settlement success. However, these biases are consistently applied across simulation years, therefore patterns of interannual variability in settlement success derived here should be qualitatively correct. The absence of the predicted GH and PH successful settlers in all or some empirically determined settlement areas (Figs. 3.3 & 3.5) could result from not including horizontal swimming behaviour (i.e., horizontal movement and speed) or tides in our models or could result from inaccurate simulations of flows in the inner shelf. Fish larvae are able to directionally swim as they grow and to seek appropriate settlement areas (Neuman & Able 1998,

Staaterman & Paris 2013). PH larvae, in particular, could actively or passively use facilitated tidal transport to reach inshore settlement areas. Finally, further studies examining the effect of expansion and reduction of favorable GH settlement areas on their settlement success are needed, since bottom water temperatures could significantly alter the size of settlement habitat, and in turn, GH settlement estimates.

CONCLUSIONS

I combined biophysical modeling, synthesis of field data, and statistical analysis to determine the settlement of 2 commercially important slope-spawning flatfish in the eastern Bering Sea. Our study constitutes a significant methodological improvement upon previous biophysical modeling of larval dispersal and settlement in the region, using a settlement algorithm that allowed preferential settlement in known favorable regions revealed from field sampling. Our results indicate that interannual variability of GH and PH settlement success is caused by interactions between early life attributes (i.e., spawning depth, and pelagic duration, preferred depths) and circulation patterns in the EBS that differentially affect the 2 species. Our study also shows an overall greater dependence of GH settlement success to variations of PLD, when compared to PH. This study provides mechanistic insights on the physical processes driving patterns of distribution, connectivity, and settlement of slope-spawning flatfish in the Bering Sea. Areas of improvements for future modeling efforts of slope-spawning flatfish larval transport in the Bering Sea are also identified.

ACKNOWLEDGEMENTS

I thank Enrique Curchitser (Rutgers University) and Kate Hedstrom (University of Alaska) for development and output of the ROMS-NEP4. I thank the officers and crew of NOAA ships Miller Freeman and Oscar Dyson for collecting field data. I also thank Mary Hunsicker for reviewing an earlier version of the manuscript. This research was supported by grants from the North Pacific Research Board (Project 905) and National Science Foundation (NSF-CMG grant 0934961). This research is contribution 0792-RAA to NOAA's Ecosystem and Fisheries-Oceanography Coordinated Investigations program and is NPRB publication number XX. The

findings and conclusions of the paper are those of the authors and do not necessarily represent the views of the National Marine Fisheries Service.

Table 3.1. Dispersal pathway simulation parameters for Greenland halibut and Pacific halibut eggs to newly-settled juveniles used in the Dispersal Model for Early Life Stages (DisMELS). Transformation larvae are competent to settle after 15 days.

Species	Development stage	Duration	Cumulative day	Depth range	Vertical swimming speed	Vertical diffusion
Greenland halibut	Eggs	60 days	0 – 59	500 – 700 m	0.00004 m/s	0.0001 m/s
	Yolksac larvae	40 days	60 – 99	200 – 500 m	0.003 m/s	0.001 m/s
	Preflexion larvae	30 days	100 – 129	10 – 200 m	0.003 m/s	0.001 m/s
	Flexion/Postflexion larvae	70 days	130 – 199	10 – 100 m	0.008 m/s	0.001 m/s
	Transformation	50 days	200 – 249	10 – 100 m	0.01 m/s	0.001 m/s
	Newly-settled juveniles	21 days	250 – 270	10 – 100 m	0.02 m/s	0.001 m/s
Pacific halibut	Eggs	20 days	0 – 19	400 – 500 m	0.00006 m/s	0.0001 m/s
	Yolksac/Preflexion larvae	55 days	20 – 74	100 – 400 m	0.002 m/s	0.001 m/s
	Flexion larvae	45 days	75 – 119	10 – 100 m	0.004 m/s	0.001 m/s
	Postflexion larvae	35 days	120 – 154	10 – 100 m	0.006 m/s	0.001 m/s
	Transformation	25 days	155 – 179	10 – 100 m	0.01 m/s	0.001 m/s
	Newly-settled juveniles	21 days	180 – 200	10 – 100 m	0.02 m/s	0.001 m/s

Table 3.2. Results of the effect of sampling location on Greenland halibut (≤ 100 mm total length, TL) and Pacific halibut (≤ 150 mm TL) presence/absence from the binomial generalized additive model (GAM).

Species	Sampling location (p – value)	R-squared	Deviance explained (%)	Un-Biased Risk Estimator (UBRE)	No. of samples
Greenland halibut	$\ll 0.001$	0.63	63.3%	-0.54	376
Pacific halibut	$\ll 0.001$	0.42	44.4 %	-0.42	376

Table 3.3. Correlations between successful settlement for Greenland halibut and Pacific halibut and annual along-shelf and cross-shelf transport indices (Vestfals et al. 2014) in the eastern Bering Sea (*' = p-value ≤ 0.1 , '**' = p-value ≤ 0.05 , '***' = p-value ≤ 0.01 , '****' = p-value ≤ 0.001). F-M: February-March and A-M: April-May.

Indices	Transect	Section	Greenland halibut		Pacific halibut	
			F-M	A-M	F-M	A-M
Along-shelf transport	Bering Canyon (South)	Basin	0.02	0.25	-0.48**	-0.20
		Main	0.15	-0.04	-0.55****	-0.52**
		Shelf	0.33	0.58***	-0.31	-0.11
	Pribilof Canyon (Central)	Basin	-0.06	-0.23	-0.27	-0.04
		Main	0.21	0.17	-0.56****	-0.03
		Shelf	0.41*	0.52**	-0.32	-0.37*
	Zhemchug Canyon (North)	Basin	-0.04	0.07	-0.23	-0.15
		Main	0.24	0.09	-0.60****	-0.25
		Shelf	0.51**	0.54**	-0.26	-0.22
Cross-shelf transport	Bering Canyon		0.12	0.19	-0.25	-0.02
	Pribilof Canyon		0.38*	0.16	-0.14	-0.35
	Zhemchug Canyon		-0.10	-0.02	-0.07	-0.19
	100 m isobath		-0.35	-0.34	0.07	0.05
	200 m isobath		0.18	0.34	-0.41*	-0.23

Table 3.4. Results from sensitivity analyses testing changes in Greenland halibut and Pacific halibut settlement success in relation to changes in pelagic larval duration length (25% increase or 25% decrease) for dispersal pathway simulations from 1996/1997 to 1999/2000.

Species	Pelagic larval duration (No. of days)	Successful settlers			
		96/97	97/98	98/99	99/00
Greenland halibut	Base: 271 days	12358	1690	6207	678
	- 25%: 229 days	4948	101	132	0
	+25%: 314 days	15256	3870	17929	10231
Pacific halibut	Base: 201 days	5446	12502	2858	6255
	- 25%: 170 days	4030	8807	2298	6471
	+ 25%: 232 days	5069	14523	2452	8469

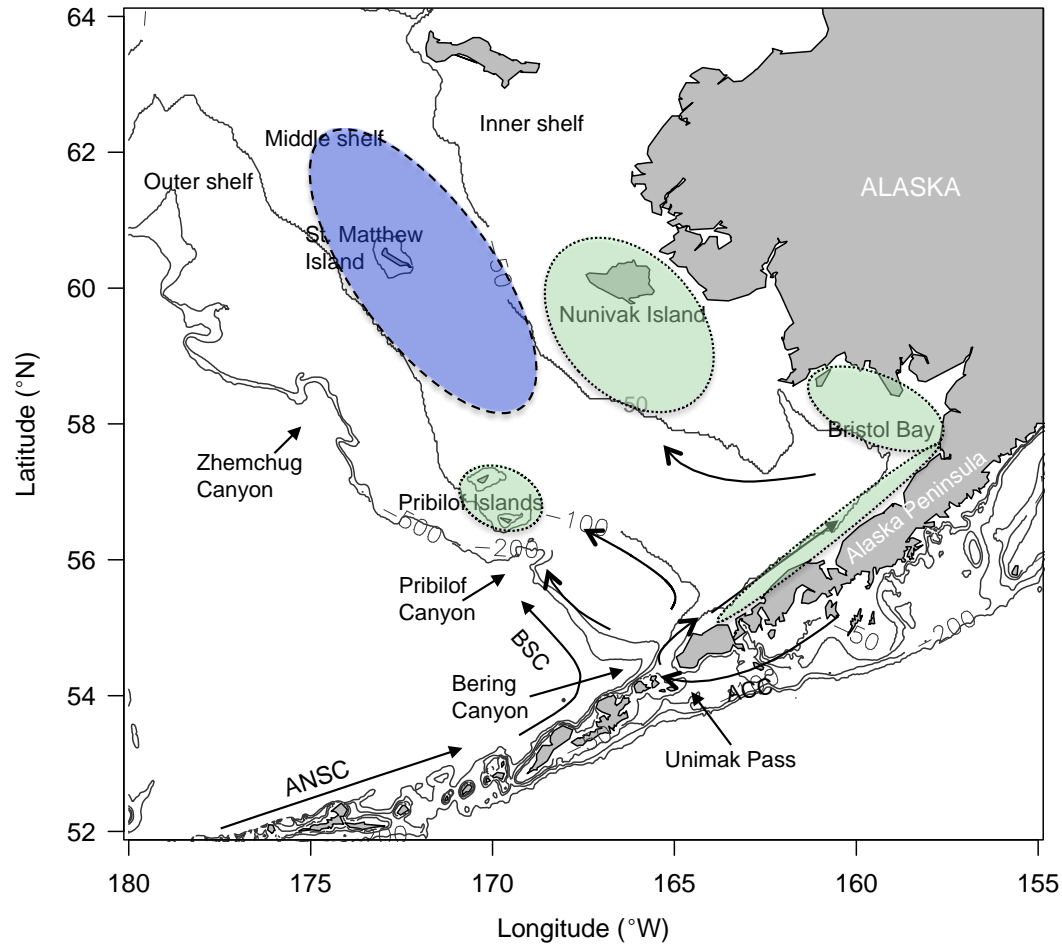


Fig. 3.1. Study area with major currents in the eastern Bering Sea. Aleutian North Slope Current (ANSC) and Bering Slope Current (BSC). Also shown is the Alaska Coastal Current (ACC) along the Alaska Peninsula. Circles indicate known settlement areas for age-0 Greenland halibut (dashed with blue color) and age-0/age-1 Pacific halibut (dotted with green color).

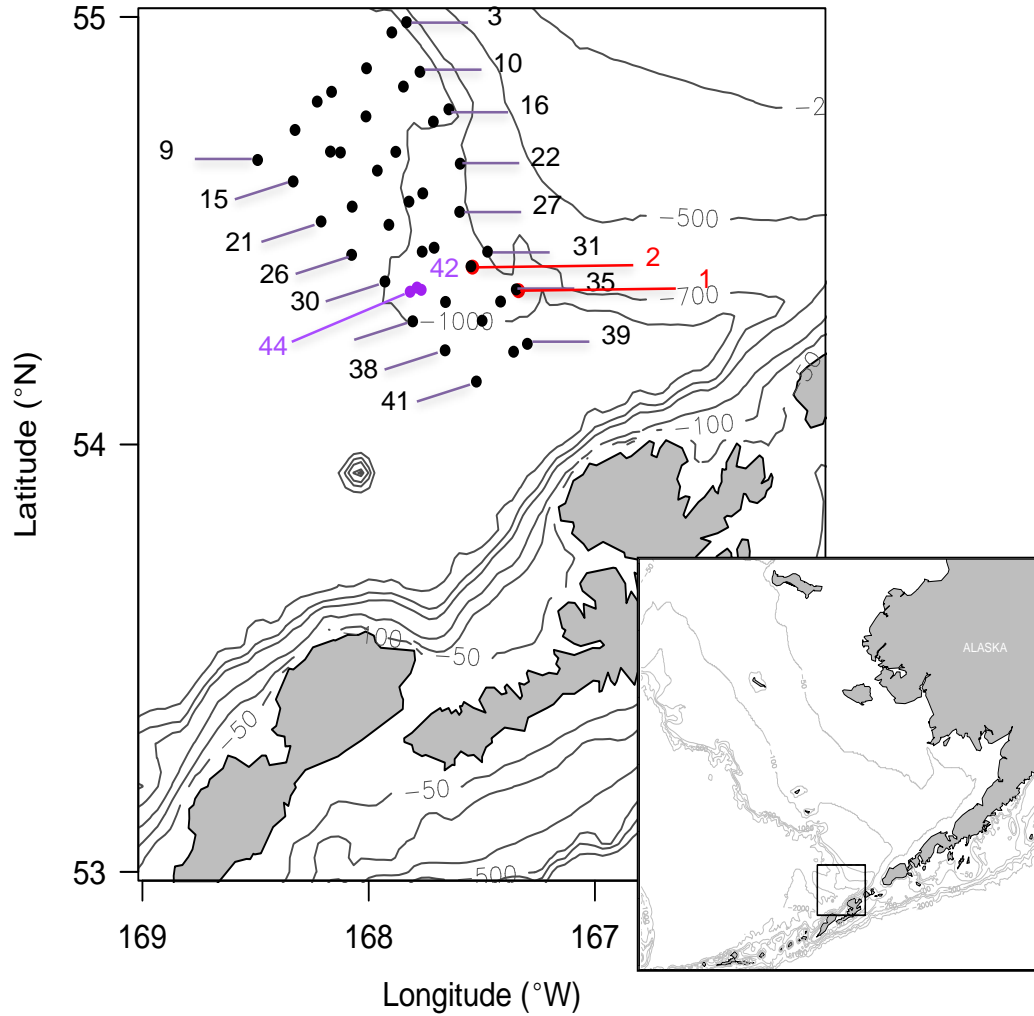


Fig. 3.2. Greenland halibut and Pacific halibut egg release locations for the DisMELS dispersal pathway simulations in the eastern Bering Sea. 1 and 2 were two locations from preliminary analysis. Three potential spawning locations (location 42-44; purple circles) were closely spaced (< 4 km) in order to check small-scale spatial variability.

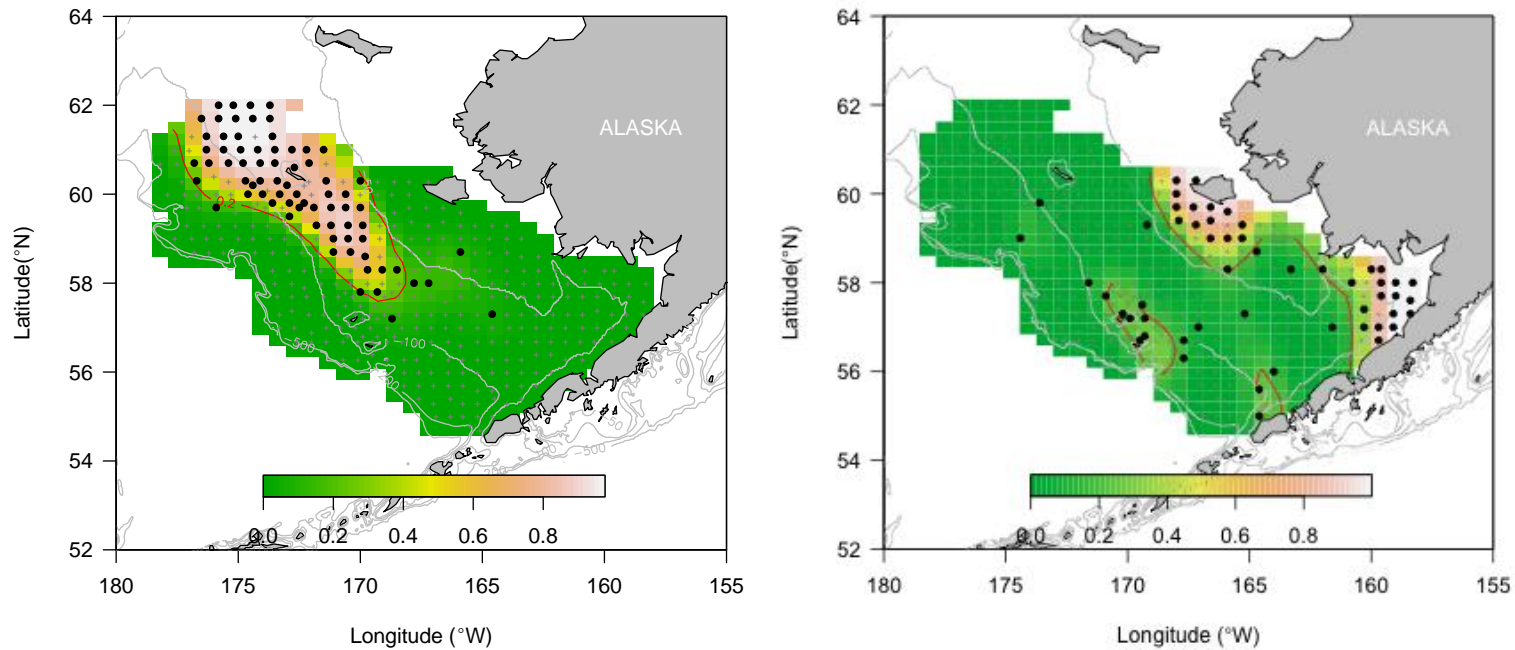


Fig. 3.3. The probability map of age-0 Greenland halibut (≤ 100 mm total length, TL; left) and age-0/age-1 Pacific halibut (≤ 150 mm TL; right) occurrence predicted by a binomial generalized additive model (GAM) using data from the eastern Bering Sea summer Groundfish Survey between 1982 to 2011. The color image shows the effect of station position on the presence/absence of each species estimated from the GAM. Red contours indicate the occurrence probability value for Greenland halibut (left; 0.2) and Pacific halibut (right; 0.2) that identify potential settlement locations for each species. Beige color indicates a relatively higher occurrence and green color indicates a relatively lower occurrence.

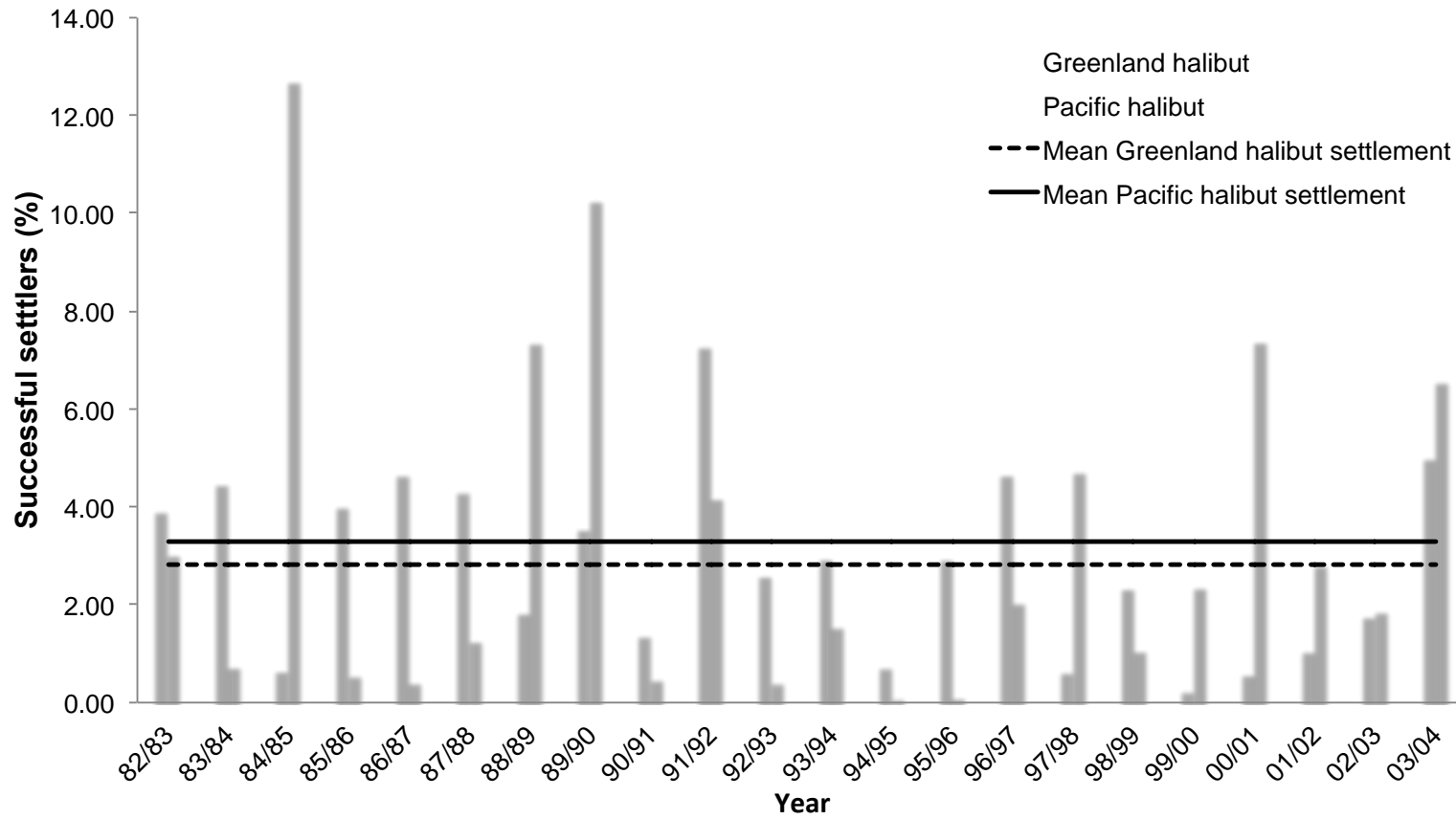


Fig. 3.4. Percentage of successful settlers for Greenland halibut (blue) and Pacific halibut (red) from the DisMELS dispersal pathway simulations between 1982/1983 and 2003/2004.

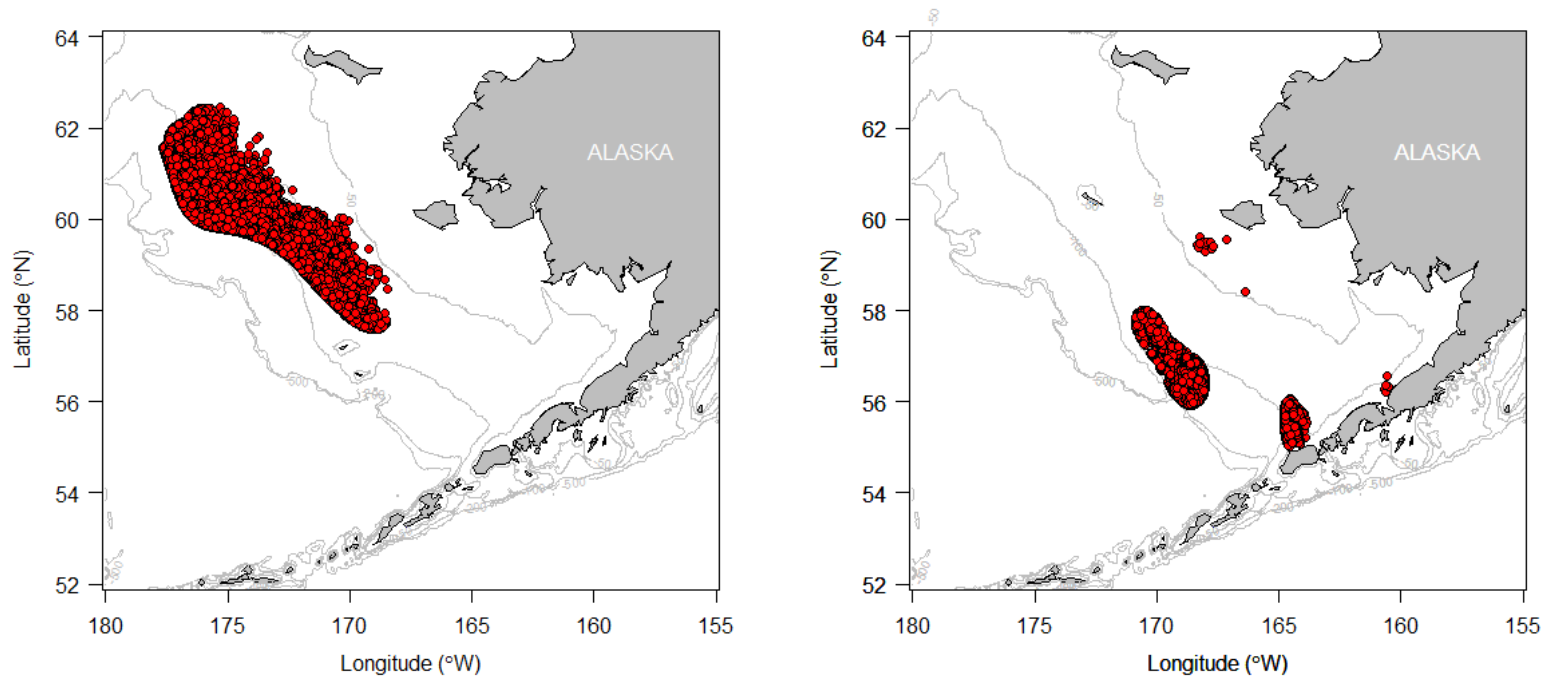


Fig. 3.5. The horizontal distributions of predicted Greenland halibut (left) and Pacific halibut (right) successful settlers over all simulation years. Red circles indicate an individual successful settler for each species that have probability of occurrence above 0.2 for Greenland halibut and Pacific halibut from 1982/1983 to 2003/2004.

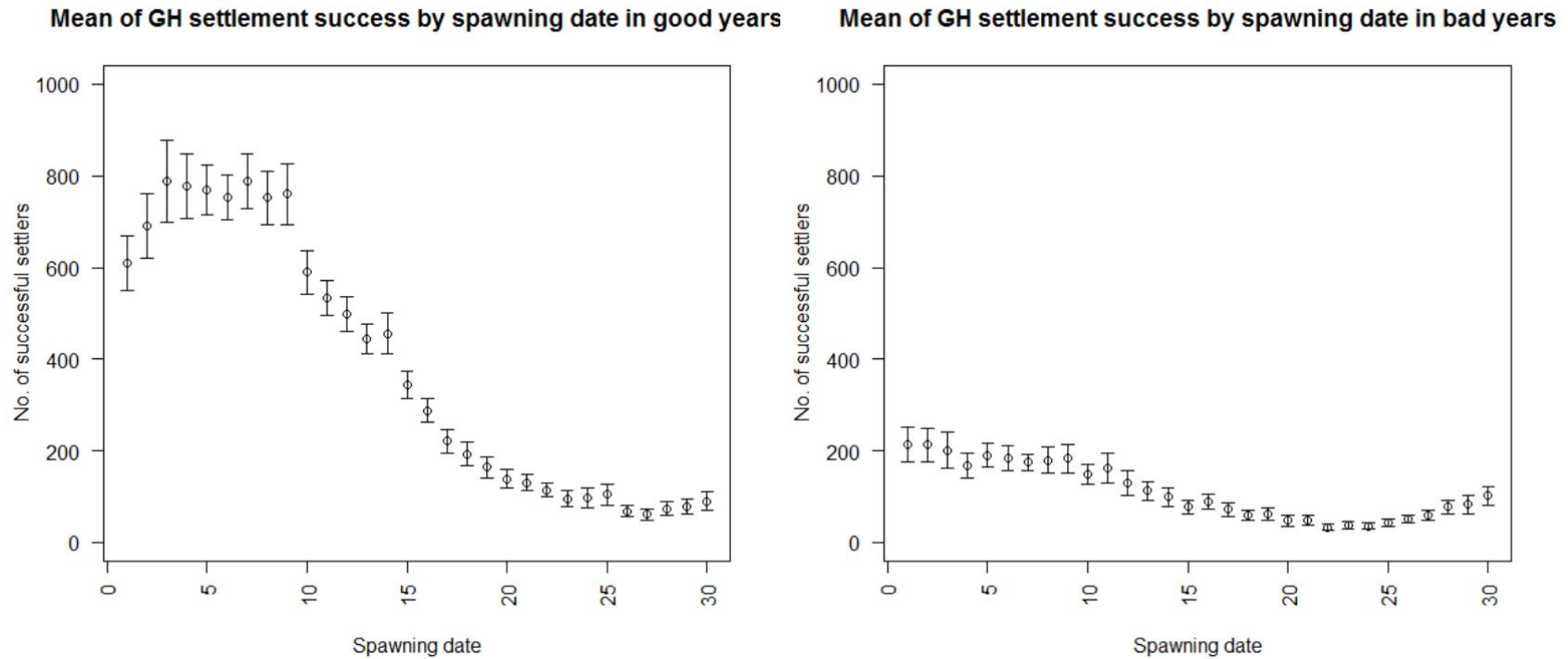


Fig. 3.6. Mean number of successful settlers by spawning date for Greenland halibut in good years (above multi-year mean; please see Fig. 3.3) and in bad years (below multi-year mean; please see Fig. 3.3). Error bars represent standard error. Spawning date 1 indicates November 2 and spawning date 30 indicates February 26 (four-day intervals).

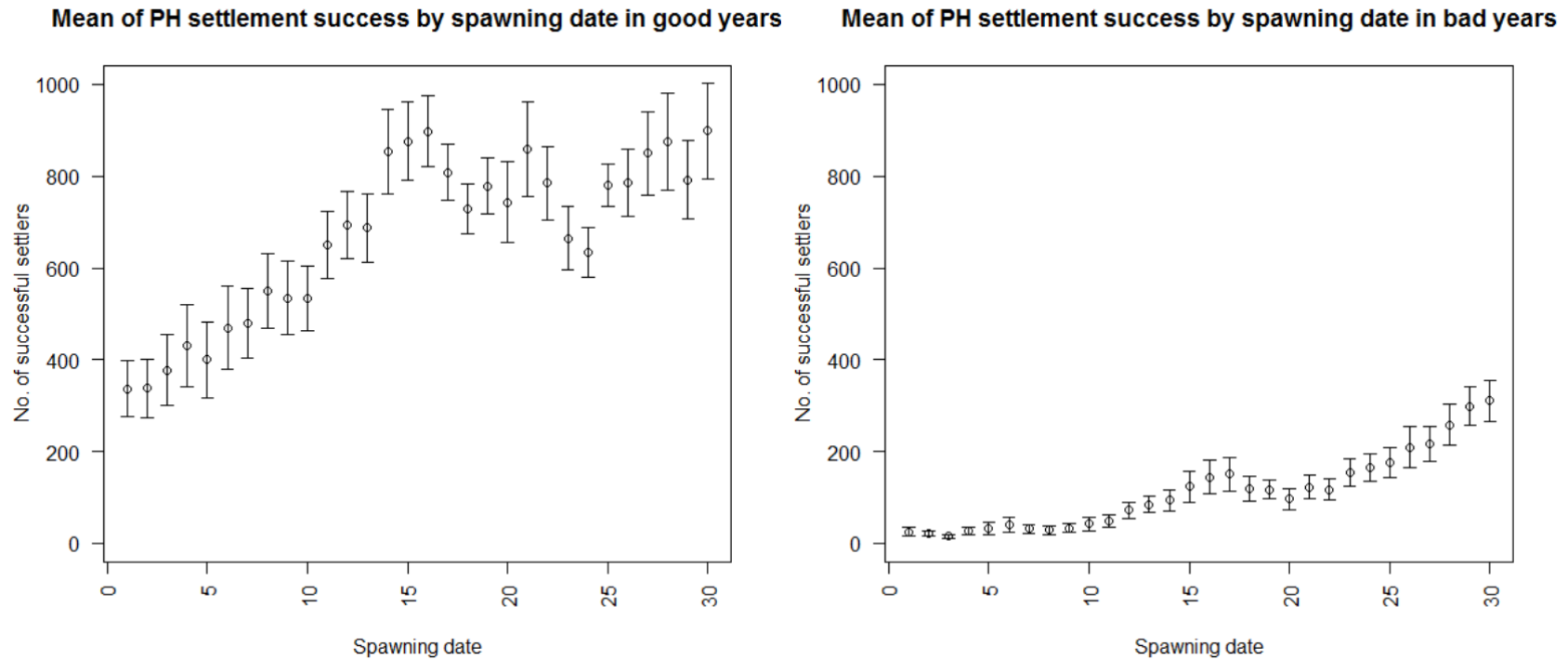


Fig. 3.7. Mean number of successful settlers by spawning date for Pacific halibut in good years (above multi-year mean; please see Fig. 3.3) and in bad years (below multi-year mean; please see Fig. 3.3). Error bars represent standard error. Spawning date 1 indicates November 2 and spawning date 30 indicates February 26 (four-day intervals).

Chapter 4. Interannual variability of size at settlement and distributions for two slope-spawning flatfish in the eastern Bering Sea

Dongwha Sohn, Lorenzo Ciannelli, Jessica A. Miller, Janet T. Duffy-Anderson,
and Delsa Anderl

In preparation:

ICES Journal of Marine Science

Oxford University Press

Great Clarendon Street

Oxford, UK

ABSTRACT

Changes in environmental conditions in marine ecosystems could directly or indirectly influence dispersal trajectories and duration, size at settlement, spatial distribution and abundance of flatfish. The slope-spawning flatfishes arrowtooth flounder (ATF; *Atheresthes stomias*) and Greenland halibut (GH; *Reinhardtius hippoglossoides*) are commercially and ecologically important in the eastern Bering Sea (EBS), which has experienced alternation between warm and cold periods since 2000. In this study, I test three hypotheses concerning the effects of environmental variables on size at settlement, distribution, and abundance, namely: (1) annual average of water temperature positively affects body length at settlement of both ATF and GH, (2) the amount of available settlement habitat increases for GH during cold years whereas that of ATF increases during warm years, and (3) habitat condition (e.g., water temperature) during the age-0 stage influences next year's age-1 abundance. To test these hypotheses, I (1) estimated body length at settlement for ATF and GH using otolith microstructure analysis and then linked size at settlement with environmental variables and (2) examined the effect of bottom temperature, and other environmental variables, on the distribution and abundance of each age-0 and age-1 stages. Results from this study showed that size at settlement for both species varied over the examined years. For ATF size at settlement was positively associated with the latitude of sampling location where ATF settled juveniles were caught. Interannual variability of size at settlement for GH was negatively correlated with ice extent and positively correlated with bottom water temperature. Collectively, these results only in part supported our initial hypotheses and indicate that other variables, most likely related to transport from spawning to settlement habitats, may be involved in determining flatfish size at settlement and distribution. The potential implications of these other variables are also investigated and further discussed in the study. Findings from this study improve the understanding of the effects of physical factors on body size at settlement and habitat variability for ATF and GH juveniles with implications for population dynamics in the EBS. Results from our study also indicate how slope-spawning flatfish will react to projected decreases in sea ice coverage and temperature increases in the EBS.

INTRODUCTION

Climate change impacts the distribution and population dynamics of ecologically and commercially important fish in marine ecosystems (Perry et al. 2005, Poloczanska et al. 2013, Pinsky et al. 2013). Changes in environmental conditions due to climate change could directly or indirectly influence the spatial distribution, abundance, and dispersal trajectories and duration with consequences on survival, body size and success of settlement of marine fish, including flatfish (Duffy-Anderson et al. 2014, Wilderbuer et al. 2002, Hufnagel et al. 2013, Petitgas et al. 2013). Slope-spawning flatfish whose offspring rely on extensive drift from the slope (spawning) to the shelf (settlement) and which require specific habitat for settlement could be especially vulnerable to environmental variability (Bailey et al. 2005, Duffy-Anderson et al. 2014). Flatfish have a variety of life-history adaptations especially during early life (Bailey et al. 2005) and a variety of habitat requirements through ontogeny. Thus, survival of flatfish in response to environmental changes could vary based on species-specific and age-specific differences in life history traits, physiological tolerances, and habitat fidelities (Rijnsdorp et al. 2009, Petitgas et al. 2013, Ciannelli et al. 2015). Improving our understanding of species-specific and age-specific reactions to climate variability and change is therefore necessary for maintaining commercially important flatfish stocks.

The eastern Bering Sea (EBS) supports many commercially and ecologically important marine organisms, including flatfish (Fig. 4.1). The EBS has experienced a prolonged cold period (2007–2012) after a prolonged warm period (2001–2005) linked to variations in areal extent of sea ice and the timing of sea ice retreat (Stabeno et al., 2012). These multiyear patterns of environmental conditions are different from conditions prior to 2000, when sea ice coverage and water temperature varied interannually (Stabeno et al. 2012). Typically, bottom water temperature in the middle shelf of the EBS during the summer, negatively correlates with sea ice extent of the previous winter (Stabeno et al. 2012). Extensive sea ice coverage during cold years results in the cold bottom layer of the middle shelf ('cold pool'; $< 2^{\circ}\text{C}$ bottom water temperature) to extend south near the Alaska Peninsula during the summer (Stabeno et al. 2012, Baker and Hollowed 2014). Variations of the cold pool extent have a strong influence on species distribution (Kotwicki and Lauth 2013, Mueter and Litzow 2008, Spencer 2008). Alternations of sea ice extent and water temperature also influence patterns in water circulations (Stabeno et al. 2012). Over the southern EBS shelf, typically the mean current flows predominantly westward in

cold years, becoming more variable in warm years (Stabeno et al. 2012). Furthermore, the position and strength of the Bering Slope Current exhibits strong seasonal and interannual variability, with stronger flow occurring close to the shelf-break during the winter and weaker flow offshore during the summer (Ladd 2014). Changes of water temperature and ocean currents in the EBS impact dispersal trajectories, dispersal duration, settlement success, and recruitment of flatfish (Duffy-Anderson et al. 2013, Ladd 2014, Vestfals et al. 2014, Sohn in preparation, Vestfals 2015).

The slope-spawning flatfishes arrowtooth flounder (ATF; *Atheresthes stomias*) and Greenland halibut (GH; *Reinhardtius hippoglossoides*) are two ecologically important species in the EBS. The former is a boreal species at the northernmost range of its distribution in the EBS, while the latter is of Arctic origin, at the southernmost range of its distribution. Both species spawn in deep water (≥ 400 m) along the continental slope during winter and have a relatively long pelagic larval duration before settlement, usually more than 6 months for GH (Sohn et al. 2010), and about 4 months for ATF (Bouwens et al. 1999, De Forest et al. 2014). After hatching, their larvae ascend through the water column as they develop. Late larvae cross onto the continental shelf (nursery) from the slope (spawning) for settlement. However, ATF and GH show different habitat associations during settlement. Juvenile GH (≤ 100 mm total length (TL)) are mostly found around St. Matthew Island in the middle shelf region (Sohn et al. 2010), but since 2009 their range of distribution has expanded to south of the Pribilof Islands due to the increasing size of the cold pool in the bottom layer of the EBS middle shelf (Ianelli et al. 2010, Sohn et al. 2016). Juvenile arrowtooth flounder (≤ 100 mm TL) concentrate mostly on the southeastern outer shelf area (De Forest et al. 2014; Table 4.1 and Fig. 4.1). The adult biomass and recruitment trends of ATF and GH in the EBS have fluctuated differentially during the last three decades. GH adult biomass has declined while ATF has increased (Ianelli et al. 2011, Spies et al. 2014). In recent years (2007-2010), GH age-0 recruitment has increased while ATF age-1 recruitment has decreased, especially in 2009 and 2010 (below average recruitment from 1961 to 2015) (Ianelli et al. 2011, Spies et al. 2014). These latest signs of GH age-0 recruitment coincided with the decreasing average bottom temperature (cold years) in the EBS. Unlike ATF, GH expanded their distribution and increased in abundance in cold years. Diverging recruitment dynamics between the two species in the EBS could result from species-specific responses to

changes in water temperature and circulation that are encountered during both pre-settlement and post-settlement stages.

Water temperature, and current direction and speed have been shown to be the most important factors influencing size at settlement, distributions, and abundance of flatfish. Water temperature directly affects flatfish growth rates, which in turn, impacts dispersal duration and size at settlement for flatfish (Nash and Geffen 2005, Laurel et al. 2014). For example, based on laboratory experiments (Laurel et al. 2014), size at settlement of northern rock sole was smaller with longer larval duration in colder temperatures. Fedewa et al. (2016) also found that the timing of metamorphosis (eye migration) of northern rock sole in the Gulf of Alaska was earlier in warmer years although fish size at metamorphosis was similar across years based on observation data and otolith microstructure analysis. During the settlement phase, slower growing and smaller individuals in cold temperature can suffer high mortality due to size-dependent predation and feeding success (Ellis and Gibson 1995, Van der Veer et al. 1997). Also, changes in temperature can alter the distribution and abundance of flatfish throughout ontogeny due to changes in habitat availability (Spencer 2008, Mueter and Litzow 2008, Cooper et al. 2014, Baker and Hollowed 2014). For example, suitable habitat for northern rock sole juveniles in the EBS has been reduced with decreasing water temperature (Cooper et al. 2014). Change in prevailing circulation patterns is another important physical factor that affects dispersal trajectories and durations from spawning to settlement areas (Wilderbuer et al. 2002, Duffy-Anderson et al. 2013, Hufnagel et al. 2013, Petitigas et al. 2013, Vestfals 2015). This could cause variation in size at settlement and recruitment variability of flatfish.

Several authors, using modeling approaches, are examining how changes in EBS environmental conditions have affected dispersal trajectory, duration, settlement success and recruitment of several flatfish, focusing mostly on pre-settlement stages (Wilderbuer et al. 2002, Duffy-Anderson et al. 2013, Vestfals et al. 2014, Vestfals 2015, Sohn et al. in preparation). For example, Wilderbuer et al. (2002) showed that recruitment variability of flatfish including ATF coincided with decadal scale changes in wind-driven advection of their larvae to juvenile nursery grounds; their recruitment increased with increasing on-shelf transport. Duffy-Anderson et al. (2013) also reported that interannual variability in currents possibly alters dispersal trajectory during the pelagic larval duration of GH, which could cause variations in their survival.

Currently, there still is a knowledge gap with respect to how changes in temperature and circulation patterns affect variations in size at settlement, distribution and abundance during early juvenile stages of ATF and GH.

In this study, I address three hypotheses; (1) body length at settlement for both ATF and GH is larger during warm years than during cold years due to temperature, (2) the amount of available settlement habitat increases for GH during cold years whereas that of ATF increases during warm years, and (3) bottom water temperature experienced during age-0 for both species affects next year's age-1 abundance. To address these three hypotheses, I (1) estimated body length at settlement for ATF and GH using otolith microstructure analysis, (2) examined the relationship between body length at settlement and environment variables such as bottom water temperature, sampling location (bottom depth and latitude), ice cover index, and along-shelf and on-shelf winds using a correlation analysis, and (3) examined the effect of bottom water temperature on the spatial distribution and abundance of the two species from age-0 to age-1.

MATERIALS AND METHODS

Data sources

To estimate body length at settlement (transition phase from pelagic to benthic habitats) for ATF and GH using otolith microstructure analysis, I obtained available otoliths (sagittae) for the two species (≤ 170 mm total length (TL)) collected between 2000 and 2011 from the Alaska Fisheries Science Center (AFSC). The otolith samples for both species were collected during the EBS shelf summer bottom trawl groundfish survey (hereafter: Groundfish Survey) conducted by the National Oceanic and Atmospheric Administration (NOAA) AFSC's groundfish assessment program. The Groundfish Survey has been conducted annually beginning early May or June and extending into late October to sample stations within a systematic grid design (Lauth and Nichol 2013). Samples were collected by bottom trawling at 376 fixed stations that centered in each 20×20 nautical mile grid square (or corner station, in the case of high-density strata) in the continental shelf region of the EBS (Lauth and Nichol 2013). The gear used is a 25.5×34.1 m eastern otter trawl with a 25.5 m headrope and a 34.1 m footrope. The net consists of 10.2 cm stretched mesh in the body and wing, 8.9 cm stretched mesh in the intermediate and codend, and 3.2 cm mesh in the codend liner (Stauffer 2004). The net is attached to paired chains and

dandy lines, and a net mensuration system is used to measure net height and width while towing. Tows are typically 30 min. in duration at a speed of 3 knots. Estimates of net width are used in calculations of area swept. During the surveys, taxa were identified and total counts and weights were recorded for each individual of both species at each tow. Also, body length for a subset of individuals was measured to the nearest mm total length for flatfish. Species abundance data for each sampling station were standardized as catch per unit effort (CPUE; catch weight (kg) divided by area swept (ha) estimated as mean net width multiplied by distance towed).

Environmental data, including sea surface temperature, bottom temperature, and bottom depth, were recorded at each station using a Sea-Bird SBE-39 datalogger attached to the headrope of the trawl (Lauth 2011). More specific information about the Groundfish Surveys can be found in Lauth (2011) and Stauffer (2004). For establishing relationships between otolith size and body length of each species, I also obtained body length for each fish for ATF and GH corresponding with otolith samples. To examine the effects of environmental variables on the spatial distribution and abundance of ATF and GH age-0 and age-1, catch (CPUE), body length, and environmental data between 1982 and 2012 were obtained from the Groundfish Survey.

Otolith analysis and criteria for settlement check mark on ATF and GH otoliths

Otoliths are useful for estimating growth and age of fish (Pannella 1971, Campana and Neilson 1985). Otolith size is often proportional to fish body length. Otolith size and microstructure have also been used to infer developmental (e.g., metamorphosis) and behavioral (e.g., settling from pelagic to benthic) changes through different life stages of fish (Campana and Neilson 1985). For example, in GH larvae collected in the Atlantic Ocean, early check marks indicate hatching and first feeding or change in larval vertical distribution associated with temperature changes (Stenberg 2007). In flatfish otoliths, accessory primordia are often formed at the outer edge of the sagittae during eye migration (Sogard 1991, Modin et al. 1996, Joh et al. 2005, Fedewa 2015, Fedewa et al. 2016). Prior to accessory primordial formation, otoliths are circular and symmetrical.

Bouwens et al. (1999) found a settlement check mark in ATF otoliths from the Gulf of Alaska corresponding to the translucent band immediately surrounding the inner portion (“kernel”; a dense and opaque structure) of an ATF otolith (Fig. 4.2). For GH, like ATF, I

assumed that a similar check mark, delineated by discontinuity or contrast pattern, would also correspond to the settlement time. To verify this assumption, I assessed whether the putative settlement check mark was present in otoliths from settled individuals and absent in otoliths from individuals that had already undergone metamorphosis and were still in the pelagic phase at the time of capture. Pelagic post-metamorphosis (eye migration) GH larvae samples that were still in the water column were obtained from the Bering-Aleutian Salmon International Survey (BASIS) cruises (mid-water trawling) from 2009 to 2011. Each individual GH was measured in standard length (SL; from the tip of the snout to the end of the caudal peduncle mm) and then sagittal otoliths were removed. GH otoliths from settled individuals were obtained from the Groundfish survey (bottom trawling). Both pelagic larvae including postflexion and transform stages and settled juveniles were used to establish a relationship between fish body length and otolith length (Fig. 4.3). All settled juveniles were larger than >89 TL mm, while pelagic larvae were <75 SL mm. Otolith lengths of pelagic larvae ranged between 0.6 mm to 1.4 mm, and none of the otoliths had a opaque zone. In contrast, all otoliths from settled juveniles (>89 mm) caught in the bottom trawls had a translucent zone around the dense opaque area, corroborating the presence of a settlement mark at the interface between the translucent and opaque zone of the otolith. Kernel length did not change with increasing GH body length (Fig. 4.3), but there was a clear relationship between otolith length and body length. Based on these observations, I concluded that the observed check in GH otoliths is indeed a settlement check.

Otolith measurements

Right and left otoliths for ATF (2004 – 2006, 2008 – 2009) and GH (2000 – 2003, 2007 – 2011) were imaged using a Leica (DFC290) camera and a dissecting microscope with reflected light. All otoliths were examined against a black background that made the translucent zones appear dark and the opaque zone appear light. Image analysis software (Imaging Software Integrates Leica Automated Microscopes and Digital Cameras Leica Application Suite 4.1 version) was used to measure otolith and kernel sizes (length; longest axis from anterior to posterior and width; longest perpendicular axis from dorsal to ventral) on both right and left otolith images. I measured 208 and 376 otolith sizes for ATF and GH, respectively (Table 4.1).

Statistical analysis

I assessed the difference between the left and right otolith sizes for ATF and GH using a paired t-test. For ATF, there was no significant difference ($t = -1.79$, $df = 185$, and $p\text{-value} = 0.07$). For GH, I found that there were significant differences between left and right otolith length ($t = -29.07$, $df = 342$, and $p\text{-value} < 0.01$) and left and right otolith width ($t = 12.73$, $df = 331$, and $p\text{-value} < 0.01$). In this study, for GH, I used the width of the right otolith to establish a relationship between body length and otolith sizes (width) using simple linear regression models. I chose the width for GH instead of the length because the former had a better (higher R^2) relationship with body size. For ATF, the relationship between body length and otolith width was not significant. Therefore, I used otolith length to establish a linear relationship between body length and otolith size (Fig. 4.4). For both ATF and GH, I found a positive linear relationship between body length and otolith size (length (ATF) and width (GH); Figs. 4.4 and 4.5).

After estimating body length at settlement based on the relationship between the otolith length (ATF) and otolith width (GH), I performed correlation analyses between mean size at settlement in each year and environmental variables, including sampling location (latitude), bottom depth, bottom temperature, Ice Cover Index (ICI), and winds (along-shelf and cross-shelf) using the Pearson's correlation. The latitude and bottom depth data were obtained from the Groundfish survey. Bottom temperature was also extracted from the Groundfish survey at all sampling stations in the middle shelf and was then used to calculate the average bottom temperature in each year in order to serve as an index of warm and cold years in the EBS (Appendix 4.1). The ICI was obtained from NOAA's Bering Climate website (<http://www.beringclimate.noaa.gov/data/index/php>) and is the average ice concentration for winter (January 1st-May31st) in the $2^\circ \times 2^\circ$ box in the EBS ($56^\circ\text{-}58^\circ\text{N}$, $163^\circ\text{-}165^\circ\text{W}$) for each year from 1979 to 2013 (Appendix 4.1). Monthly mean u and v surface winds in April (1000 mb) were obtained from the NCEP-DOE Reanalysis 2 data provided by the NOAA/OAR/ESRL PSD, Boulder, Colorado, USA, from their website (<http://www.esrl.noaa.gov/psd/data/gridded/data.ncep.reanalysis2.html>; Kanamitsu et al. 2002) and were averaged over the area $54^\circ\text{-}58^\circ\text{N}$ and $165^\circ\text{-}175^\circ\text{W}$. The obtained u surface wind was rotated 315° counterclockwise into the along-shelf direction (northwesterly; blowing from northwest (negative value) to southeast (positive value) and the v surface wind was also rotated

315° counterclockwise into the on-shelf direction (southwesterly; blowing from southwest (negative value) to northeast (positive value)) (Appendix 4.1).

Effect of water temperature on abundance and distribution of ATF and GH from age-0 to age-1

ATF and GH age-0 and age-1 were identified by body length categories based on the estimated size at settlement, the groundfish survey data, and stock assessment (Spies et al. 2014, Barbeaux et al. 2014). The range of ATF body lengths was ≤ 100 mm for age-0 and 110 - 160 mm for age-1. For GH, the range was ≤ 120 mm for age-0 and 130 - 180 mm for age-1. The numerical catch of individuals from each age group was standardized by area swept.

To examine effects of environmental variables on age-0 and age-1 ATF and GH spatial distribution and abundance and to test the second hypothesis that the amount of available settlement habitat increases for GH during cold years whereas that of ATF increases during warm years due to temperature, I used a variable coefficient generalized additive model (GAM) (Ciannelli et al. 2004, Bartolino et al. 2011, Ciannelli et al. 2012, Hunsicker et al. 2013), where the effect of a covariate is allowed to change gradually over space in relation to other covariates included in the model. In my model, the relationship between species abundance and local bottom temperature is spatially variable and locally linear (Hunsicker et al. 2013). Environmental variables in the fully fitted model included local bottom temperature, and sampling location (latitude and longitude). For this GAM analysis, I used the bottom temperature in the sampling location where each species was collected during the Groundfish survey. The value for bottom temperature was standardized based on the mean and standard deviation of the full dataset. The full model for age-0 ATF and GH was formulated as follows:

$$x_{y,(\varphi,\lambda)} = y + s_1(\varphi, \lambda) + s_2(\varphi, \lambda)T_{y,(\varphi,\lambda)} + e_{y,(\varphi,\lambda)}$$

where $x_{y,(\varphi, \lambda)}$ is the natural logarithm of numerical CPUE (+ 1) of age-0 ATF and GH at a particular location φ, λ (identified by longitude and latitude degrees), in year y (as factor). T indicates local bottom temperature. s_1 is a 2-dimensional smoothing function (thin plate regression spline, Wood 2006) that captures the underlying spatial distribution of the flatfish which is not otherwise captured by the other covariates. s_2 is a two-dimensional smoothing function that define the local linear effect of bottom temperature (T) on the dependent variable x .

To test the third hypothesis, about the effect of annual average of bottom temperature experienced during the age-0 on the age-1 stage abundance, the mean bottom temperature from age-0 habitat for each species was used as factor in the full model for age-1. The full model for age-1 ATF and GH was formulated as follows:

$$x_{y,(\varphi,\lambda)} = BT_{y-1} + s_1(\varphi,\lambda) + s_2(\varphi,\lambda)T_{y,(\varphi,\lambda)} + e_{y,(\varphi,\lambda)}$$

where $x_{y,(\varphi,\lambda)}$ is the natural logarithm of numerical CPUE (+ 1) of age-1 ATF and GH at a particular location φ, λ (identified by longitude and latitude degrees). BT indicates the mean bottom temperature experienced during the age-0 stage for each species and is used as factor. A backwards selection process was used for determining the best model by minimizing the Akaike Information Criterion (AIC) and the generalized cross validation (GCV). The GAM analysis was conducted using the mgcv-package (version 1.7-24; Wood 2006) in R version 3.0.1 (2013). To calculate mean bottom temperature experienced during age-0 stage (BT), occurrence probability maps of settlement locations for ATF and GH were estimated from the Groundfish Survey data from 1992 to 2012 for ATF and from 1982 to 2012 for GH, using a binomial GAM with the logit link function. Sampling location, captured through the interaction between latitude and longitude, was the only model covariate used in the presence/absence GAM. The analysis was restricted to individuals ≤ 100 mm TL for both species. To define ATF and GH settlement regions, I selected the threshold value for the probability of ATF and GH occurrence that produced the greatest difference between the percentage of presence stations minus the percentage of absence stations included within the threshold (see chapter 3). Thus, the selected probability threshold for delineating settlement locations contained the highest number of presence stations and the lowest number of absence stations for the target species.

RESULTS

Interannual variability of size at settlement

Estimated size at settlement varied over time for both species (Fig. 4.6). The median size at settlement for ATF was the smallest in 2004 (warm year; 44.5 mm TL) and largest in 2008 (cold year; 65.1 mm TL; Fig. 4.6). However, no significant correlation was found between ATF

size at settlement and mean summer bottom temperature in the middle shelf of the EBS and the ICI (Table 4.2). The latitude of sampling locations was the only significant variable to affect ATF size at settlement – ATF significantly increased with increasing latitude (Table 4.2).

For GH, the median of estimated body length at settlement was larger in 2001- 2003 (warm years; range of size at settlement between 95.5 mm and 125.2 mm TL) than in 2007-2011 (cold years; range of size at settlement between 84.7 mm and 92.8 mm TL) (Fig. 4.6). GH size at settlement significantly increased with increasing mean bottom temperature in the middle shelf of the EBS (Table 4.2). Also, when the ICI increased, size at settlement for GH significantly decreased (Table 4.2). There was no significant relationship between GH size at settlement and bottom depth and between GH size at settlement and latitude of sampling location (Table 4.2). Like ATF, neither on-shelf wind (southwesterly; blowing from southwest to northeast; Table 4.2) nor along-shelf wind (northwesterly; blowing from northwest to southeast; Table 4.2) significantly correlated with GH size at settlement in each year (Table 4.2).

Effect of water temperature on the abundance and distribution of ATF and GH juveniles

Based on results from the best-fitted variable coefficient GAM, settled age-0 ATF abundance and distribution were significantly influenced by local bottom temperature (Table 4.3 and Fig. 4.7). Age-0 ATF abundance increased and their distribution expanded to the middle shelf when local temperature increased (Fig. 4.7). Age-1 ATF abundance and distribution were significantly affected by sampling location, local bottom temperature, and mean bottom temperature of age-0 fish habitat (Table 4.4 and Fig. 4.8). Age-1 ATF distribution expanded to the middle shelf from the outer shelf with increasing local bottom temperature (Fig. 4.8). Although the bottom temperature experienced during age-0 ATF has a significant effect on abundance in all years, there is no consistent trend across the study period (Table 4.4 and Appendix 4.3).

For age-0 GH, sampling location and bottom temperature had significant effects on their abundance and distribution (Table 4.3 and Fig. 4.9). Opposite to age-0 ATF, age-0 GH distribution expanded their distribution to the outer shelf when local bottom temperature decreased (Fig. 4.9). Age-0 GH were highly concentrated in the middle and outer shelves between 57°N and 62°N. Age-1 abundance increased in the outer shelf with decreasing local

bottom temperature, but increased in the middle shelf around St. Matthew Island with increasing local bottom temperature (Fig. 4.10). The bottom temperature range experienced during the GH age-0 significantly affects the abundance of age-1 GH in some years; age-1 abundance increased when average bottom temperature experienced during age-0 was relatively low (Table 4.4 and Appendix 4.4).

DISCUSSION

Using combined historical field observations and laboratory work, this study addressed (1) interannual variation in size at settlement for ATF and GH in relation to changes in environmental variables, (2) the effect of bottom temperature on age-0 and age-1 ATF and GH abundance and distribution, and (3) the effect of bottom temperature experienced during age-0 habitat of each species on their age-1 abundance and distribution. Prior to this study, there was no knowledge about size at settlement for ATF and GH and how environmental factors could affect changes in size at settlement for the two species in the EBS. Furthermore, little is known about the effect of factors such as bottom temperature on distribution and abundance of ATF and GH settled juveniles (age-0 and age-1) in the EBS, although previous studies (i.e., Mueter and Litzow 2008, Spencer 2008, Kotwicki and Lauth 2013, and Vestfals 2015) in the EBS showed significant effect of bottom temperature on abundance and distribution of the adult stage. Results from our study will have implications for understanding species-specific response of slope-spawning flatfish to projected decreases in sea ice coverage and temperature increases in the EBS.

Our results from otolith microstructure analysis showed that the range in median estimated size at settlement for ATF is 44.5 mm to 65.1 mm TL in the EBS. This result is similar to previous research in the Gulf of Alaska although the degree of variation in the range of size at settlement is larger in this study. Bouwens et al (1999) showed that ATF settle at 40 to 45 mm SL based on otolith analysis and field observation data - pelagic ATF > 40 mm SL were not caught in the Gulf of Alaska. For GH, our results indicate that the range of estimated median body length at settlement was between 78.1 mm and 125.2 mm TL. This result is consistent with historical field observation data in the EBS. Based on the historical Groundfish survey data, the

smallest size of settled GH juvenile was 60 mm TL. The size of the largest GH pelagic larvae in the BASIS survey was 100 mm SL. Therefore, otolith analyses including kernel size measurement and the relationship between otolith size (length or width) and body length for ATF and GH proved to be a useful tool to estimate size at settlement for both species.

The estimated size at settlement for ATF and GH varied by year, in correlation with environmental variables such as latitude of sampling location for ATF and the ICI and mean summer bottom temperature in the middle shelf of the EBS for GH. However, results did not support our hypothesis that size at settlement for both ATF and GH is larger during warm years than during cold years. Size at settlement for GH is larger during warm years than during cold years, but not for ATF. Water temperature is one of the dominant factors that directly influences growth and development rates of flatfish (Nash and Geffen 2014). Growth and development rates of most flatfish increase with warmer temperatures and up to an optimal high temperature threshold if there is no food limitation, resulting in metamorphosis and settlement at larger sizes (Burke et al. 1999, Benoit and Pepin 1999, Laurel et al. 2014). For example, growth rate and size at settlement of northern rock sole increased at higher temperature (Laurel et al. 2014).

Other environmental factors including currents that influence dispersal trajectory and dispersal duration of ATF and GH from spawning to settlement could also differentially influence size at settlement for each species. Although there is a lack of significant correlation between size at settlement for ATF and GH and April mean on-shelf wind (blowing from southwest to northeast)/along-shelf wind (blowing from northwest to southeast), there was a significant negative correlation between April mean on-shelf wind and the ICI in the EBS; on-shelf wind significantly increased when the ICI decreased (Appendix 4.2). This result indicates that it is possible that strong southwesterly on-shelf wind in warm years could generate southeastward Ekman transport that delay GH larval transport to their settlement area, located on the northern side of the EBS middle shelf. Based on the NEP4 (Northeast Pacific version 4) ROMS (Regional Ocean Model System) model, Vestfals et al. (2014) found that along-shelf transport decreased when winter (December-March) southwesterly on-shelf wind increased. Also, Vestfals et al. (2014) found on-shelf transport across the 200 m isobath was negatively correlated with ice coverage. The strong on-shelf transport across the shelf break in the EBS could favor ATF larvae that are competent to settle, allowing them to reach their settlement area

faster, resulting in a decrease in size at settlement. In cold years, extensive sea ice coverage to the south close to Bering Canyon and to the west up to 200 m isobath could decrease on-shelf transport, which would likely impede ATF larval transport to their settlement area in the southern outer shelf. When northwestward Ekman transport increases, ATF larvae may take a longer time to reach their settlement area or may advect to unsuitable habitat.

Our results from the GAM analysis for age-0 ATF and GH support the second hypothesis that the amount of available settlement habitat increases for GH during cold years whereas that of ATF increases during warm years. ATF and GH require different habitats for their settlement and nursery areas in the EBS. ATF settle initially in the outer shelf of the southern part of the EBS. GH settle in the middle shelf of the northern part of the EBS around St. Matthew Island and then move to a deeper depth as they grow (Sohn et al. 2010). Both age-0 and age-1 GH abundance was higher with decreasing bottom temperature, and they expanded their distribution from the middle shelf to the outer shelf. However, both age-0 and age-1 ATF abundance was higher with increasing bottom temperature, and they also expanded their distribution from the outer shelf to the middle shelf. These results are consistent with previous studies and field observations (Ianelli et al. 2011, Ciannelli et al. 2012, Hunsicker et al. 2013, Sohn et al. 2016). Settled juvenile GH (<100 mm TL) expand their range to the south of the Pribilof Islands in cold years, which is likely due to an increase in the extent of the cold pool due to expanded winter sea ice coverage (Ianelli et al. 2011 and Sohn et al. 2016). ATF (> 200 mm TL) spatial distribution and abundance have increased with warming temperature, resulting in increasing habitat overlap with their prey (age-0/age-1 pollock) (Ciannelli et al. 2012, Hunsicker et al. 2013). Additionally, various environmental variables not included in my study, including sediment type and depth as well as water temperature could influence adult ATF and GH spatial distribution and abundance after settlement (Swartzman et al. 1992, McConnaughey and Smith 2000, Mueter and Litzow 2008, Spencer 2008 and Kotwicki and Lauth 2013).

Based on our results about variations in size at settlement and distribution in relation to changes in environmental variables, in cold years, GH larvae would reach their settlement area faster and would have a smaller size at settlement due to the expansion of their settlement habitat and strong along-shelf transport compared to warm years. ATF may exhibit exactly the opposite pattern. In warm years, expanded settlement habitat and weak along-shelf and strong on-shelf

transport for ATF would allow them to reach suitable settlement locations earlier and they would therefore have a smaller size at settlement.

In the presence of size-selective predation mortality, it is likely that variation of size and location at settlement influences survival. Larger individuals can avoid high mortality due to size-dependent predation and feeding success. However, if the amount of suitable habitat after settlement is smaller, there may be a decrease in survival due to increased competition for limited resources. Based on stock assessment, ATF age-0 recruitment decreased in recent cold years (2009-2011; Spies et al. 2014). This result may indicate that ATF age-0 survival is low in cold years although their size at settlement is relatively large. For GH, age-0 recruitment increased in recent cold years (2007-2010; Barbeaux et al. 2014). This result may indicate that GH age-0 survival is high in cold years although their size at settlement is relatively small. Therefore, available habitat size could be more important than size selective predation mortality for their survival.

My results support the hypothesis that bottom temperature experienced during age-0 for both species affects next year's age-1 abundance. Survival during age-0 associated with habitat bottom temperature could directly influence age-1 abundance, especially for GH. I found no clear relationship between age-1 ATF abundance and water temperature during the age-0 phase, indicating that a combination of small size at settlement (warm years) and high extent of the settlement habitat (warm years), contribute to the recruitment success of ATF. Given that ATF settle in locations that are densely populated by piscivorous groundfish (e.g., Pacific cod, other adult flatfish and pollock), one would expect that both physical (habitat extent) and biological (settlement size and predation pressure) factors contribute to their recruitment success.

CONCLUSION

Understanding variability of size at settlement, distribution, and abundance is important for predicting and managing the population dynamics of ATF and GH in the EBS. Interannual variability of size at settlement for the two species is directly or indirectly related to changes in environmental variables including bottom water temperature and ice extent, which influence growth rate and currents. Our results imply that there are species-specific differences in size at

settlement and habitat size of ATF and GH in response to environmental variability. Our results improve our understanding of the effect of physical factors on body-size at settlement and habitat variability for ATF and GH juveniles. Also, results from our study have implications for how the two slope-spawning flatfish may react to projected decreases in sea ice coverage and temperature increases in the EBS. While I characterized the effect of environmental variables on size at settlement and habitat size for age-0 and age-1 ATF and GH, there is still a lack of knowledge about growth rates, food availability, and predation pressure for the two species during early life stages in the EBS. These aspects relating to changes in size at settlement and habitat size for the two species in the EBS need to be further investigated.

ACKNOWLEDGEMENTS

I thank the officers and crew of NOAA ships Miller Freeman and Oscar Dyson for collecting field data. This research was supported by grants from the North Pacific Research Board (Project 1205). This research is contribution 0792-RAA to NOAA's Ecosystem and Fisheries-Oceanography Coordinated Investigations program and is NPRB publication number XX.

Table 4.1. Number of useful otolith samples for Greenland halibut pelagic larvae (< 80 mm standard length) and settled juvenile arrowtooth flounder and Greenland halibut (\leq 170 mm total length) in the eastern Bering Sea.

Year	Year	No. otolith of arrowtooth flounder	No. otolith of Greenland halibut
Pelagic larvae	2009	-	12
	2010	-	17
	2011	-	7
Settled juveniles	2000	-	22
	2001	-	20
	2002	-	15
	2003	-	8
	2004	18	-
	2005	29	-
	2006	36	-
	2007	-	57
	2008	24	60
	2009	33	46
	2010	36	108
2011	32	40	

Table 4.2. Correlations coefficients between size at settlement for arrowtooth flounder and Greenland halibut and environmental variables in the eastern Bering Sea ('*' = p-value ≤ 0.1 , '**' = p-value ≤ 0.05 , '***' = p-value ≤ 0.01 , '****' = p-value ≤ 0.001).

Environmental variables	Arrowtooth flounder (n = 7)	Greenland halibut (n = 9)
Along-shelf wind ¹	-0.55	0.06
On-shelf wind ²	-0.43	0.40
Ice cover index ³	0.43	-0.66**
Bottom temperature ⁴	-0.42	0.63 *
Sampling location (latitude) ⁵	0.71 *	-0.04
Sampling location (bottom depth) ⁶	0.29	0.12

¹ Along-shelf wind: April mean along-shelf wind (northwesterly; blowing from northwest (negative value) to southeast (positive value) and 54°-58°N, 165°-175°W)

² On-shelf wind: April mean on-shelf wind (southwesterly; blowing from southwest (negative value) to northeast (positive value) and 54°-58°N, 165°-175°W)

³ Ice Cover Index: Mean ice concentration for winter (January 1st-May31st and 56°-58°N, 163°-165°W)

⁴ Bottom temperature: Mean summer bottom temperature in the middle shelf (50 – 100 m isobaths) of the eastern Bering Sea from the Groundfish survey between 1982 and 2012

⁵ Sampling location (latitude): Latitude information where settled juveniles were caught

⁶ Sampling location (bottom depth): Bottom depth information where settled juveniles were caught

Table 4.3. Model selection results of variable coefficient generalized additive models for age-0 arrowtooth flounder (≤ 100 mm total length) abundance/CPUE between 1992 and 2012 and age-0 Greenland halibut (≤ 120 mm total length) abundance between 1982 and 2012 from summer groundfish surveys in the eastern Bering Sea. GCV stands for generalized cross validation score and AIC stands for akaike information criterion. The values corresponding to the smooth terms of lat and lon indicate the respective p-values and significance (*'= p-value ≤ 0.1 , **'= p-value ≤ 0.05 , ***'= p-value ≤ 0.01 , ****'= p-value ≤ 0.001).

Species	Model	R-square	Deviance explained	No. fish	GCV	AIC	s(lon,lat)	s(lon,lat) *BT	Factor
ATF	1	0.216	32.4 %	202	0.07	35.057	0.3223	0.045 *	Year
ATF	2	0.221	32.6 %	202	0.069	33.294	excluded	0.001 **	Year
GH	1	0.128	19.3 %	543	0.1281	423.859	0.046*	0.113	Year
GH	2	0.13	20.0 %	543	0.1289	426.589	0.553	excluded	Year
GH	3	0.03	4.96 %	543	0.1354	457.187	0.0414*	0.1025	excluded

Table 4.4. Results of variable coefficient generalized additive models for age-1 arrowtooth flounder (110 mm – 160 mm total length) abundance between 1992 and 2012 and age-1 Greenland halibut (130 mm -180 mm total length) abundance between 1982 and 2012 from summer groundfish surveys in the eastern Bering Sea. GCV stands for generalized cross validation score and AIC stands for akaike information criterion. BT stands for bottom temperature in present survey year and BT1 stands for bottom temperature of age-0 habitat in previous survey year. The values corresponding to the smooth terms of lat and lon indicate the respective p-values and significance (*'= p-value \leq 0.1, '**'= p-value \leq 0.05, '***'= p-value \leq 0.01, '****'= p-value \leq 0.001).

Species	Model	R-square	Deviance explained	No. fish	GCV	AIC	s(lon,lat)	s(lon,lat)*BT	Factor
ATF	1	0.284	30.7 %	1368	0.3346	2385.10	< 0.001 ***	<0.001 ***	BT1
GH	1	0.508	55.6 %	612	0.2245	818.113	<0.001 ***	0.0209 *	BT1

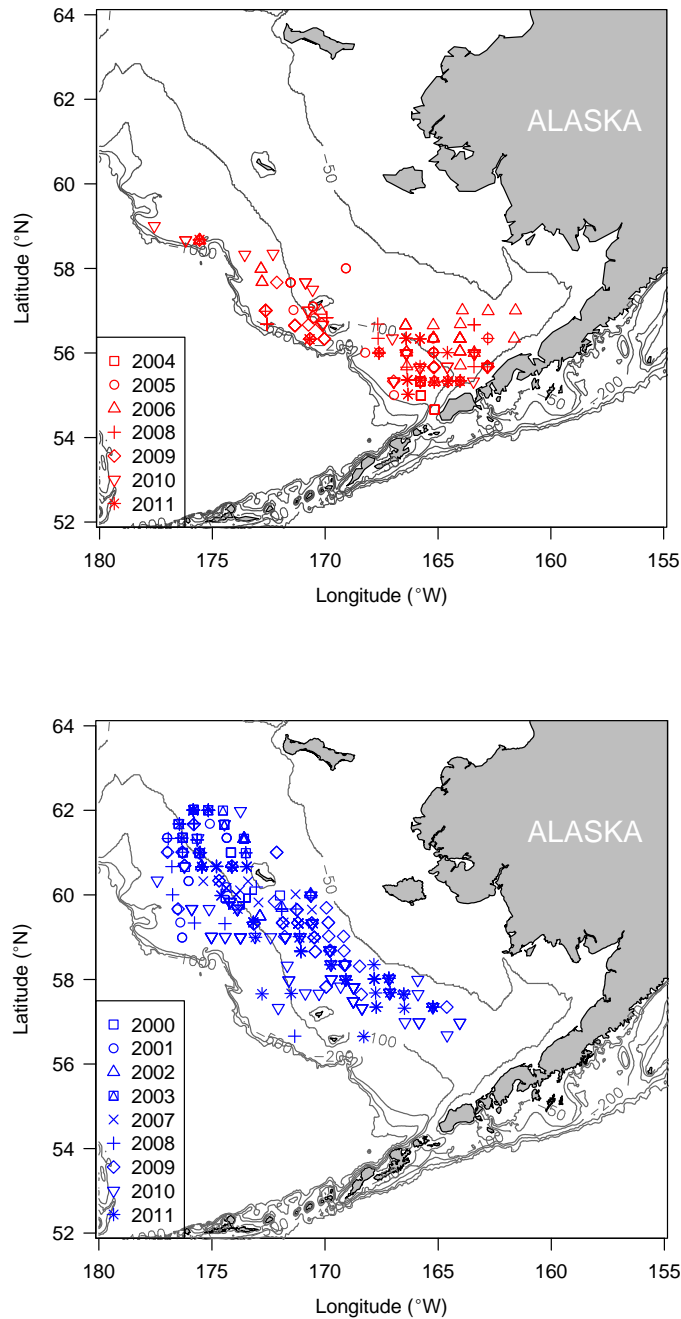


Fig. 4.1. Sampling locations of otoliths for arrowtooth flounder (≤ 170 mm total length; 2004-2006, 2008-2011; upper panel) and Greenland halibut (≤ 170 mm total length; 2000-2003, 2007-2011; bottom panel), collected during summer bottom trawl groundfish surveys in the eastern Bering Sea.

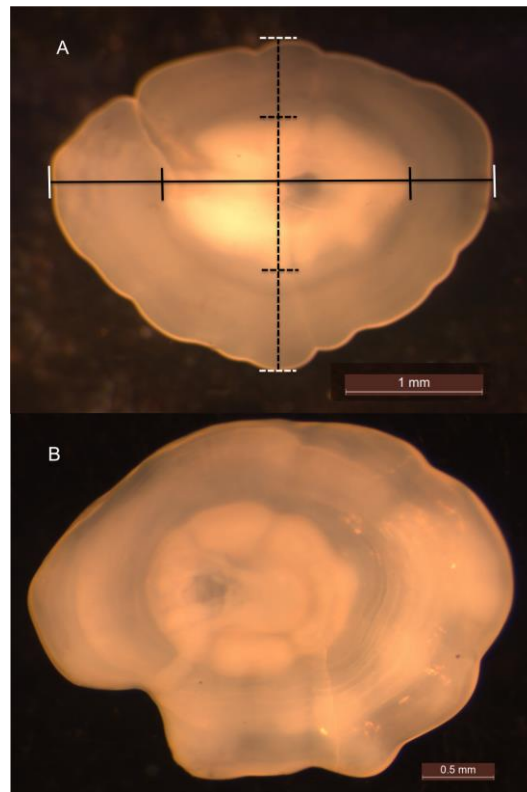


Fig. 4.2. Right otolith pictures for (A) arrowtooth flounder and (B) Greenland halibut juveniles from summer bottom trawl groundfish surveys in the eastern Bering Sea. In (A), dashed lines and intervals indicate otolith and kernel widths, while solid lines and intervals indicate otolith and kernel lengths. Similar structural metrics were used in Greenland halibut otoliths.

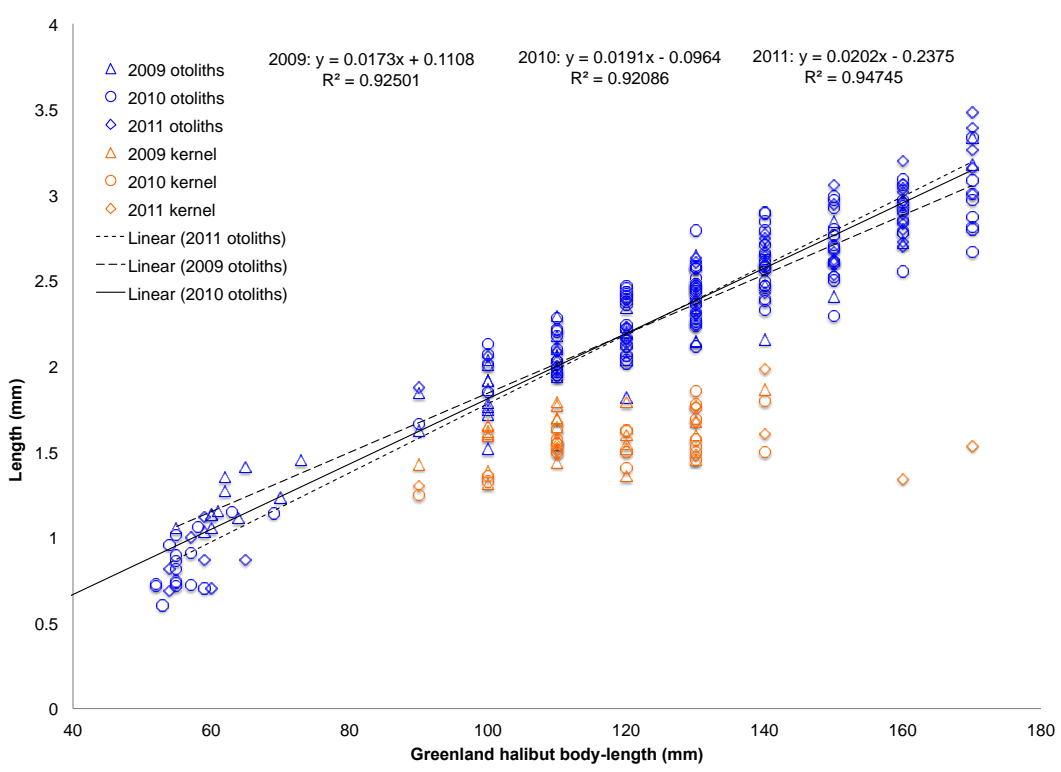


Fig. 4.3. Relationships between otolith length (mm) and body length (mm) and between kernel length (mm) and body length (mm) for Greenland halibut larvae and juveniles in 2009-2011.

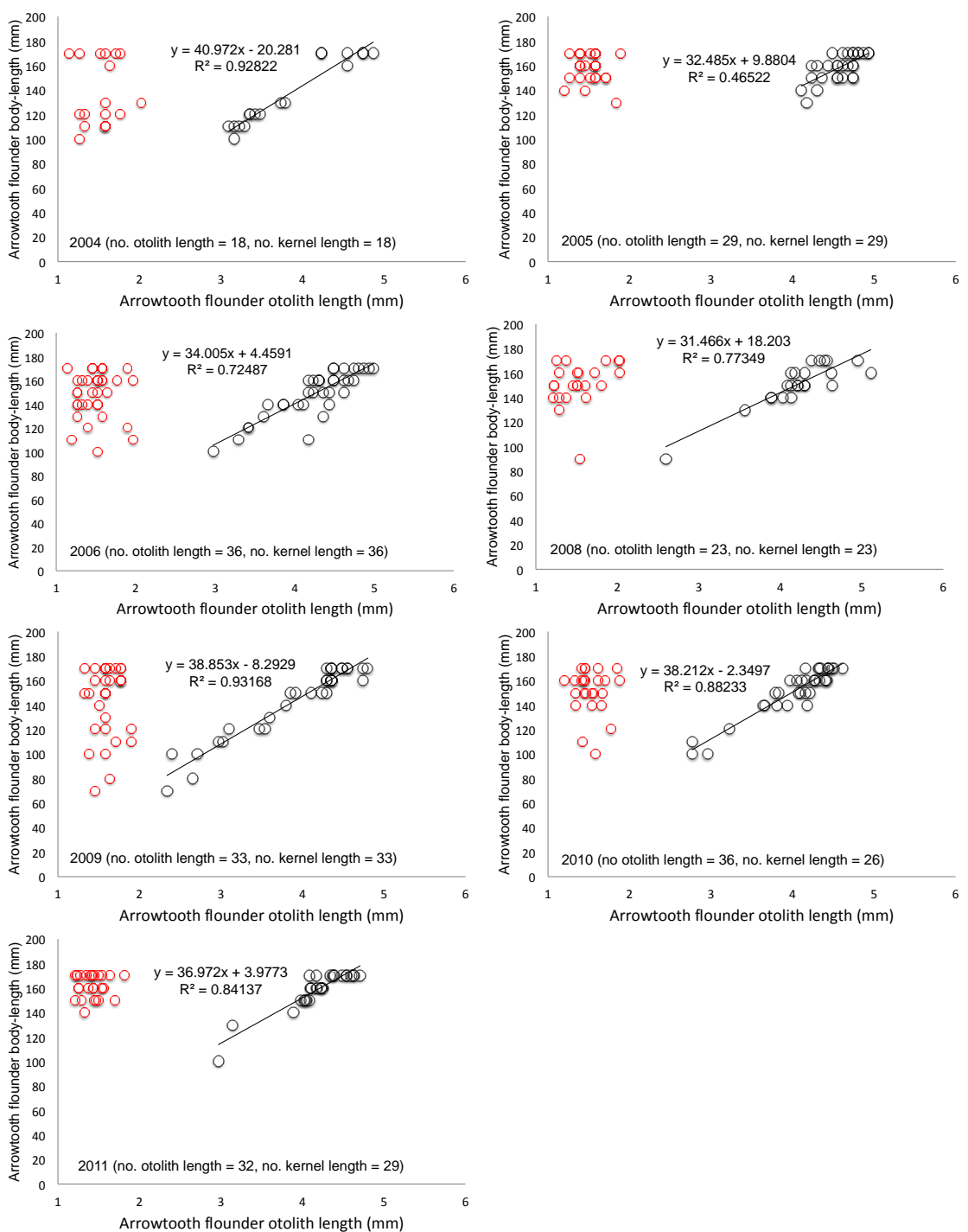


Fig. 4.4. Relationships between body length (mm total length) and otolith length (mm) of arrowtooth flounder (≤ 170 mm total length) in 2004-2006 and 2008-2011 from summer bottom trawl groundfish surveys in the eastern Bering Sea. Red dots indicate kernel length on otoliths of arrowtooth flounder.

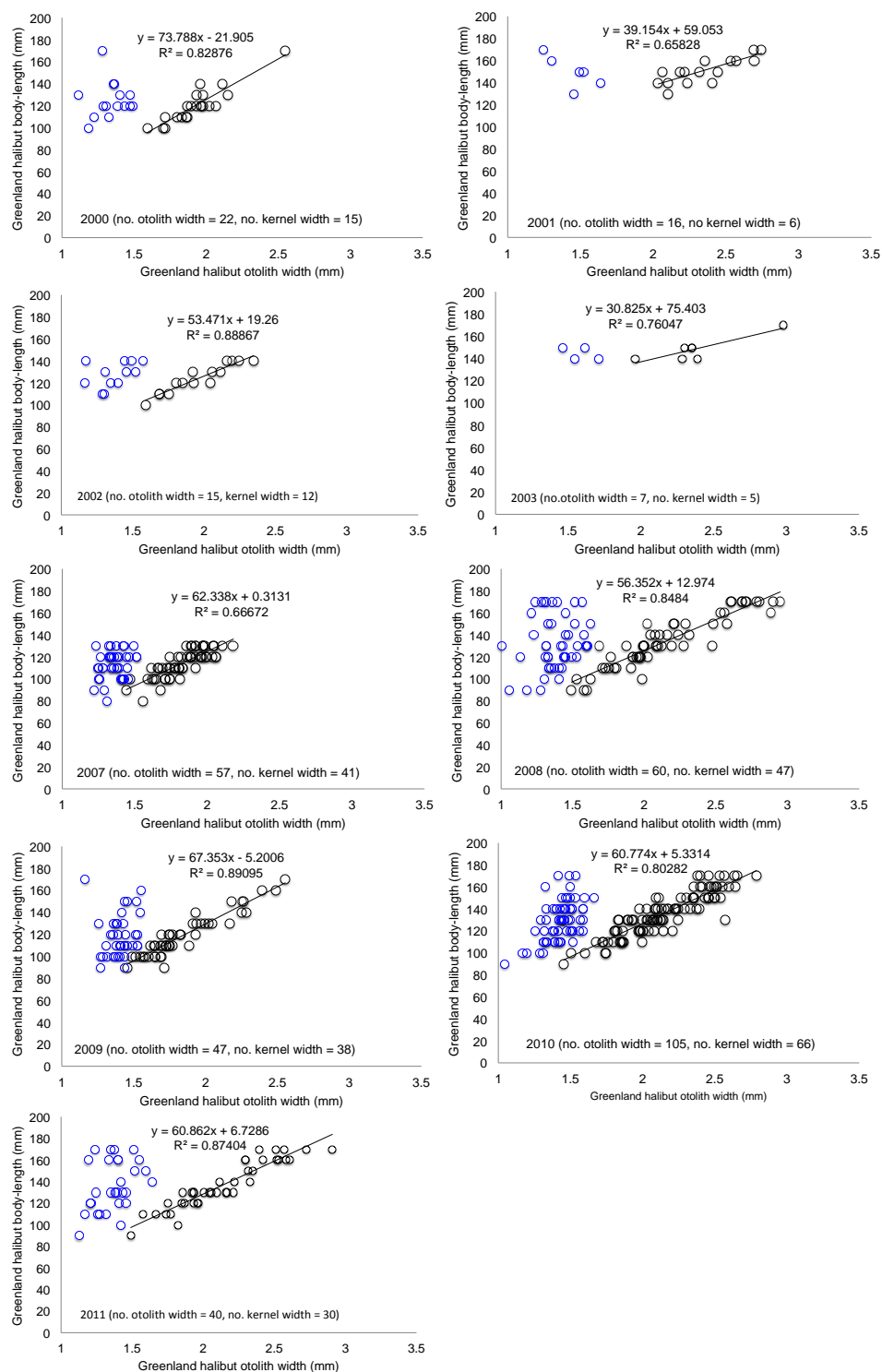


Fig. 4.5. The relationships between body length (mm total length) and otolith width (mm) of Greenland halibut (≤ 170 mm total length) in 2000-2003 and 2007-2011 from summer bottom trawl groundfish surveys in the eastern Bering Sea. Blue dots indicate kernel width on otoliths of Greenland halibut.

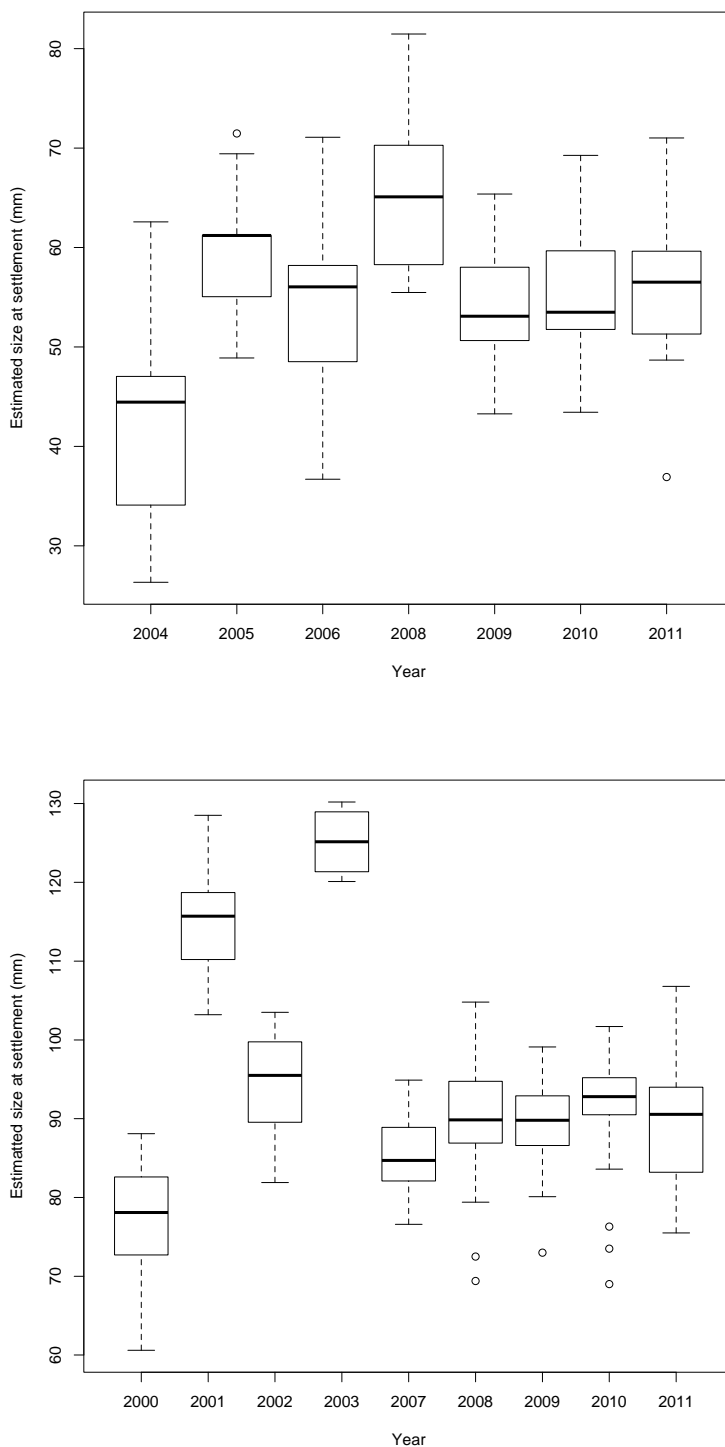


Fig. 4.6. Box plots for the estimated body length at settlement (mm total length) based on relationships between body length and otolith length for arrowtooth flounder (upper panel; 2004-2006 and 2008-2011) and between body length and otolith width for Greenland halibut (bottom panel; 2000-2003, 2007-2011) in the eastern Bering Sea.

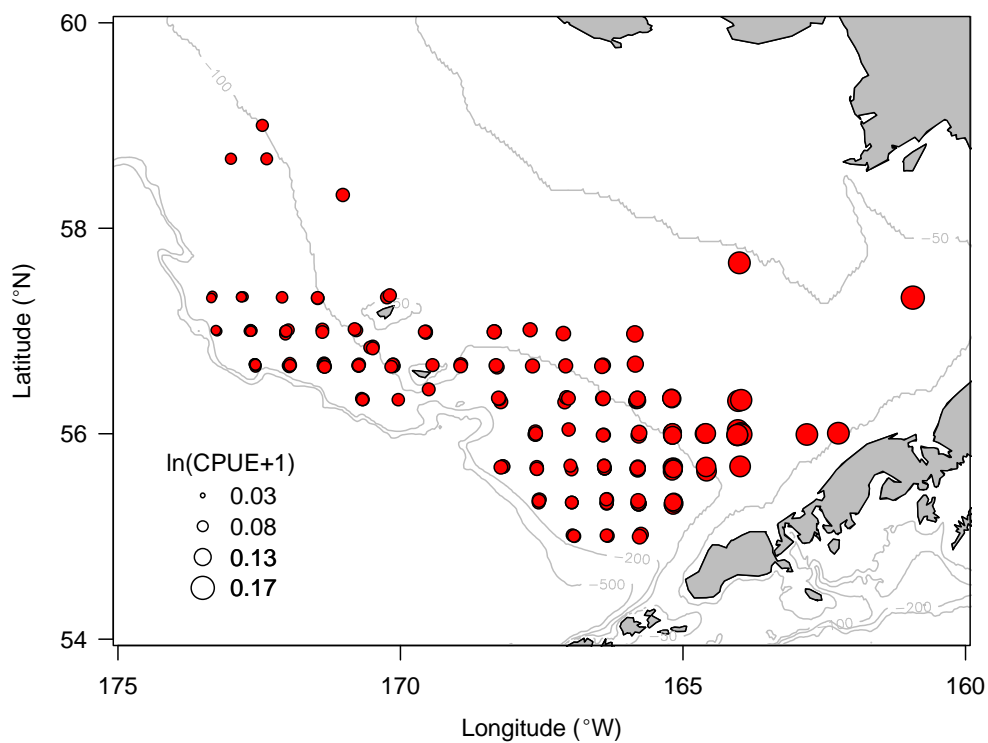


Fig. 4.7. Rate of change (proportional to bubble size) of local age-0 arrowtooth flounder (≤ 100 mm total length) abundance in relation to unit changes of bottom temperature from the best-fitted variable coefficient generalized additive model.

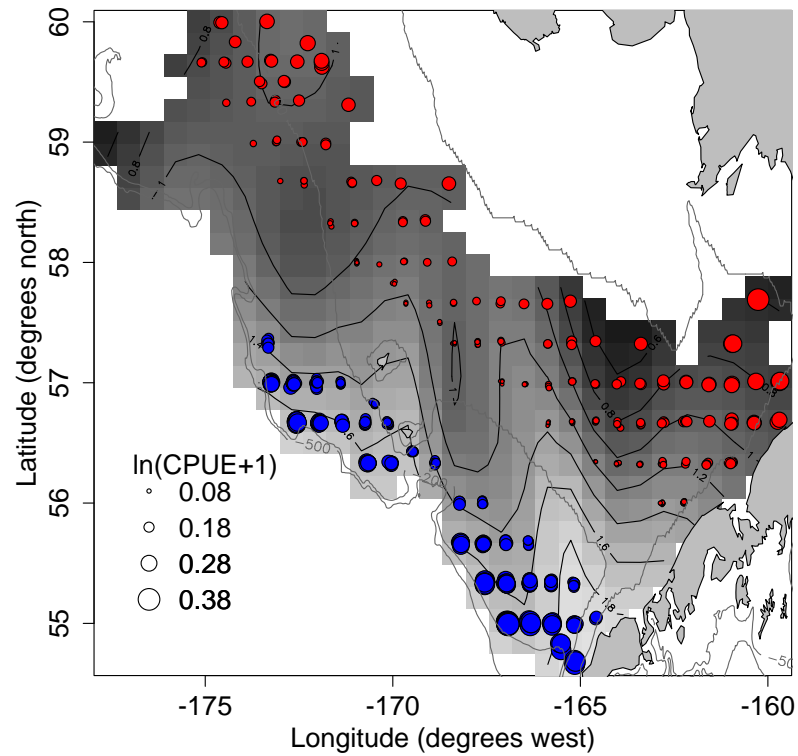


Fig. 4.8. Rate of change (proportional to bubble size) of local age-1 arrowtooth flounder (110 mm – 160 mm total length) abundance in relation to unit changes of bottom temperature (blue = negative, red = positive). The shaded regions indicate the average distribution of age-1 arrowtooth flounder abundance estimated from the best-fitted variable coefficient generalized additive model. Light and dark shading show areas of high and low abundance, respectively.

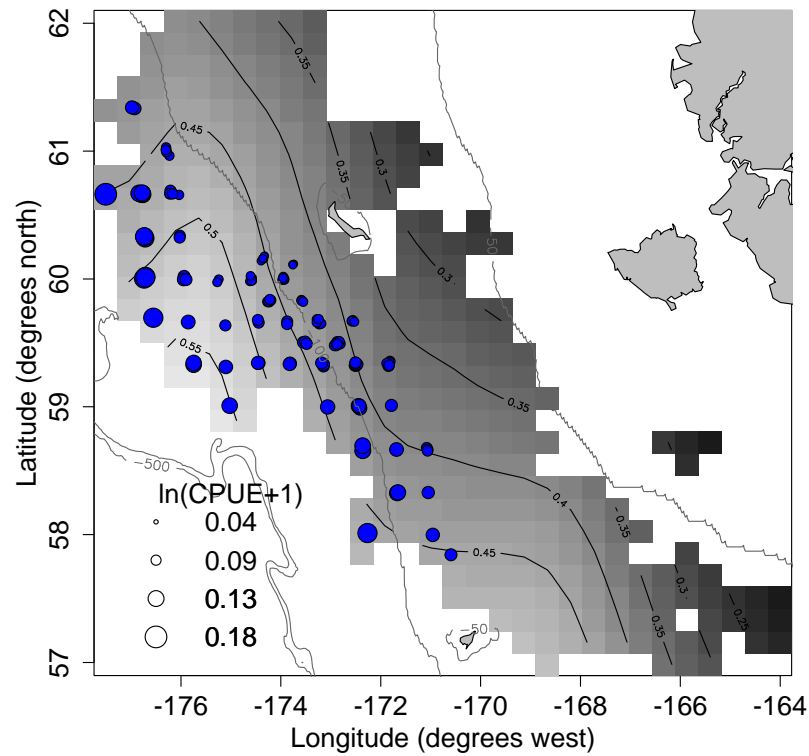


Fig. 4.9. Rate of change (proportional to bubble size) of local age-0 Greenland halibut (≤ 120 mm total length) abundance in relation to unit changes of bottom temperature (blue = negative). The shaded regions indicate the average distribution of age-0 Greenland halibut abundance estimated from the best-fitted variable coefficient generalized additive model. Light and dark shading show areas of high and low abundance, respectively.

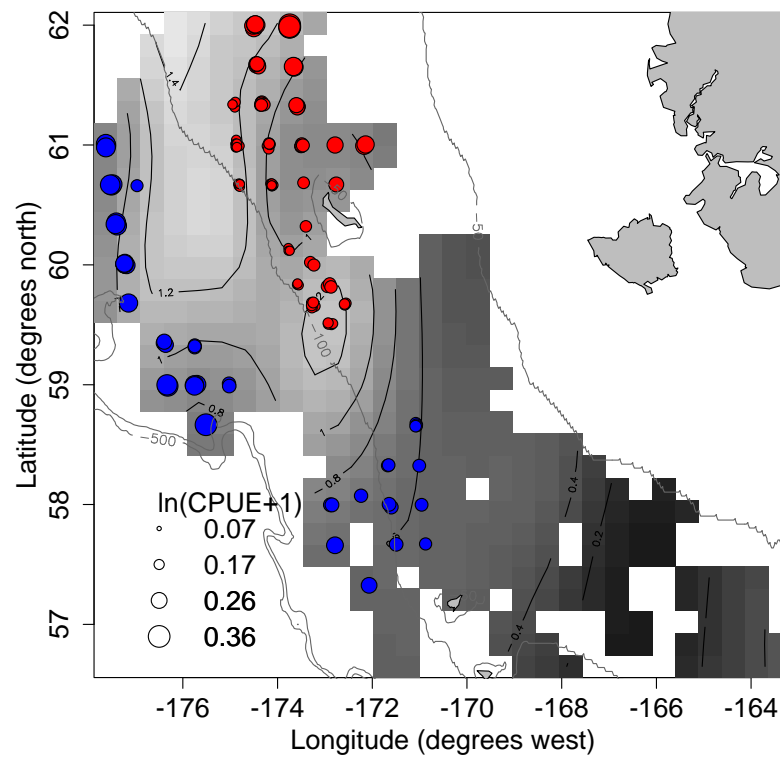


Fig. 4.10. Rate of change (proportional to bubble size) of local age-1 Greenland halibut (130 mm – 180 mm total length) abundance in relation to unit changes of bottom temperature (blue = negative, red = positive). The shaded regions indicate the average distribution of age-1 Greenland halibut abundance estimated from the best-fitted variable coefficient generalized additive model. Light and dark shading show areas of high and low abundance, respectively.

Chapter 5. Summary and implication

The overarching goal of this dissertation was to understand physical processes affecting distribution, abundance, settlement success, and settlement size of slope-spawning flatfish in the eastern Bering Sea, with a focus on arrowtooth flounder, Greenland halibut, and Pacific halibut. These three species were selected because they are commercially (the last two) and ecologically important and show different temporal patterns in their recruitment and population dynamics despite sharing many similar life history attributes. Applying statistical analysis of field observations, bio-physical modeling, and laboratory work on otolith microstructure, I related the aforementioned traits of these three slope-spawning flatfish to environmental variability in the eastern Bering Sea. Understanding species-specific and age-specific responses to environmental variability is important for understanding differences in their recruitment and population dynamics. This understanding provides valuable insight into the potential adaptability of these three species to observed variability and potential future climate change in the North Pacific and Bering Sea in particular, knowledge which is important for making management decisions.

In chapter 2, based on analysis of ichthyoplankton field observations, I found species-specific differences in the spatial distribution (vertically and horizontally) and juvenile nursery areas between Greenland halibut and Pacific halibut in the eastern Bering Sea. Pacific halibut larvae abruptly ascend to shallower water as they grow, and cross-onto the shelf earlier than Greenland halibut. This ontogenetic movement has the benefit of allowing Pacific halibut larvae to take advantage of near-surface on-shelf transport to reach their settlement locations. However, an early transition from the slope to the shelf may not equally benefit Greenland halibut, whose settlement locations are more distant from the spawning ground. Prior to this study, little was known about the vertical and horizontal distribution of Pacific halibut early life stages in the eastern Bering Sea. Results from chapter 2 have helped fill this critical knowledge gap. Understanding the vertical distribution of Pacific halibut larvae is important because strength and direction of transport could be different throughout the water column as found by Duffy-Anderson et al. (2013). Differences in early life traits (e.g., distribution, pelagic larval duration, and nursery areas) between Greenland halibut and Pacific halibut, interacting with variability of water temperature and prevailing currents, could result in diverging settlement and recruitment

patterns. The field observations summarized in Chapter 2 provide critical baseline data for parameterizing a dispersal trajectory model used to examine variability in settlement success (chapter 3).

In chapter 3, using a bio-physical modeling approach, I found that differences in interannual variability of Greenland halibut and Pacific halibut settlement in the eastern Bering Sea is caused by differences in early life attributes, especially spawning depth, pelagic duration, and ontogenetic movement combined with interannual and seasonal variations in prevailing currents. Greenland halibut settlement increased with increasing along-shelf (northwestward) flow whereas Pacific halibut settlement decreased. Early winter spawning (i.e., November and December) benefitted Greenland halibut settlement success, while Pacific halibut settlement was most successful when they spawned in January and February. Furthermore, Greenland halibut settlement is altered by the temperature dependence of pelagic larval duration; their settlement decreased (increased) with decreasing (increasing) PLD, but the same was not observed for Pacific halibut. These results indicate that Pacific halibut may have a stronger resilience to changes in temperature in comparison to Greenland halibut in the eastern Bering Sea. This study builds on previous modeling work (e.g., Duffy-Anderson et al. 2013) by including behavioral parameters on the dispersal of Greenland halibut and Pacific halibut. This study also provides novel methodological and data-driven approaches to define settlement success of dispersal trajectories in the EBS.

After characterizing differences in early life history traits (Chapter 2), and their role in determining settlement success (Chapter 3), I focused on environmental factors affecting individual size, spatial distribution, and abundance during settlement and post-settlement stages (Chapter 4). I was particularly interested in understanding whether environmental variability (i.e., water temperature and currents) have the potential to affect individual size and distribution during settlement, and if so, whether such dependencies would also affect survival and distribution during post-settlement stages. I approached this last part of my study using a combination of laboratory work on otolith microstructure, and statistical analyses of field observations for arrowtooth flounder and Greenland halibut juveniles (age-0 and age-1). Prior to my study, featured in chapter 4, there had been no attempt to estimate size at settlement for arrowtooth flounder and Greenland halibut in the eastern Bering Sea using otolith microstructure

analysis. There is also a lack of knowledge about what physical factors drive variation in size at settlement for these species in the eastern Bering Sea. I found that variations in size at settlement for arrowtooth flounder are associated with the latitude of sampling locations where arrowtooth flounder settled juveniles were caught, which could be influenced by currents – their size at settlement increased with increasing latitude. For Greenland halibut, variations in their size at settlement are correlated with summer mean bottom temperature in the middle shelf of the eastern Bering Sea and ice coverage. Greenland halibut size at settlement decreased with decreasing bottom water temperature and increasing ice extent. Furthermore, there is a strong negative correlation between ice coverage and mean April on-shelf wind (southwesterly; blowing from southwest to northeast) although there was no significant correlation between along-shelf/on-shelf winds and size at settlement of both species. Results from the spatial analysis of settled individuals showed that the extent of settlement habitat increases for Greenland halibut in cold years whereas that of arrowtooth flounder increases in warm years. These environmental variations, including bottom temperature, ice coverage, and on-shelf wind, which can influence growth rate, dispersal pathways and duration, and settlement habitat extent, can in part help explain variations in individual size at settlement. For example, in cold years, the extent of the suitable settlement habitat increases for Greenland halibut and decrease in arrowtooth flounder, making it possible for individuals of the former species to reach their settlement locations earlier in the dispersal phase. Also, in cold years, on-shelf winds are weaker in comparison to arm years, which generate relatively weak Ekman transport from northwest to southeast at the surface. This would likely enhance Greenland halibut larval transport to the northwest and would reduce the time needed for them to reach their settlement in the northern middle shelf around St. Matthew Island.

Our results from Chapter 4 also show that the bottom temperature of the Greenland halibut age-0 habitat negatively affects Greenland halibut age-1 abundance in the next year. For arrowtooth flounder, I found a dependence of age-1 abundance on the temperature experienced during the age-0 stage, but with no a clear directionality. The dependence of age-1 abundance on current as well as past conditions may help explain why only during the later stanza of cold years (2007-2012) Greenland halibut has shown signs of increased recruitment and abundance, in spite of earlier isolated, but not consecutive, cold years (e.g., 1999). Results from chapter 4 have

provided valuable insight into the ways in which physical factors influence variations in size at settlement, habitat size, and abundance of these two ecologically important species in the eastern Bering Sea.

The findings from these three studies have greatly improved our understanding of settlement success and recruitment of important slope-spawning flatfish in the eastern Bering Sea. Specifically, I have developed a better understanding of the effects of water temperature and prevailing currents on distribution, abundance, settlement success, and size at settlement of arrowtooth flounder, Greenland halibut, and Pacific halibut. In most cold years when along-shelf flow is generally strong, the level of larval supply of Greenland halibut to their settlement areas is higher than in warm years (Fig. 5.1). Greenland halibut larvae have benefits from these favorable along-shelf currents and are able to reach their settlement more quickly (Fig. 5.1). Size at settlement for Greenland halibut therefore decreases in cold years, which could in turn lead to higher mortality due to predation pressure and lower feeding success (Fig. 5.1). However, the larger amount of suitable habitat for settlement and post-settlement stages could result in lower competition and less predation in comparison to warm years (Fig. 5.1). On the other hand, in cold years, Pacific halibut, which have their settlement habitat in the southern part of the eastern Bering Sea, have lower numbers of successful settlers (Fig. 5.2). This is because prevailing currents carry them away from settlement locations. Although information about size at settlement for Pacific halibut is still limited, if it resembles that of arrowtooth flounder, I would expect their size at settlement to increase in cold years because strong along-shelf transport could bring arrowtooth flounder larvae far away from their settlement area or might advect them to unsuitable habitat (Fig. 5.2). Although arrowtooth flounder size at settlement is larger in cold years, the amount of suitable habitat after settlement is smaller, which may cause a decrease in recruitment due to increased competition for limited resources in the eastern Bering Sea (Fig. 5.2).

In agreement with the above expectations, I found that Greenland halibut have higher age-1 abundance (a proxy for recruitment) in cold years while Pacific halibut have higher age-1 abundance in warm years. Findings from my dissertation work are also consistent with stock assessment report for Greenland halibut (Barbeaux et al. 2014). Stock assessment for age-0 Greenland halibut recruitment increased in recent cold years (2007-2010). These results indicate

that Greenland halibut survival is higher in cold years, particularly during protracted cold conditions, than in warm years despite size at settlement being relatively small. Therefore, settlement success and available habitat size during settlement and post-settlement phases could be more critical to the survival of Greenland halibut, and most likely Pacific halibut, than size at settlement.

Wang et al. (2012) projected that surface air temperature in the eastern Bering Sea would increase by about 2 °C due to global warming over the next 50 years. It is expected that the southeastern Bering Sea would be more strongly influenced by warming than the northeastern Bering Sea, with decreasing sea ice coverage accompanying the temperature increase (Stabeno et al. 2012). Arrowtooth flounder and Pacific halibut are of sub-Arctic origin, at the northernmost ranges of their distribution while Greenland halibut is a boreal species at the southernmost range of its distribution in the eastern Bering Sea. They are, therefore, affected differently by warming. If such a warming scenario holds true, I anticipate that Greenland halibut settlement and recruitment, as well as adult populations will decrease and they will move into deeper habitats off the shelf and northward due to decreasing nursery habitat availability, while Pacific halibut populations will increase and they will extend their distribution to the north. Greenland halibut settlement is very sensitive to changes in pelagic larval duration, which could be affected by temperature and currents. With a warming trend, Greenland halibut pelagic larval duration would decrease with increasing water temperature, settlement success would be relatively low, and size at settlement and extent of nursery habitat would decrease. Therefore, Greenland halibut recruitment is more constrained and less adaptable to future climate variability compared to Pacific halibut, which appears more adaptable to future warming.

This research makes a vital methodological and ecological contribution to address the effects of physical factors on the distribution, abundance, settlement, body-size at settlement, and habitat availability of slope spawning flatfish in the eastern Bering Sea and elsewhere. By studying how physical factors and their variability influence these three flatfish during early life stages, I have gained valuable insight into the response of flatfish stocks to past and future climate changes in the eastern Bering Sea, that is especially vulnerable to warming.

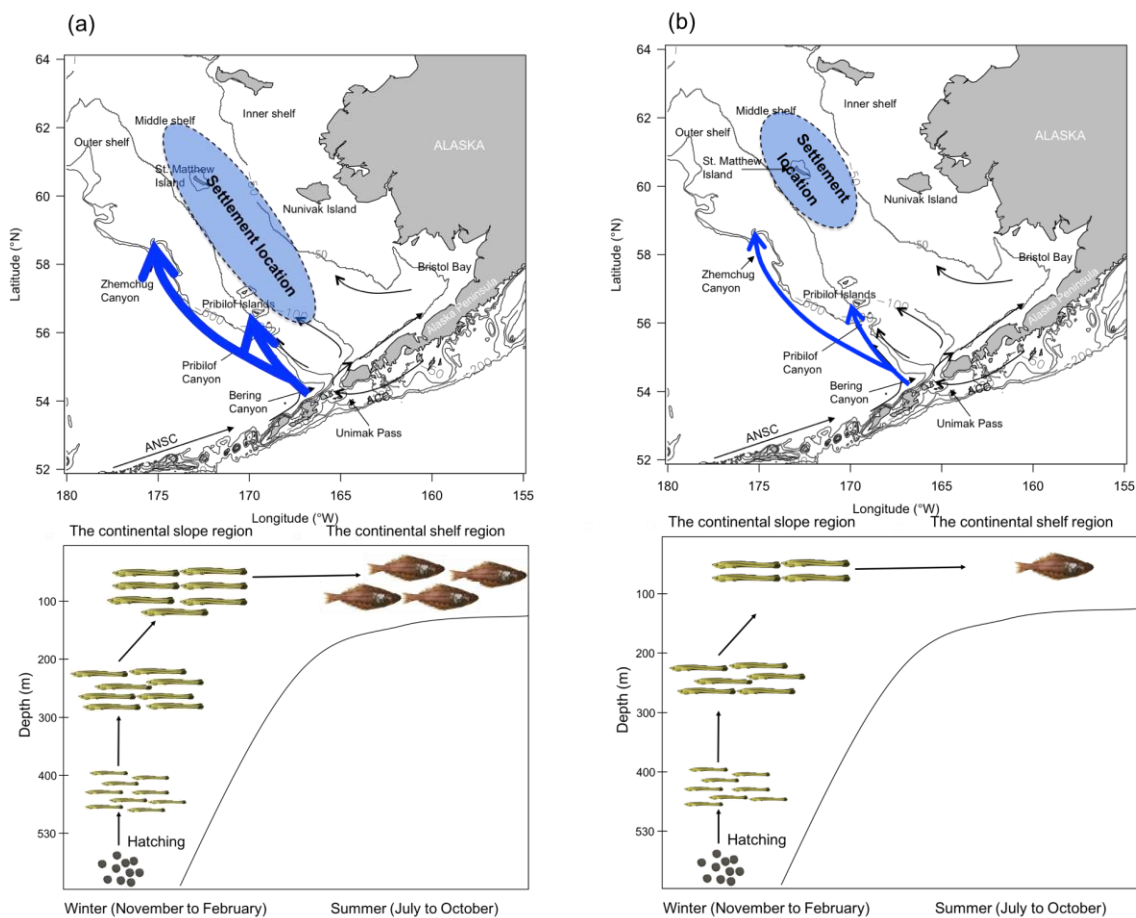


Fig. 5.1. Schematic representations of Greenland halibut settlement, size at settlement, and habitat availability in cold years (a) and warm years (b) in the eastern Bering Sea. Blue arrows represent the strength of along-shelf transport. The size of settling individuals is representative of their observed size at settlement (i.e., smaller in (a) and larger in (b)). Circles indicate known settlement areas for age-0 Greenland halibut (dashed with blue color).

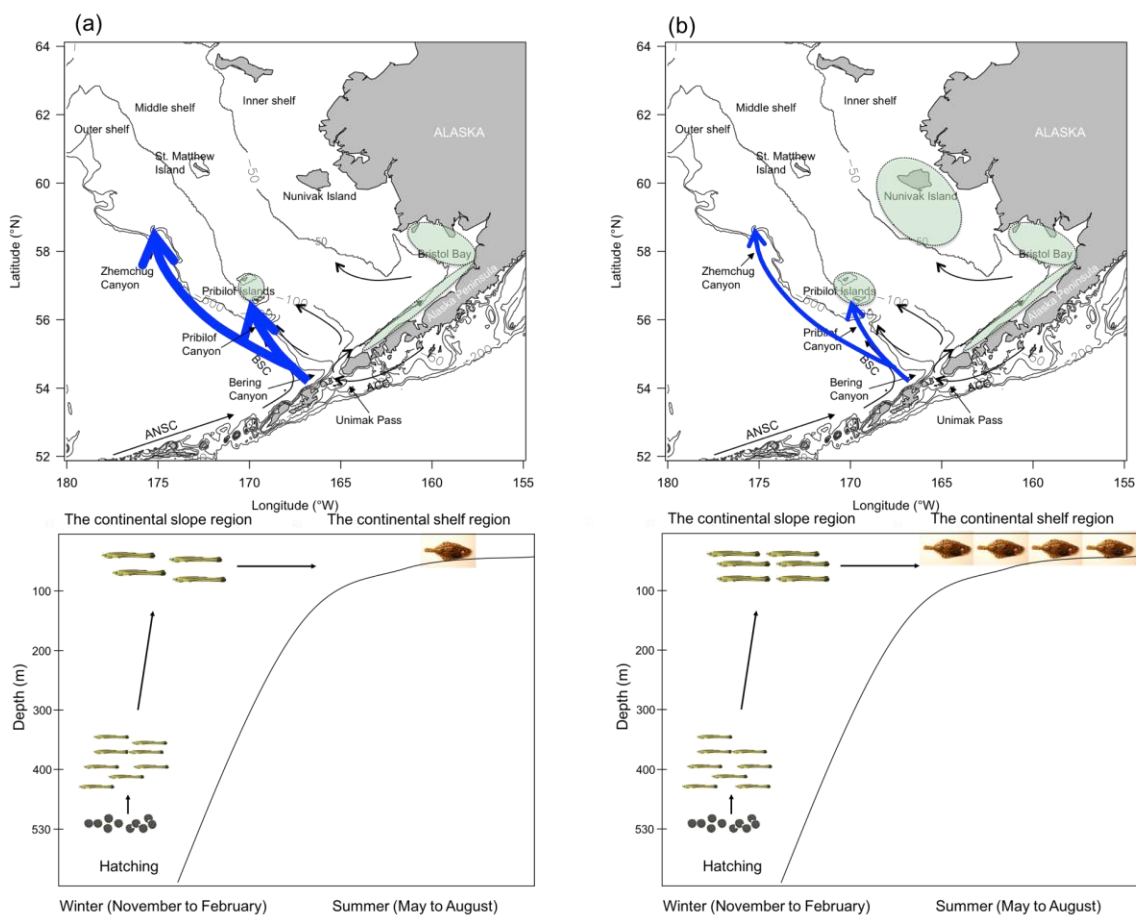


Fig. 5.2. Schematic representations of Pacific halibut settlement, size at settlement, and habitat availability in cold years (a) and warm years (b) in the eastern Bering Sea. Blue arrows represent the strength of along-shelf transport. The size of settling individuals is representative of their observed size at settlement (i.e., larger in (a) and smaller in (b)). Circles indicate known settlement areas for age-0/age-1 Pacific halibut (dotted with green color).

BIBLIOGRAPHY

Alton MS, Bakkala RG, Walters GE, Munro PT (1988) Greenland turbot *Reinhardtius hippoglossoides* of the east Bering Sea and the Aleutian Islands region. NOAA Technical Report NMFS 71.

Aydin K, Mueter FJ (2007) The Bering Sea - a dynamic food web perspective. Deep Sea Research II: Topical Studies in Oceanography, 54:2501–2525.

Baker MR, Hollowed AB (2014) Delineating ecological regions in marine systems: integrating physical structure and community composition to inform spatial management in the eastern Bering Sea. Deep-Sea Research II: Topical Studies in Oceanography, 109:215-240.
doi:10.1016/j.dsr2.2014.03.001

Bailey KM (1994) Predation on juvenile flatfish and recruitment variability. Netherlands Journal of Sea Research, 32(2):175-189.

Bailey KM, Picquelle SJ (2002) Larval distribution patterns of offshore spawning flatfish in the Gulf of Alaska: sea valleys as transport trajectories and enhanced inshore transport during ENSO events. Marine Ecology Progress Series, 236:205-217.

Bailey KM, Nakata H, Van der Veer H (2005) The planktonic stages of flatfish: physical and biological interactions in transport processes. pp. 94-119. In Gibson, R. (Ed.). Flatfishes: Biology and Exploitation. Blackwell Science Ltd, Oxford, UK, pp. 94-119.

Bailey KM, Abookire AA, Duffy-Anderson JT (2008) Pathways in the sea: A comparison of spawning areas, larval advection patterns and juvenile nurseries of offshore spawning flatfishes in the Gulf of Alaska. Fish and Fisheries, 9:44-66.

Barbeaux SJ, Ianelli J, Nichol D, Hoff J (2013) Assessment of the Greenland Turbot (*Reinhardtius hippoglossoides*) in the Bering Sea and Aleutian Islands. In Stock assessment and fishery evaluation document for groundfish resources in the Bering Sea/Aleutian Islands region as projected for 2014. Section 5. North Pacific Fishery Management Council, Anchorage, AK.

Barbeaux SJ, Ianelli J, Nichols D, Hoff J (2014) Assessment of Greenland Turbot (*Reinhardtius hippoglossoides*) in the Bering Sea and Aleutian Islands. In Stock Assessment and Fishery Evaluation Document for Groundfish Resources in the Bering Sea/Aleutian Islands Region. Section 5. Anchorage: North Pacific Fishery Management Council.

Bartolino V, Ciannelli L, Bacheler NM, Chan KS (2011) Ontogenetic and sex-specific differences in density-dependent habitat selection of a marine fish population. Ecology, 92(1):189-200.

Benoît HP, Pepin P (1999) Interaction of rearing temperature and maternal influence on egg development rates and larval size at hatch in yellowtail flounder (*Pleuronectes ferrugineus*).

Canadian Journal of Fisheries and Aquatic Sciences, 56:785-794.

Benoît HP, Pepin P, Brown JA (2000) Patterns of metamorphic age and length in marine fishes, from individuals to taxa. Canadian Journal of Fisheries and Aquatic Sciences, 57(4):856-869.

Best EA (1974) Juvenile halibut in the eastern Bering Sea: trawl surveys, 1970-1972. International Pacific Halibut Commission Technical Reports 11.

Best EA (1977) Distribution and abundance of juvenile halibut in the southeastern Bering Sea. International Pacific Halibut Commission Science Reports 62.

Best EA (1981) Halibut ecology. [IN]The Bering Sea shelf: Oceanography and resources. D.W. Hood and J.A. Calder (Ed.), 1, pp. 495-509.

Best EA, Hardman WH (1982) Juvenile halibut surveys, 1973-1980. International Pacific Halibut Commission Technical Reports 20.

Bolle LJ, Dickey-Collas M, van Beek JKL, Erfmeijer PLA, Witte IJJ, van der Veer HW, Rijnsdorp AD (2009) Variability in transport of fish eggs and larvae III. Effects of hydrodynamics and larval behaviour on recruitment in plaice. Marine Ecology Progress Series, 390:195–211.

Bond NA, Overland JE (2005) The importance of episodic weather events to the ecosystem of the Bering Sea shelf. Fisheries Oceanography, 14(2):97-111.

Bouwens KA, Smith RL, Paul AJ, Rugen W (1999) Length at and timing of hatching and settlement for arrowtooth flounders in the Gulf of Alaska. Alaska Fishery Research Bulletin, 6(1):41-48.

Brodeur RD (2001) Habitat-specific distribution of Pacific Ocean perch (*Sebastes alutus*) in Pribilof Canyon, Bering Sea. Continental Shelf Research, 21:207-224.

Burke JS, Seikai T, Tanaka Y, Tanaka M (1999) Experimental intensive culture of summer flounder, *Paralichthys dentatus*. Aquaculture 176:135-144.

Campana SE, Neilson JD (1985) Microstructure of fish otoliths. Canadian Journal of Fisheries and Aquatic Sciences, 42:1014-1032.

Chen K, Ciannelli L, Decker MB, Ladd C, Cheng W, Zhou Z, Chan KS (2014) Reconstructing source-sink dynamics in a population with a pelagic dispersal phase. PLOS One 9(5) e5316

Ciannelli L, Chan KS, Bailey KM, Stenseth NC (2004) Nonadditive effects of the environment on the survival of a large marine fish population. Ecology, 85(12):3418-3427.

Ciannelli L, Bartolino V, Chan KS (2012) Nonadditive and nonstationary properties in the spatial distribution of a large marine fish population. Proceeding of the Royal Society of London

B, 279: 3635-3642. doi:10.1098/rspb.2012.0849

Ciannelli L, Bailey K, Olsen EM (2015) Evolutionary and ecological constraints of fish spawning habitats. *ICES Journal of Marine Science*, 72(2):285-96. doi:10.1093/icesjms/fsu145

Coachman LK (1986) Circulation, water masses, and fluxes on the southeastern Bering Sea shelf. *Continental Shelf Research*, 5:32–108.

Cooper DW, Duffy-Anderson JT, Stockhausen WT, Cheng W (2012) Modeled connectivity between northern rock sole (*Lepidopsetta polyxystra*) spawning and nursery areas in the eastern Bering Sea. *Journal of Sea Research*, 84:2-12. doi:10.1016/j.seares.2012.07.001

Cooper DW, Duffy-Anderson JT, Norcross B, Holladay B, Stabeno P (2014) Nursery areas of juvenile northern rock sole (*Lepidopsetta polyxystra*) in the eastern Bering Sea in relation to hydrography and thermal regimes. *ICES Journal of Marine Science*, 71:1683-1695.

Cowen RK, Sponaugle S (2009) Larval dispersal and marine population connectivity. *Annual Review of Marine Science*, 1:443–466.

Curchitser EN, Haidvogel DB, Hermann AJ, Dobbins EL, Powell TM, Kaplan A (2005) Multi-scale modeling of the North Pacific Ocean: assessment and analysis of simulated basin-scale variability (1996-2003). *Journal of Geophysical Research*, 110(C11021) doi:10.1029/2005JC002902

Danielson S, Curchitser E, Hedstrom K, Weingartner T, Stabeno P (2011) On ocean and sea ice modes of variability in the Bering Sea. *Journal of Geophysical Research*, 116, C12034, doi:10.1029/2011JC007389.

De Forest L, Duffy-Anderson JT, Heintz RA, Matarese AC, Siddon EC, Smart TI, Spies IB (2014) Taxonomy of the early life stages of arrowtooth flounder (*Atheresthes stomias*) and Kamchatka flounder (*A. evermanni*) in the eastern Bering Sea, with notes on distribution and condition. *Deep Sea Research Part II: Topical Studies in Oceanography*, 109:181-189.

Domínguez-Petit R, Ouellet P, Lambert Y (2013) Reproductive strategy, egg characteristics and embryonic development of Greenland halibut (*Reinhardtius hippoglossoides*). *ICES Journal of Marine Science*, 70(2): 342-351. doi:10.1093/icesjms/fss180

Duffy-Anderson JT, Busby M, Mier KL, Deliyianides CM, Stabeno P (2006) Spatial and temporal patterns in summer ichthyoplankton assemblages on the eastern Bering Sea shelf 1996-2000. *Fisheries Oceanography*, 15(1):80-94.

Duffy-Anderson JT, Blood DM, Cheng W, Ciannelli L, Matarese AC, Sohn D, Vance TC, Vestfals C (2013) Combining field observations and modeling approaches to examine Greenland halibut (*Reinhardtius hippoglossoides*) early life ecology in the southeastern Bering Sea. *Journal of Sea Research*, 75:96-109.

- Duffy-Anderson JT, Bailey KM, Cabral H, Nakata H, van der Veer H (2014) The planktonic stages of flatfishes: physical and biological interaction in transport process. In *Flatfish: Biology and Exploitation*, 2nd edn Ed. by R.N. Gibson, R.D.M. Nash, A.J. Geffen, and H.W. van der Veer. John Wiley & Sons, Ltd, Oxford, UK.
- Ellis T, Gibson RN (1995) Size-selective predation of 0-group flatfishes on a Scottish coastal nursery ground. *Marine Ecology Progress Series*, 127(1):27-37.
- Fedewa EJ (2015) Pre- and post-settlement processes of northern rock sole (*Lepidopsetta polyxystra*) in relation to interannual variability in temperature and productivity in the Gulf of Alaska. Doctoral Dissertation, Oregon State University, Corvallis, OR.
- Fedewa EJ, Miller JA, Hurst TP (In press) Pre-settlement processes of northern rock sole (*Lepidopsetta polyxystra*) in relation to interannual variability in the Gulf of Alaska. *Journal of Sea Research*.
- Forrester CR, Alderdice DF (1973) Laboratory observations on early development of the Pacific halibut. *International Pacific Halibut Commission Technical Reports* 9.
- Gibson RN, Robb L, Wennhage H, Burrows MT (2002) Ontogenetic changes in depth distribution of juvenile flatfishes in relation to predation risk and temperature on a shallow-water nursery ground. *Marine Ecology Progress Series*, 229:233-244.
- Fox CJ, McCloghrie P, Young EF, Nash RDM (2006) The importance of individual behaviour for successful settlement of juvenile plaice (*Pleuronectes platessa L.*): a modelling and field study in the eastern Irish Sea. *Fisheries Oceanography*, 15(4): 301-313.
- Gunderson DR, Ellis IE (1986) Development of a plumb staff beam trawl for sampling demersal fauna. *Fisheries Research*, 4:35-41.
- Harden Jones F R (1968) *Fish Migration*. Edward Arnold, London, UK. 325 pp.
- Herrmann M, Bouffard J, Béranger K (2009) Monitoring open-ocean deep convection from space. *Geophysical Research Letters* 36, L03606
- Hjort J (1914) Fluctuations in the great fisheries of Northern Europe viewed in the light of biological research. *Rapports et Procès-Verbaux des Reunions du Conseil International pour l'Exploration de la Mer*. 20:1-228.
- Hoff GR (2008) A nursery site of the Alaska skate (*Bathyraja parmifera*) in the eastern Bering Sea. *Fisheries Bulletin*, 106:233-244.
- Hoff GR (2010) Identification of skate nursery habitat in the eastern Bering Sea. *Marine Ecology Progress Series*, 403:243-254.

Houde ED (2008) Emerging from Hjort's Shadow. *Journal of Northwest Atlantic Fishery Science*, 41:53-70.

Hufnagl M, Peck MA, Nash RDM, Pohlmann T, Rijnsdorp AD (2013) Changes in potential North Sea spawning grounds of plaice (*Pleuronectes platessa* L.) based on early life stage connectivity to nursery habitats. *Journal of Sea Research*, 84:26–39.

Hunsicker ME, Ciannelli L, Bailey KM, Zador S, Stige LC (2013) Climate and Demography Dictate the Strength of Predator-Prey Overlap in a Subarctic Marine Ecosystem. *PLoS ONE* 8(6): e66025. doi:10.1371/journal.pone.0066025

Hunt GL, Coyle KO, Eisner LB, Farley EV, Heintz RA, Mueter F, Napp JM, Overland JE, Ressler PH, Salo S (2011) Climate impacts on eastern Bering Sea foodwebs: a synthesis of new data and an assessment of the Oscillating Control Hypothesis. *ICES Journal of Marine Science: Journal du Conseil*, 68(6):1230.

Huret M, Runge JA, Chen C, Cowles G, Xu Q, Pringle JM (2007) Dispersal modeling of fish early life stages: sensitivity with application to Atlantic cod in the western Gulf of Maine. *Marine Ecology Progress Series*, 347:261-274.

Ianelli JN, Barbeaux S, Honkalehto T, Kotwicki S, Aydin K, Williamson N (2010) Assessment of the walleye pollock stock in the eastern Bering Sea. Stock Assessment and Fishery Evaluation Report for the Groundfish Resources of the Bering Sea/Aleutian Islands Regions. North Pacific Fishery Management Council, Anchorage, AK.

Ianelli JN, Wilderbuer TK, Nichol D (2011) Assessment of Greenland turbot in the eastern Bering Sea and Aleutian Islands. Bering Sea and Aleutian Islands Stock Assessment and Fishery Evaluation report. North Pacific Fishery Management Council, Anchorage, AK. 696 pp.

Iles TD, Sinclair M (1982) Atlantic herring: stock discreteness and abundance. *Science*, 215: 627–633.

Joh M, Takatsu T, Nakaya M, Higashitani T, Takahashi T (2005) Otolith microstructure and daily increment validation of marbled sole (*Pseudopleuronectes yokohamae*). *Marine Biology*, 147:59-69.

Kanamitsu M, Ebisuzaki W, Woollen J, Yang S-K, Hnilo JJ, Fiorino M, Potter GL (2002) NCEP–DOE AMIP-II Reanalysis (R-2). *Bulletin of the American Meteorological Society*, 83:1631-1643. doi: <http://dx.doi.org/10.1175/BAMS-83-11-1631>

Kim JJ, Stockhausen W, Kim S, Cho Y-K, Seo G-H, Lee J-S (2015) Understanding interannual variability in the distribution of, and transport processes affecting, the early life stages of *Todarodes pacificus* using behavioral-hydrodynamic modeling approaches. *Progress in Oceanography*, 138(Part B):571-583. doi: 10.1016/j.pocean.2015.04.003

Kotwicki S, Lauth RR (2013) Detecting temporal trends and environmentally-driven changes in the spatial distribution of bottom fishes and crabs on the eastern Bering Sea shelf. *Deep Sea*

Research Part II: Topical Studies in Oceanography, 94:231-243.

Laurel BJ, Danley C, Haines S (2014) The effects of temperature on growth, development and settlement of northern rock sole larvae (*Lepidopsetta polyxystra*). Fisheries Oceanography, 23:495-505.

Ladd C, Hunt GJ, Mordy CW, Salo SA, Stabeno PJ (2005) Marine environment of the eastern and central Aleutian Islands. Fisheries Oceanography, 14:22–38.

Ladd C, Stabeno PJ (2009) Freshwater transport from the Pacific to the Bering Sea through Amukta Pass. Geophysical Research Letter 36

Ladd C (2014) Seasonal and interannual variability of the Bering Slope Current. Deep-Sea Research Part II: Topical Studies in Oceanography, 109: 5-13.

Lanksbury JA, Duffy-Anderson JT, Mier KL, Busby MS, Stabeno PJ (2007) Distribution and transport patterns of northern rock sole, *Lepidopsetta polyxystra*, larvae in the southeastern Bering Sea. Progress in Oceanography, 72:39-62.

Lauth RR (2011) Results of the 2010 eastern and northern Bering Sea continental shelf bottom trawl survey of groundfish and invertebrate fauna. U.S. Dept. Commerce NOAA Technical Memorandum NMFS- AFSC-227, 256 p.

Lauth RR, Nichol DG (2013) Results of the 2012 eastern Bering Sea continental shelf bottom trawl survey of groundfish and invertebrate resources. U.S. Dept. Commerce NOAA Technical Memorandum NMFS-AFSC-256, 162 p.

Leggett WC, Frank KT (1997) A comparative analysis of recruitment variability in North Atlantic flatfishes--testing the species range hypothesis. Journal of Sea Research, 37(34):281-299.

Levin LA (2006) Recent progress in understanding larval dispersal: new directions and digressions. Integrative and Comparative Biology, 46:282-97.

Liu HW, Stickney RR, Dickhoff WW, McCaughran DA (1993) Early larval growth of Pacific halibut (*Hippoglossus stenolepis*). Journal of the World Aquaculture Society, 24:482-485.

Liu HW, Stickney RR, Dickhoff WW, McCaughran DA (1994) Effects of environmental factors on egg development and hatching of Pacific halibut *Hippoglossus stenolepis*. Journal of the World Aquaculture Society, 25(2):317-321.

Loher T, Seitz A (2008) Characterization of active spawning season and depth for Eastern Pacific halibut (*Hippoglossus stenolepis*), and evidence of probable skipped spawning. Journal of Northwest Atlantic Fishery Science, 41: 23-36.

Matarese AC, Kendall Jr AW, Blood DM, Vinter BM (1989) Laboratory guide to early life history stages of Northeast Pacific fishes. NOAA Technical Report NMFS 80. 652 pp.

- Matarese AC, Blood DM, Picquelle SJ, Benson JL (2003) Atlas of abundance and distribution patterns of ichthyoplankton from the Northeast Pacific Ocean and Bering Sea ecosystems based on research conducted by the Alaska Fisheries Science Center (1972–1996). NOAA Professional Paper NMFS 1. 281 pp.
- McConnaughey RA, Smith KR (2000) Associations between flatfish abundance and surficial sediments in the eastern Bering Sea. *Canadian Journal of Fisheries and Aquatic Sciences*, 57:2410–2419.
- Methot RD (1986) Frame trawl for sampling juvenile fish. *California Cooperative Oceanic Fisheries Investigations Reports* 27, 267-278.
- Mizobata K, Wang J, Saitoh S (2006) Eddy-induced cross-slope exchange maintaining summer high productivity of the Bering Sea shelf break, *Journal of Geophysical Research*, 55(16-17):1717-1728.
- Modin J, Fagerholm B, Gunnarsson B, Pihl L (1996) Changes in otolith microstructure at metamorphosis of plaice, *Pleuronectes platessa* L. *ICES Journal of Marine Science*, 53:745-748
- Mordy CW, Stabeno PJ, Ladd C, Zeeman SI, Wisegarver DP, Hunt GL Jr (2005) Nutrients and primary production along the eastern Aleutian Island Archipelago. *Fisheries Oceanography*, 14:55–76.
- Nash RDM, Geffen AJ (2005) Age and growth. *In Flatfishes: biology and exploitation. Edited by R.N. Gibson. Blackwell, Oxford, UK.* pp. 138–163.
- Mueter FJ, Litzow MA (2008) Sea ice retreat alters the biogeography of the Bering Sea continental shelf. *Ecological Applications*, 18 (2):309-320.
- Nash RDM, Geffen AJ (2012) Mortality through the early life-history of fish: what can we learn from European plaice (*Pleuronectes platessa* L.)? *Journal of Marine Systems*, 93:58–68.
- Nash RDM, Geffen AJ (2014) Age and growth. R.N. Gibson (Ed.), *Flatfishes: Biology and Exploitation* (2nd ed.), Blackwell Science, Oxford (2014), pp. 207-227
- Neuman MJ, Able KW (1998) Experimental evidence of sediment preference by early life history stages of windowpane (*Scophthalmus aquosus*). *Journal of Sea Research*, 40:33-41.
- Nielsen JL, Graziano SL, Seitz AC (2010) Fine-scale population genetic structure in Alaskan Pacific halibut *Hippoglossus stenolepis*. *Conservation Genetics*, 11:999-1012.
- Norcross BL, Muter FJ, Holladay BA (1997) Habitat models for juvenile pleuronectids around Kodiak Island, Alaska. *Fishery Bulletin US*, 95:504-520.

Overland JE, Spillane MC, Hurlburt HE, Wallcraft AJ (1994) A numerical study of the circulation of the Bering Sea basin and exchange with the north Pacific Ocean. *Journal of Physical Oceanography*, 24(4):736-758.

Overland JE, Adams JM, Bond NA (1999) Decadal Variability of the Aleutian Low and Its Relation to High-Latitude Circulation. *Journal of Climate*, 12(5):1542-1548.

Overland JE, Bond NA, Adams JM (2002) The relation of surface forcing of the Bering Sea to large-scale climate patterns. *Deep-Sea Research Part II: Topical Studies in Oceanography*, 49B:5855-5868.

Parada C, Armstrong DA, Ernst B, Hinckley S, Orensanz, J.M. (2010) Spatial dynamics of snow crab (*Chionoecetes opilio*) in the eastern Bering Sea, putting together the pieces of the puzzle. *Bulletin of Marine Science*, 86(2):413-437.

Pannella G (1971) Fish Otoliths: Daily Growth Layers and Periodical Patterns. *Science* 173:1124-1127

Petitgas P, Rijnsdorp AD, Dickey-Collas M, Engelhard GH, Peck MA, Pinnegar J K, Drinkwater K, Huret M, Nash RDM (2013) Impacts of climate change on the complex life cycles of fish. *Fisheries Oceanography*, 22: 121-139.

Pinsky ML, Worm B, Fogarty MJ, Sarmiento JL, Levin SA (2013) Marine taxa track local climate velocities. *Science*, 341:1239-1242.

Poloczanska ES, Brown CJ, Sydeman WJ, Kiessling W, Schoeman DS, Moore PJ, Brander K, Bruno JF, Buckley LB, Burrows MT, Duarte CM, Halpern BS, Holding J, Kappel CV, O'Connor MI, Pandolfi JM, Parmesan C, Schwing F, Thompson SA, Richardson AJ (2013) Global imprint of climate change on marine life. *Nature Climate Change*, 3:919-925.

Rijnsdorp AD, Van Beek FA, Flatman S, Millner RM, Riley JD, Giret M, De Clerck R (1992) Recruitment of sole stocks, *Solea solea* (L.), in the northeast Atlantic. *Netherlands Journal of Sea Research*, 29(1-3):173-192.

Rijnsdorp AD, Peck MA, Engelhard GH, Mo'llmann C, Pinnegar JK (2009) Resolving the effect of climate change on fish populations. *ICES Journal of Marine Science*, 66: 1570-1583. doi: 10.1093/icesjms/fsp056.

Schumacher J, Bond NA, Brodeur RD, Livingston PA, Napp JM, Stabeno PJ (2003) Climate change in the southeastern Bering Sea and some consequences for biota. *Large Marine Ecosystems of the World: Trends in Exploitation, Protection, and Research*:17-40.

Seitz AC, Loher T, Nielsen JL (2007) Seasonal movements and environmental conditions experienced by Pacific halibut in the Bering Sea, examined by pop-up satellite tags. *International Pacific Halibut Commission Science Reports* 84.

Seitz A, Loher T, Norcross BL, Nielsen JL (2011) Dispersal and behavior of Pacific halibut *Hippoglossus stenolepis* in the Bering Sea and Aleutian Islands region. *Aquatic Biology*, 12:225-239.

Siddon EC, Duffy-Anderson JT, Mueter FJ (2011) Community-level response of fish larvae to environmental variability in the southeastern Bering Sea. *Marine Ecology Progress Series*, 426:225-239.

Skud BE (1977) Regulations of the Pacific halibut fishery, 1924-1976. International Pacific Halibut Commission Technical Reports 15.

Sogard SM (1991) Interpretation of Otolith Microstructure in Juvenile Winter Flounder (*Pseudopleuronectes americanus*) - Ontogenic Development, Daily Increment Validation, and Somatic Growth Relationships. *Canadian Journal of Fisheries and Aquatic Sciences*, 48:1862-1871.

Sohn D (2009) Ecology of Greenland Halibut (*Reinhardtius hippoglossoides*) during the Early Life Stages in the Eastern Bering Sea and Aleutian Islands. Master's thesis. College of Oceanic and Atmospheric Sciences, Oregon State University, Oregon, USA (June, 2009).

Sohn D, Ciannelli L, Duffy-Anderson JT (2010) Distribution and drift trajectories of Greenland halibut (*Reinhardtius hippoglossoides*) during early life stages in the eastern Bering Sea and Aleutian Islands. *Fisheries Oceanography*, 19(5):339-353.

Sohn D, Ciannelli L, Duffy-Anderson JT (2016) Distribution of early life Pacific Halibut and comparison with Greenland halibut in the eastern Bering Sea. *Journal of Sea Research* 107:31-42.

Spencer PD (2008) Density-independent and density-dependent factors affecting temporal changes in spatial distributions of eastern Bering Sea flatfish. *Fisheries Oceanography*, 17(5):396-410.

Spies I, Wilderbuer TK, Nichol DG, Aydin K (2014) Assessment of the arrowtooth flounder stock in the Eastern Bering Sea and Aleutian Islands. In Stock assessment and fishery evaluation report for the groundfish resources of the Bering Sea/Aleutian Islands region. North Pacific Fishery Management Council, Anchorage, Alaska. pp. 921-1012.

Staaterman E, Paris CB (2013) Modeling larval fish navigation: the way forward. *ICES Journal of Marine Science*, 71:918-924. doi:10.1093/icesjms/fst103

Stabeno PJ, Schumacher JD, Ohtani K (1999) The physical oceanography of the Bering Sea. In: Loughlin, T., Ohtani, K. (Eds.), University of Alaska Sea Grant, Fairbanks, AK, pp. 1-28. 825 pp.

Stabeno PJ, Meurs PV (1999) Evidence of episodic on-shelf flow in the southeastern Bering Sea.

Journal of Geophysical Research, 104:715-720.

Stabeno PJ, Reed RK, Napp JM (2002) Transport through Unimak Pass, Alaska. Deep-Sea Research II: Topical Studies in Oceanography, 49(26):5931-5943.

Stabeno PJ, Kachel DG, Kachel NB, Sullivan ME (2005) Observations from moorings in the Aleutian Passes: temperature, salinity and transport. Fisheries Oceanography, 14:39-54.

Stabeno P, Moore S, Napp J, Sigler M, Zerbini A (2012) Comparison of warm and cold years on the southeastern Bering Sea shelf. Deep-Sea Research Part II: Topical Studies in Oceanography, 65-70:31-45.

Stabeno PJ, Hristova HG (2014) Observations of the Alaskan Stream near Samalga Pass and its connection to the Bering Sea: 2001–2004. Deep Sea Research Part I: Oceanographic Research, 88:30-46.

Stauffer G (2004) NOAA protocols for groundfish bottom trawl surveys of the Nation's fishery resources. U.S. Dept. Commerce NOAA Technical Memorandum AFSC-SPO-65.

Stenberg C (2007) Recruitment processes in west Greenland waters with special focus on Greenland halibut (*Reinhardtius hippoglossoides*, W.), Doctoral Dissertation, University of Bergen, Bergen, Norway.

Stene A, Gundersen AC, Albert OT, Nedreaas KH, Solemdal P (1999) Early development of Northeast Arctic Greenland halibut (*Reinhardtius hippoglossoides*). Journal of Northwest Atlantic Fishery Science, 25: 171-177.

Stewart IJ, Leaman BM, Martell S, Webster RA (2013) Assessment of the Pacific halibut stock at the end of 2012. International Pacific Halibut Commission. Report of Assessment and Research Activities, 2013:93-186.

St-Pierre G (1984) Spawning location and season for Pacific halibut. International Pacific Halibut Commission Science Reports 70.

St-Pierre G (1989) Recent studies of Pacific halibut postlarvae in the Gulf of Alaska and eastern Bering Sea. International Pacific Halibut Commission Scientific Reports 73.

Swartzman G, Uang C, Kaluzny S (1992) Spatial analysis of Bering Sea groundfish survey data using generalized additive models. Canadian Journal of Fisheries & Aquatic Sciences, 49(7):1366-1378.

Thompson WF, Van Cleve R (1936) Life history of the Pacific halibut Distribution and early life history. International Fisheries Commission Reports 9.

Van der Veer HW, Ellis T, Miller JM, Pihl L, Rijnsdorp AD (1997) Size selective predation on juvenile North Sea flatfish and possible implications for recruitment. In Chambers, R.C. and E.A. Trippel (Eds.). Early life history and recruitment in fish populations. Chapman and Hall, London, UK, pp. 279-303.

Van der Veer HW, Ruardij P, Van den Berg AJ, Ridderinkho H (1998) Impact of interannual variability in hydrodynamic circulation on egg and larval transport of plaice *Pleuronectes platessa* L. in the southern. North. Sea. Journal of Sea Research, 39: 29-40.

Van der Veer HW, Berghahn R, Miller JM, Rijnsdorp AD (2000) Recruitment in flatfish, with special emphasis on North Atlantic species: progress made by the Flatfish Symposia. ICES Journal of Marine Science, 57(2):202.

Vestfals C, Ciannelli L, Ladd C, Duffy- Anderson JT (2014) Effects of seasonal and inter-annual variability in along-shelf and cross- shelf transport on groundfish recruitment in the eastern Bering Sea. Deep Sea Research Part II: Topical Studies in Oceanography, 109:190–203. <http://dx.doi.org/10.1016/j.dsr2.2013.09.026>.

Vestfals C (2015) The responses of slope-spawning flatfish to environmental variability in the eastern Bering Sea. Doctoral Dissertation, Oregon State University, Corvallis, OR.

Wang M, Overland JE, Stabeno P (2012) Future climate of the Bering and Chukchi Seas projected by global climate models. Deep Sea Research II: Topical Studies in Oceanography, 65-70: 46-57.

Wiebe PH, Burt KH, Boyd SH, Morton AW (1976) A multiple opening/closing net and environmental sensing system for sampling zooplankton. Journal of Marine Research, 34:313-326.

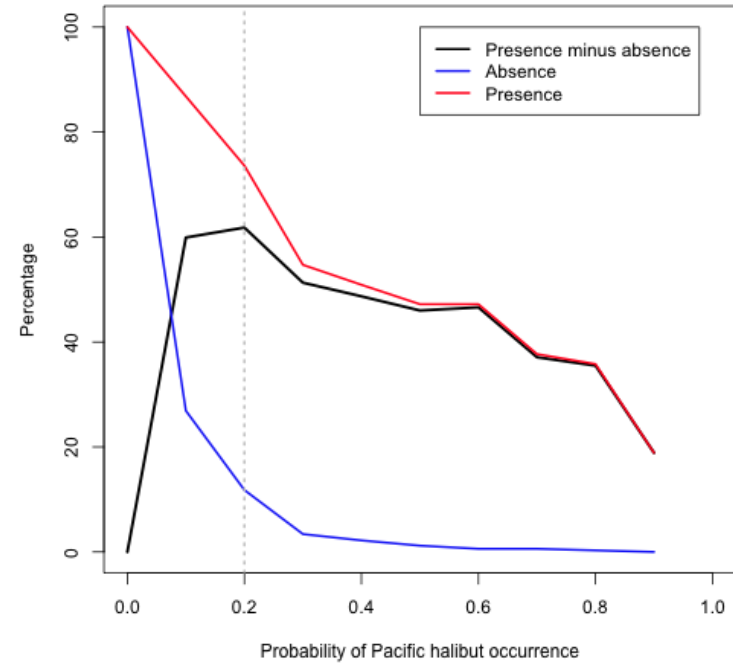
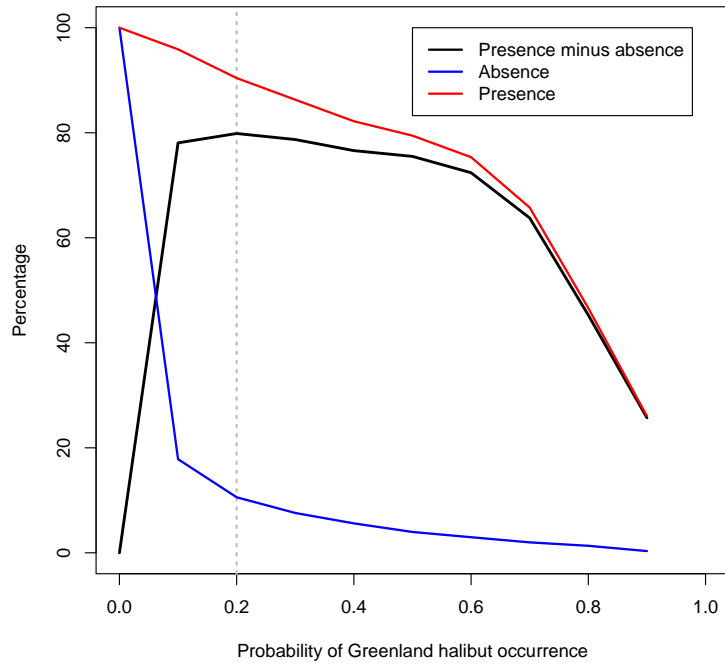
Wilderbuer TK, Hollowed AB, Ingraham WJ, Spencer PD, Connors ME, Bond NA, Walters GE (2002) Flatfish recruitment response to decadal climate variability and ocean conditions in the eastern Bering Sea. Progress Oceanography, 55: 235-248.

Wood SN (2004) Stable and efficient multiple smoothing parameter estimation for generalized additive models. Journal of the American Statistical Association, 99:673-686.

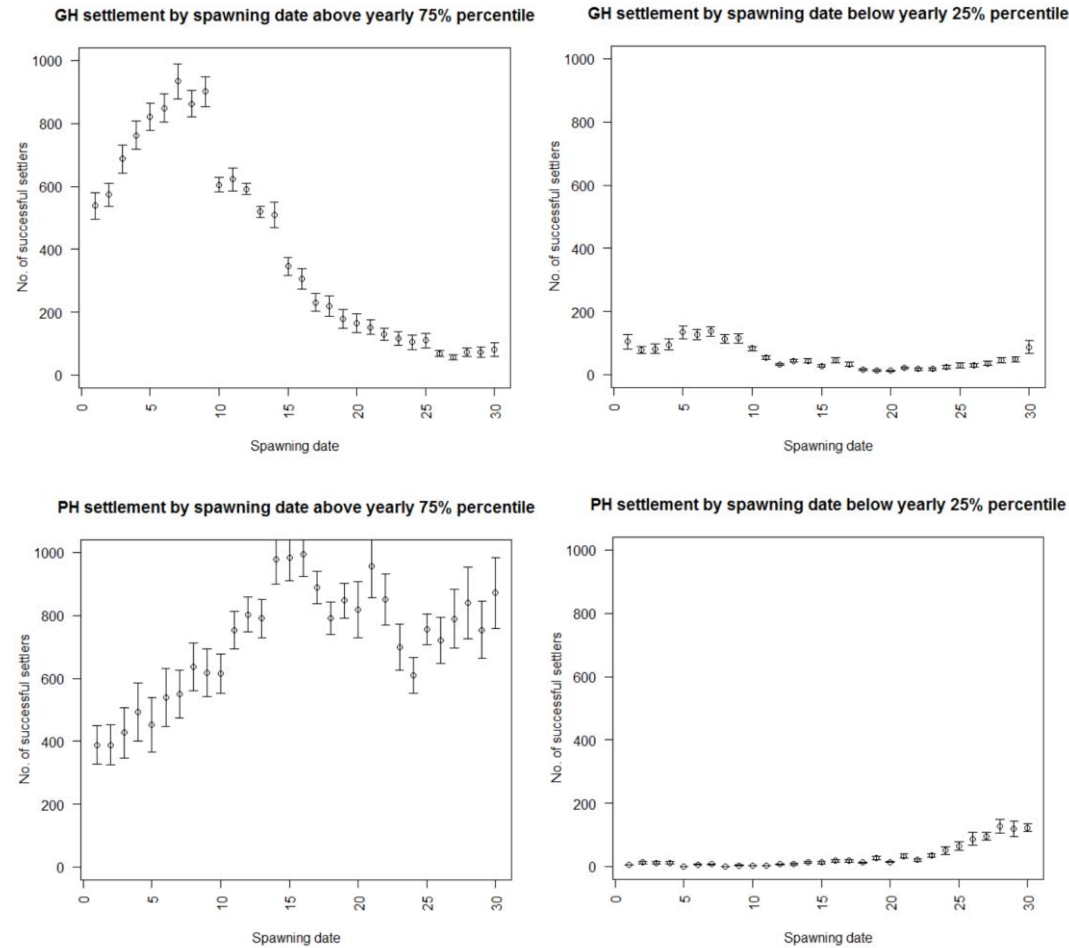
Wood SN (2006) Generalized Additive Models: An Introduction with R. Boca Raton: Chapman & Hall/CRC, 319 pp.

APPENDICES

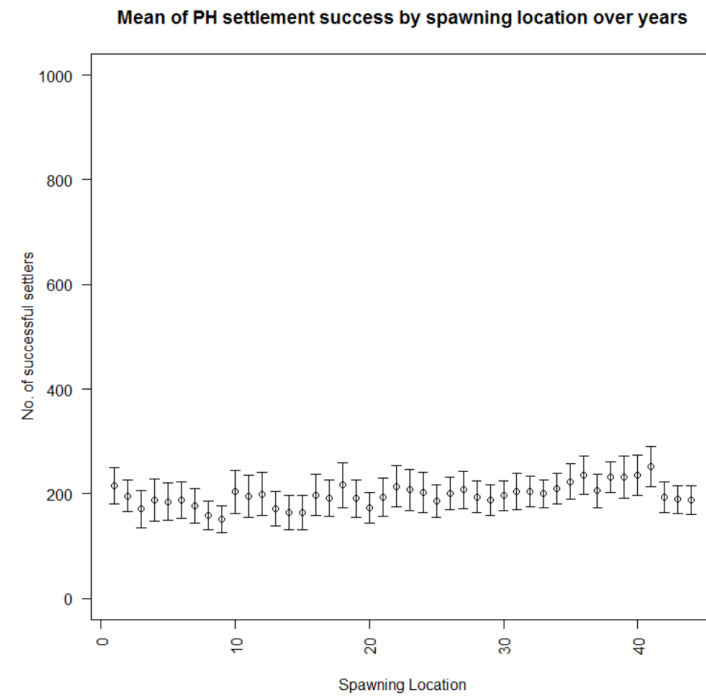
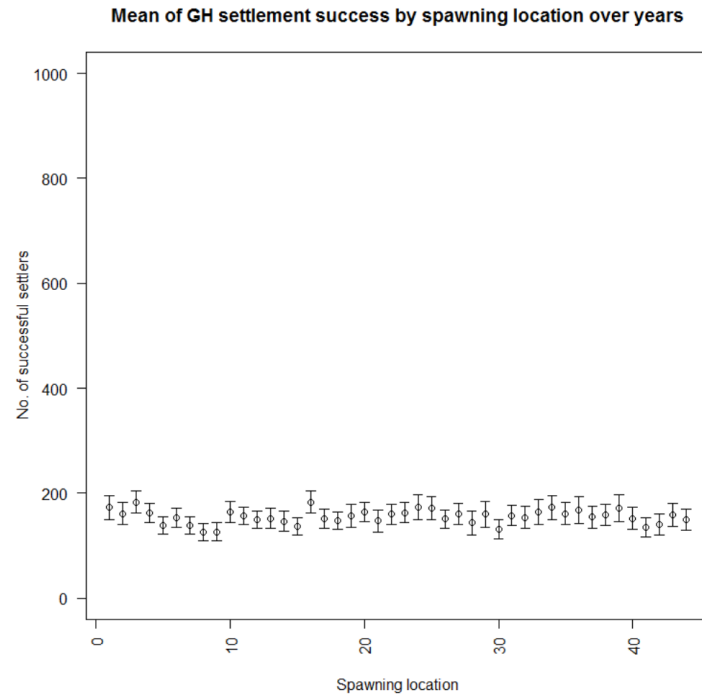
Appendix 3.1. The relationship between observed percentage of presence stations (red line), percentage of absence stations (blue line), and percentage of presence stations minus percentage of absence stations and predicted probability of occurrence for Greenland halibut (left panel) and Pacific halibut (right panel).



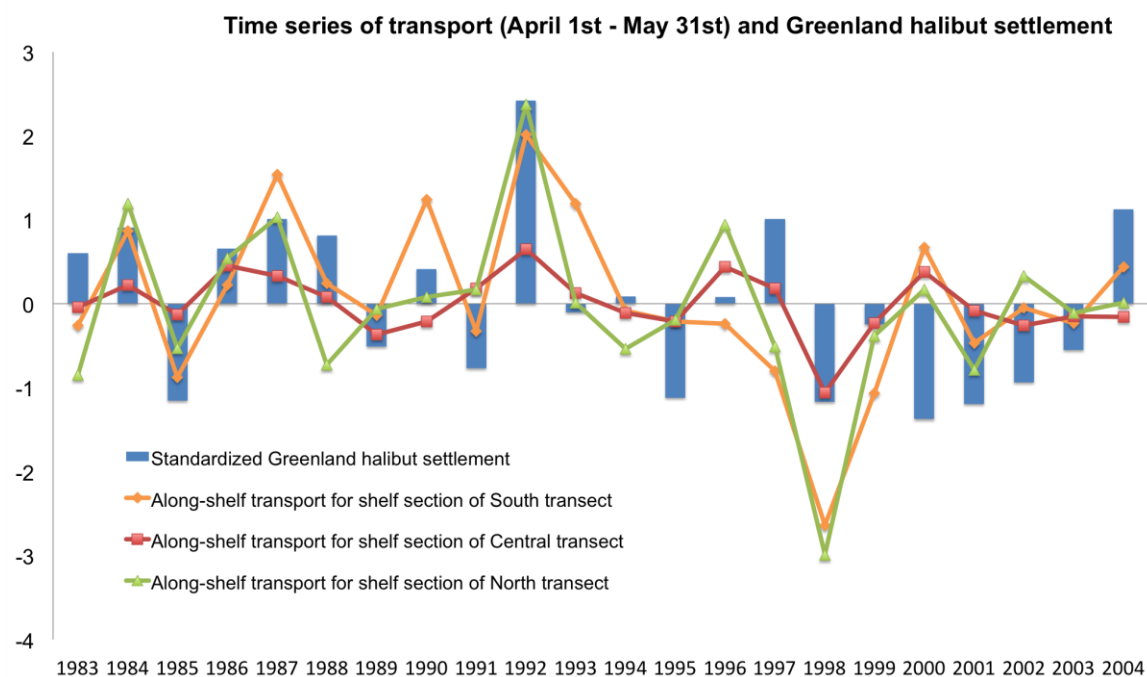
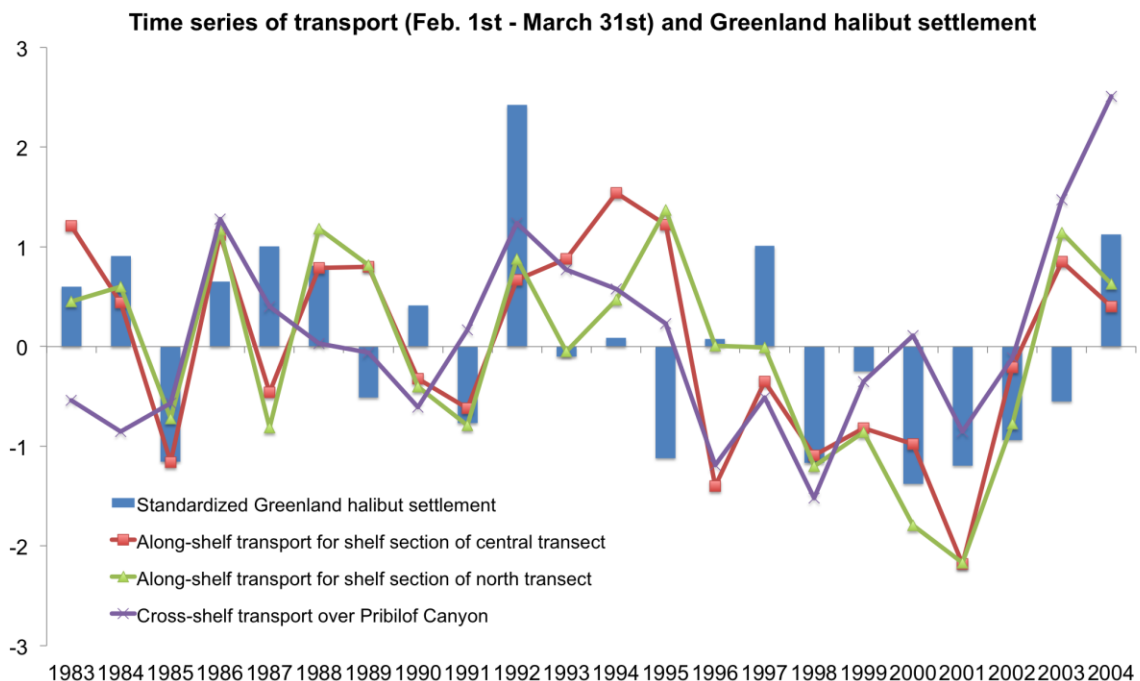
Appendix 3.2. Mean number of successful settlers by spawning date in 75th percentile years and in 25th percentile years for Greenland halibut (upper panels) and Pacific halibut (bottom panels). Error bars represent standard error. Spawning date 1 indicates November 2 and spawning date 30 indicates February 26 (four-day intervals).



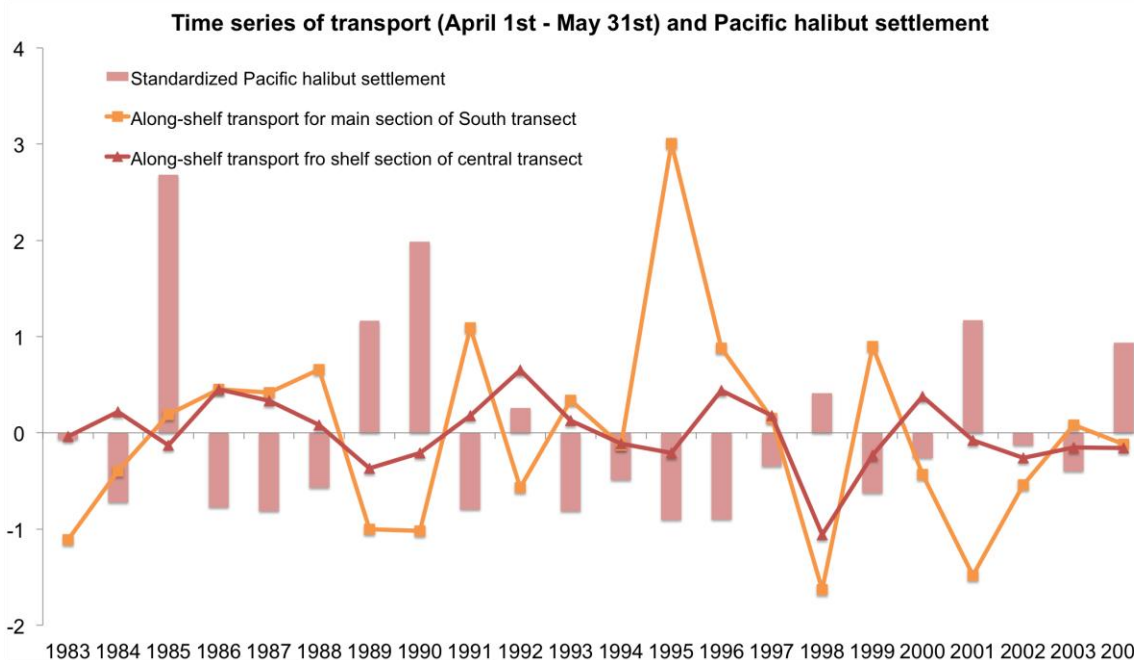
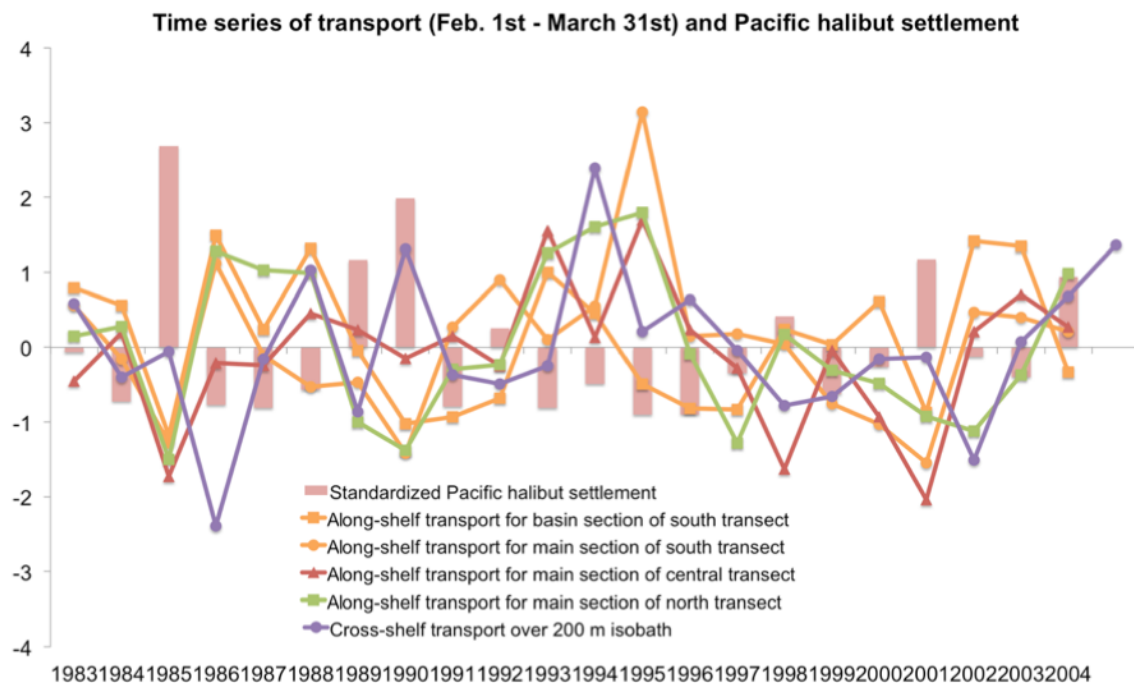
Appendix 3.3. Mean number of successful settlers by spawning location over the simulated years for Greenland halibut (left panel) and Pacific halibut (right panel). Error bars represent standard error.



Appendix 3.4. Time series of standardized average annual transport in the Bering Slope Current between Feb. 1st and March 31st (upper panel) and between April 1st – May 31st (bottom panel) and standardized annual Greenland halibut settlement. Transport has been standardized to transect length (Sv/km) to facilitate comparison between transects. Positive values represent northwestward transport; negative values represent southeastward transport.



Appendix 3.5. Time series of standardized average annual transport in the Bering Slope Current between Feb. 1st and March 31st (upper panel) and between April 1st – May 31st (bottom panel) and standardized annual Pacific halibut settlement. Transport has been standardized to transect length (Sv/km) to facilitate comparison between transects. Positive values represent northwestward transport; negative values represent southeastward transport.



Appendix 4.1. Mean value for environmental variables including along-shelf/on-shelf winds, ICI, and bottom temperature in the eastern Bering Sea.

Year	Along-shelf wind ¹	On-shelf wind ²	Ice Cover Index ³	Bottom temperature ⁴
2000	-0.44	-3.58	1.23	1.52
2001	1.68	3.82	-1.76	2.11
2002	2.05	2.18	-0.52	2.62
2003	-1.05	-0.71	-1.71	3.06
2004	2.01	1.50	-1.47	2.51
2005	-0.21	0.58	-1.77	2.66
2006	-1.96	4.54	-0.36	0.81
2007	-1.89	-0.78	0.76	0.41
2008	-1.78	-3.92	3.11	0.30
2009	4.11	-0.08	3.54	0.12
2010	0.75	-5.12	3.28	0.19
2011	0.37	2.53	0.82	1.63

¹ Along-shelf wind: April mean along-shelf wind (northwesterly; blowing from northwest (negative value) to southeast (positive value) and 54°-58°N, 165°-175°W)

² On-shelf wind: April mean on-shelf wind (southwesterly; blowing from southwest (negative value) to northeast (positive value) and 54°-58°N, 165°-175°W)

³ Ice Cover Index: Mean ice concentration for winter (January 1st-May31st and 56°-58°N, 163°-165°W)

⁴ Bottom temperature: Mean summer bottom temperature in the middle shelf (50 – 100 m isobaths) of the eastern Bering Sea from the Groundfish survey between 1982 and 2012

Appendix 4.2. Correlations between environmental variables in the eastern Bering Sea using the Pearson's product-moment correlation (*'= p-value \leq 0.1, '**'= p-value \leq 0.05, '***'= p-value \leq 0.01, '****'= p-value \leq 0.001).

Year	Along-shelf wind ¹	On-shelf wind ²	Ice Cover Index ³	Bottom temperature ⁴
Along-shelf wind ¹	1			
On-shelf wind ²	0.188	1		
Ice Cover Index ³	0.098	-0.642**	1	
Bottom temperature ⁴	0.105	0.415	-0.869****	1

¹ Along-shelf wind: April mean along-shelf wind (northwesterly; blowing from northwest (negative value) to southeast (positive value) and 54°-58°N, 165°-175°W)

² On-shelf wind: April mean on-shelf wind (southwesterly; blowing from southwest (negative value) to northeast (positive value) and 54°-58°N, 165°-175°W)

³ Ice Cover Index: Mean ice concentration for winter (January 1st-May31st and 56°-58°N, 163°-165°W)

⁴ Bottom temperature: Mean summer bottom temperature in the middle shelf (50 – 100 m isobaths) of the eastern Bering Sea from the Groundfish survey between 1982 and 2012

Appendix 4.3. Results of variable coefficient generalized additive models for age-1 arrowtooth flounder (110 mm – 160 mm total length) between 1992 and 2012 from summer groundfish surveys in the eastern Bering Sea. Mean bottom temperature (BT) experienced during age-1 ATF habitat was used as the only factor in the model (*' = p-value \leq 0.1, '**' = p-value \leq 0.05, '***' = p-value \leq 0.01, '****' = p-value \leq 0.001). The estimate column indicates the value of the difference in average abundance between the reference intercept (BT = 2.0) and all other BT values. The p-value refers to the Ho that the estimated parameter is equal to 0.

Parametric coefficients BT (°C)	Estimate	Standard error	t-value	P-value
Intercept	1.58	0.12	13.31	<2e-16***
2.2	-0.46	0.09	-5.34	1.11e-07 ***
2.3	-0.52	0.10	-5.30	1.38e-07 ***
2.4	-0.58	0.09	-6.64	4.73e-11 ***
2.5	-0.37	0.09	-4.00	6.83e-05 ***
2.8	-0.77	0.14	-5.62	2.37e-08 ***
2.9	-0.71	0.10	-6.95	5.60e-12 ***
3.0	-0.50	0.12	-4.15	3.62e-05 ***
3.1	-0.64	0.10	-6.34	3.18e-10 ***
3.2	-0.16	0.08	-2.12	0.03458 *
3.5	-0.72	0.09	-8.26	3.63e-16 ***
3.6	-0.74	0.10	-7.39	2.52e-13 ***
3.7	-0.61	0.10	-6.11	1.31e-09 ***
3.8	-0.28	0.10	-2.89	0.00396 **
4.1	-0.50	0.10	-5.27	1.59e-07 ***
4.2	-0.44	0.09	-4.99	7.02e-07 ***

Appendix 4.4. Results of variable coefficient generalized additive models for age-1 Greenland halibut (130 mm -180 mm total length) between 1982 and 2012 from summer groundfish surveys in the eastern Bering Sea. GCV stands for generalized cross validation score and AIC stands for akaike information criterion. Mean bottom temperature (BT) experienced during age-1 GH habitat was used as the only factor in the model (*'= p-value ≤ 0.1 , **'= p-value ≤ 0.05 , ***'= p-value ≤ 0.01 , ****'= p-value ≤ 0.001). The estimate column indicates the value of the difference in average abundance between the reference intercept (BT = -0.88) and all other BT values. The p-value refers to the Ho that the estimated parameter is equal to 0.

Parametric coefficients BT (°C)	Estimate	Standard error	t-value	P-value
Intercept	0.06	0.28	0.22	0.82
-0.74	0.41	0.27	1.49	0.14
-0.65	-0.13	0.31	-0.43	0.67
-0.61	0.06	0.30	0.22	0.83
-0.59	0.20	0.29	0.71	0.48
-0.53	1.52	0.27	5.63	2.87e-08 ***
-0.51	0.14	0.31	0.44	0.67
-0.44	0.43	0.28	1.56	0.12
-0.42	0.98	0.27	3.57	0.0004 ***
-0.25	0.43	0.30	1.46	0.15
-0.22	0.24	0.33	0.71	0.48
-0.1	0.65	0.28	2.38	0.018 *
-0.04	0.21	0.30	0.68	0.50
0.13	0.27	0.31	0.87	0.39
0.35	0.40	0.30	1.33	0.18
0.51	0.48	0.27	1.76	0.08 .
0.68	0.22	0.30	0.75	0.45
0.7	0.11	0.31	0.35	0.73
0.88	0.06	0.36	0.16	0.87
0.92	0.31	0.29	1.08	0.28
1.2	0.01	0.33	0.02	0.98
1.27	-0.19	0.38	-0.52	0.61
1.3	0.23	0.31	0.74	0.46
1.46	0.23	0.33	0.71	0.48
1.49	0.12	0.38	0.31	0.76
1.57	0.05	0.42	0.13	0.90
1.74	0.46	0.28	1.62	0.11
2.02	0.44	0.29	1.52	0.13
2.17	-0.03	0.34	-0.08	0.94